Recent Developments in Testing General Relativity with Satellite Laser Ranging

L. Iorio([1])([*])

([1]) *Dipartimento di Fisica dell'Università di Bari, Via Amendola 173, 70126, Bari, Italy.*

1. – Introduction

The last decade can be characterized by an impressive diversity of techniques monitoring the artificial and natural satellite dynamics, as well as the Earth rotation: improved laser technology, renewed Doppler techniques, satellite radar altimetry, massive usage of the Global Positioning System (GPS), etc. Each of these techniques is optimally tailored to a specific type of application or scientific problem. For example, it appears that laser tracking (SLR: see on the WEB: **http://ilrs.gsfc.nasa.gov**) of passive geodynamics satellites (LAGEOS, LAGEOS II, Starlette, Stella, Ajisai, Etalon I and II) over relatively long time intervals provides an excellent method for determining the long-term variations of the geopotential [1] (including tidal effects) and many small non-gravitational phenomena [2]. It turns out that the precision reached in the latest years by such technique in measuring the position of the passive laser-ranged geodetic satellites LAGEOS and LAGEOS II amounts to 1 cm or better([1]). See, e.g., **http://earth.agu.org/revgeophys/marsha01/node1.html**

Such astonishing levels of accuracy have disclosed an unexpectedly wide field of research in space geodesy, geophysics and fundamental physics. E.g., now it is possible to plan satellite-based experiments devoted to the experimental control even of some tiny post-Newtonian features of the Earth'gravitational field predicted by Einstein' s General Relativity [3]. They are usually expressed in terms of certain solve-for least squares fits' parameters. In evaluating the precision of the results of these experiments it must be considered that, in general, the main error does not consist of the standard statistical error of the fits but of the various systematic errors. They are induced by a complete set of other physical effects acting upon the satellites to be employed [4]. Such perturbations are often quite larger than the relativistic effects investigated and induce systematic errors to be correctly evaluated and assessed. Many of these aliasing effects are traditionally investigated by geophysics and space geodesy, so that such experiments are multidisciplinary efforts which cover many scientific areas until now separated [5, 6]. Indeed, the expansion of the SLR network, together with improved system accuracies, has enabled the laser data to contribute directly to improving orbit force models. It allows one to calculate more accurately, among other things, the error budget of many

---

([*]) E–mail: Lorenzo.Iorio@ba.infn.it
([1]) In August 2001 the single-shot accuracy in tracking LAGEOS at Matera amounts to 5 mm

space-based general relativistic experiments: this is the main topic of the present work. It does not treat the measurement modelling errors specifically related to the laser-ranging technique.

1˙1. *The Lense-Thirring drag of inertial frames*. – One of the most interesting topic in General Relativity is the structure of the spacetime around a spherically symmetric rotating mass-energy distribution. Indeed, in the slow-motion and weak-field approximation, it exhibits the characteristic feature of exerting a non-central force on a test particle due to the total angular momentum of the central object, contrary to Newtonian mechanics in which the gravitational action of a body is caused only by its mass, regardless to its rotational motion. Because of the formal analogies with the electrodynamics, this effect, deduced from the equations of Einstein for the first time by Lense and Thirring in 1918 [7], is also defined as gravitomagnetism. A comprehensive review of its properties can be found in [8, 9, 10].

In the past few years we have seen increasing efforts, both from a theoretical and an experimental point of view, devoted to the measurement of the Lense-Thirring effect in the weak gravitational field of the Earth by means of artificial satellites. At present, there are two main proposals which point towards the implementation of this goal: the Gravity Probe-B mission [11], and the approach proposed in [12] which consists in using the actually orbiting LAGEOS laser-ranged satellite and launching another satellite of LAGEOS type, the LARES, with the same orbital parameters of LAGEOS except for the inclination, which should be supplementary with respect to it, the eccentricity which should be one order of magnitude larger, and the area-to-mass ratio which should be smaller so to reduce the impact of the non-gravitational orbital perturbations (see Appendix A for the LAGEOS type satellites' data). The observable would be a secular linear trend built up with the sum of the residuals of the longitudes of the ascending nodes Ω of LARES and LAGEOS (see section 2 and fig. 1 for an explanation of the Keplerian orbital elements in terms of which the orbit of a satellite can be parameterized). The proposed orbital geometry would allow one to minimize the impact of the aliasing trend due to the mismodelling in the classical nodal precessions generated by the oblateness of the Earth, which would represent the main systematic error.

The GP-B mission is aimed to the detection of the motion of a spinning particle. At present, both the GP-B and the LARES have not yet been launched: however, while the GP-B is scheduled to fly in fall 2002, the fate of LARES project is still uncertain.

Recently, Ciufolini, in ref.[14], has put forward an alternative strategy based on the utilization of the already existing LAGEOS and LAGEOS II which allowed the detection of the Lense-Thirring drag at a precision level of the order of 20% [15, 16]. While the GP-B mission is focused on the gravitomagnetic dragging of the spin of a freely falling body, in the LAGEOS experiment it is the entire orbit of the satellite which is considered to undergo the secular Lense-Thirring precession. More exactly, among the Keplerian orbital elements [17, 18], the node Ω and the perigee ω are affected by the gravitomagnetic perturbation. For LAGEOS and LAGEOS II it amounts to

$$\dot{\Omega}_{\mathrm{LT}}^{\mathrm{LAGEOS}} \simeq 31 \text{ mas/y}, \tag{1}$$

$$\dot{\Omega}_{\mathrm{LT}}^{\mathrm{LAGEOS\ II}} \simeq 31.5 \text{ mas/y}, \tag{2}$$

$$\dot{\omega}_{\mathrm{LT}}^{\mathrm{LAGEOS}} \simeq 31.6 \text{ mas/y}, \tag{3}$$

$$\dot{\omega}_{\mathrm{LT}}^{\mathrm{LAGEOS\ II}} \simeq -57 \text{ mas/y}, \tag{4}$$

where mas/y stands for milliarcseconds per year.

In section 2 a brief derivation of such results is presented. It follows ordinary linear satellite perturbation theory. Indeed, in the slow-motion and weak-field approximation, the gravitomagnetic potential is treated as a classical disturbing term with respect to the Newtonian gravitoelectric monopole.

The observable quantity proposed in [14] is a suitable combination of the orbital residuals of the nodes of LAGEOS and LAGEOS II and the perigee of LAGEOS II

$$(5) \qquad \dot{y} \equiv \delta\dot{\Omega}^{\mathrm{I}}_{\mathrm{exp}} + c_1 \times \delta\dot{\Omega}^{\mathrm{II}}_{\mathrm{exp}} + c_2 \times \delta\dot{\omega}^{\mathrm{II}}_{\mathrm{exp}} \simeq \mu_{\mathrm{LT}} \times 60.2.$$

In it $c_1 = 0.295$, $c_2 = -0.35$, μ_{LT} is the scaling, solve-for parameter, equal to 1 in General Relativity and 0 in classical mechanics, to be determined and $\delta\Omega^{\mathrm{I}}_{\mathrm{exp}}$, $\delta\Omega^{\mathrm{II}}_{\mathrm{exp}}$, $\delta\omega^{\mathrm{II}}_{\mathrm{exp}}$ are the orbital residuals, in mas, calculated with the aid of some orbit determination software like UTOPIA or GEODYN, of the nodes of LAGEOS and LAGEOS II and the perigee of LAGEOS II. The residuals account for any unmodelled or mismodelled physical phenomena acting on the observable analyzed. By dealing with the gravitomagnetism as an unmodelled physical effect, General Relativity predicts a linear trend with a slope of 60.2 mas/y

$$(6) \qquad \dot{y}_{\mathrm{LT}} \equiv (31 \text{ mas/y}) + c_1 \times (31.5 \text{ mas/y}) + c_2 \times (-57 \text{ mas/y}) \simeq 60.2 \text{ mas/y}.$$

The coefficients c_1 and c_2 have been obtained by solving for the three unknowns δJ_2, δJ_4 and μ_{LT} a nonhomogeneous algebraic linear system of three equations expressing the observed mismodelled classical precessions of the nodes of LAGEOS and LAGEOS II and the perigee of LAGEOS II (see ref.[14]). They depend on the orbital parameters of LAGEOS and LAGEOS II and are built up so to cancel out all the static and dynamical contributions of degree $l = 2, 4$ and order $m = 0$ of the Earth's gravitational field. This cancellation is required to reduce especially the impact of the first two even $(l = 2, 4)$ zonal $(m = 0)$ harmonics of the static geopotential. Indeed, at the present level of accuracy of the terrestrial gravitational field [19], the mismodelled parts of the classical orbital precessions of the node and the perigee, caused by the Earth's oblateness and parameterized with the first two even zonal coefficients J_2 and J_4 [1], for a single satellite amount to a significant part of the corresponding Lense-Thirring effect itself on the considered orbital element. The combined residuals of eq. (5) are affected by a complete set of gravitational and non-gravitational perturbations; among the former ones those generated by the solid Earth and ocean tides [20, 21] play an important role.

In section 3 the amplitudes and the periods of the most relevant tidal perturbations acting upon the nodes of LAGEOS and LAGEOS II and the perigee of LAGEOS II have been worked out [22]. This analysis covers both the solid $l = 2$ and the ocean $l = 2, 3, 4$ part of the tidal spectrum, includes the first order contributions, in the sense of the Kaula's theory of perturbations [1], and also a calculation of the mismodelling in the first order perturbative amplitudes compared to the Lense-Thirring drag over 4 years.

Section 4 is devoted to the study of the impact of the solid Earth and ocean tidal perturbations on eq. (5) with particular care to the systematic errors induced by them on the measurement of μ_{LT} [23, 24]. The left hand side of eq. (5) has been calculated by adopting the nominal values of the perturbative amplitudes worked out in section 3 in order to test if the first two even degree zonal tidal lines do not really affect the combined residuals. This is particularly important for the 18.6-year tidal constituent whose period is that of the longitude of the ascending node of the Moon, i.e. 18.6 years.

Indeed, over observational time spans of few years it could resemble a trend as well and its mismodelled part, accounted for by the residuals combination, could corrupt the measurement of μ_{LT}. The results obtained in section 3 have been employed also in order to obtain a simulated residual curve on which several tests have been performed for the various tesseral ($m = 1$) and sectorial ($m = 2$) tidal constituents, not cancelled out by the combined residuals, with the aim of assessing their contribution on the systematic uncertainty in the measurement of μ_{LT}.

1˙2. *The gravitoelectric pericenter shift*. – In section 5 the experience gained in the Lense-Thirring LAGEOS experiment is used to propose a possible experiment for measuring the general relativistic pericenter shift of a test body due to the Schwarzschild's gravitoelectric part of the terrestrial gravitational field by means of the SLR data to LAGEOS and LAGEOS II. The approach is similar to that of the current Lense-Thirring LAGEOS experiment and it is based on another suitable combination of orbital residuals of the nodes of LAGEOS and LAGEOS II and the perigee of LAGEOS II. The possibility of adopting different observables is examined as well. A discussion on the obtainable values for the Parameterized Post Newtonian parameters β and γ is also included.

1˙3. *The LARES mission*. – In section 6 we reanalyze the original LARES mission from the point of view of the sensitivity of the related observable to the departures of the LARES orbital parameters from their nominal values due to the orbital injection errors. Moreover, we propose an alternative combination of orbital residuals involving also the LAGEOS II which would yield to a smaller and more stable value of the error due to the mismodelling in the even zonal harmonics of the geopotential which turns out to be the main source of systematic error.

1˙4. *Conclusions*. – Section 7 is devoted to the conclusions and to the recommendations for future work.

2. – The Lense-Thirring effect on the orbit of a test body

2˙1. *Introduction*. – In this section an alternative strategy is presented in order to derive the Lense-Thirring effect [25]. It reveals itself useful especially in the prediction of the behavior of all the Keplerian orbital elements of the test body in the gravitational field of a rotating source. Our calculations are based on the Lagrangian planetary equations [1, 26, 27] and a non-central hamiltonian term whose existence, if from one hand can be rigorously deduced, from the other hand can be intuitively guessed by analogy from the corresponding term in electrodynamics for the Lagrangian of a charged particle acted upon by electric and magnetic fields.

For a perfectly spherical source the well known Lense-Thirring rate equations for the secular precessions of the node and the perigee are reobtained.

2˙2. *The gravitomagnetic potential*. – In general, it can be proved [9] that the general relativistic equations of motion of a test particle of mass m freely falling in a stationary gravitational field, in the weak-field and slow-motion approximation, are given by

$$(7) \qquad m\frac{d^2\mathbf{r}}{dt^2} \simeq m\left(\mathbf{E}_g + \frac{\mathbf{v}}{c} \times \mathbf{B}_g\right).$$

In eq. (7) $\mathbf{E}_g$ and $\mathbf{B}_g$ are the gravitoelectric and gravitomagnetic fields, respectively. If a perfectly spherically symmetric rotating body is assumed as gravitational source, in eq.

(7) $\mathbf{E}_g = -GM\mathbf{i}_r/r^2 + \mathcal{O}(c^{-2})$ is the Newtonian gravitational field of a spherical body, with M its mass and G the Newtonian gravitational constant([2]), while $\mathbf{B}_g$ is given by [9]

$$(8) \qquad \mathbf{B}_g = \nabla \times \mathbf{A}_g \simeq 2\frac{G}{c}\left[\frac{\mathbf{J} - 3(\mathbf{J}\cdot\mathbf{i}_r)\mathbf{i}_r}{r^3}\right],$$

in which

$$(9) \qquad \mathbf{A}_g(\mathbf{r}) \simeq -2\frac{G}{c}\frac{\mathbf{J}\times\mathbf{r}}{r^3}.$$

In eq. (9) $\mathbf{J}$ is the angular momentum of the central body. The field $\mathbf{A}_g \equiv (h_{01}, h_{02}, h_{03})$, named gravitomagnetic potential, is due to the off-diagonal components of the spacetime metric tensor

$$(10) \qquad g_{\mu\nu} = \eta_{\mu\nu} + h_{\mu\nu}, \ \mu, \nu = 0, 1, 2, 3,$$

where $\eta_{\mu\nu}$ is the Minkowski metric tensor. In obtaining eq. (9) a non-rotating reference frame $K\{x, \ y, \ z\}$ with the z axis directed along the intrinsic angular momentum of the central spinning body $\mathbf{J}$ and the $\{x, \ y\}$ plane coinciding with its equatorial plane has been used. The origin is located at the center of mass of the central body. Eq. (7) holds if $\mathbf{A}_g$ is not time-varying.

The gravitomagnetic potential generates a non-central gravitational contribute due uniquely to the angular momentum of the gravitational source that the Newtonian mechanics does not predict, though the conditions of validity of eq. (7) are the same for which the latter holds as well.([3]) So it is possible to speak of mass-energy currents whose motion exerts a non-central gravitational force on a test massive body analogous to the Lorentz force felt by a charged particle when it is moving in a magnetic field. Indeed, its equations of motions

$$(11) \qquad m\frac{d^2\mathbf{r}}{dt^2} \simeq q\left(\mathbf{E} + \frac{\mathbf{v}}{c}\times\mathbf{B}\right)$$

are formally analogous to eq. (7). Eq. (11) can be derived by means of the Lagrangian

$$(12) \qquad \mathcal{L}_{e.m.} = \frac{1}{2}mv^2 - qV + \frac{q}{c}(\mathbf{v}\cdot\mathbf{A}).$$

where $\mathbf{v}$ is the velocity of the particle and V is its scalar potential.

([2]) The terms of order $\mathcal{O}(c^{-2})$ are the post-Newtonian corrections due to the static Schwarzschild part of the metric.
([3]) Incidentally, it may be interesting to notice that eq. (7) are consistent with the fundamental Einstein assumption [28] that a non-accelerated reference frame with a gravitational field is equivalent, within certain limits, to an accelerated one without any gravitational field. Indeed, if a reference frame solidal with the rotating body is assumed, the equations of motion for a test particle are formally identical to eq. (7): the gravitomagnetic force term $\frac{m}{c}(\mathbf{v}\times\mathbf{B}_g)$ is substituted by the Coriolis force term $2m(\mathbf{v}\times\mathbf{\Omega})$ where $\mathbf{\Omega}$ is the angular velocity vector of the rotating body [29]. See also [30].

Since one of the most promising ways to detect the gravitomagnetic precession consists of employing artificial Earth satellites, it would be helpful to derive the rate equations for the change in the parameters that characterize their orbits. To this aim one could introduce "by hand" a perturbative term k $(\mathbf{v} \cdot \mathbf{A}_g)$ in the gravitational Lagrangian of the particle and use it in some particular perturbative scheme; the constant k would be determined by means of dimensional considerations and taking into account that it should be built up of universal constants. In fact it is possible to show that a non-central term analogous to $\frac{q}{c}(\mathbf{v} \cdot \mathbf{A})$ can be rigorously deduced in the Lagrangian of a test body in the gravitational field of a spinning mass-energy distribution, and that it can be exploited in deriving straightforwardly the effect of the gravitomagnetic potential on the Keplerian orbital elements of the test body.

2˙3. *The rate equations for the Keplerian orbital elements*. – The relativistic Lagrangian for a free particle in a gravitational field can be cast into the form:

$$\mathcal{L} = \mathcal{L}^{(0)} + \mathcal{L}^{(1)}. \tag{13}$$

In eq. (13) the term $\mathcal{L}^{(1)}$ is to be intended as containing the contributions of the off-diagonal terms of the metric

$$\mathcal{L}^{(1)} = \frac{m}{c} g_{0k} \dot{x}^0 \dot{x}^k. \tag{14}$$

In this case, recalling that the slow motion approximation is used, the eq. (14) becomes

$$\mathcal{L}^{(1)} \equiv \mathcal{L}_{gm} = \frac{m}{c}(\mathbf{A}_g \cdot \mathbf{v}). \tag{15}$$

For different derivations of $\mathcal{L}_{gm}$ see also [31, 32, 26]. In this section it is proposed to adopt $\mathcal{L}_{gm}$ in order to deriving the Lense-Thirring effect on the orbital elements of a particle in the field of a rotating gravitational source.

To this aim it must be assumed that under the gravitomagnetic force the departures of the test body' s trajectory from the unperturbed Keplerian ellipse are very small in time. This allows to introduce the concept of osculating ellipse. It means that, at a given instant of time, the particle may be assumed to lie on the Keplerian ellipse determined by the position and velocity at that instant thought as initial conditions for an unperturbed motion; at the next instant of time the particle will be at a point of another Keplerian ellipse, slightly different with respect to the previous one and determined by the real position and velocity of the test body at the new instant of time thought as new initial conditions for an unperturbed Keplerian orbit. In other words, the real trajectory of the test body at every instant may be approximated by an osculating Keplerian ellipse. So the perturbed motion can be described in terms of unperturbed Keplerian elements varying in time. See fig. 1.

Consider the frame $K\{x,\ y,\ z\}$ previously defined and a frame $K^{'}\{X,\ Y,\ Z\}$ with the Z axis directed along the orbital angular momentum $\mathbf{l}$ of the test body, the plane $\{X,\ Y\}$ coinciding with the orbital plane of the test particle and the X axis directed toward the pericenter. K and $K^{'}$ have the same origin located in the center of mass of the central body. The Keplerian orbital elements are [1]

- a, e, the semimajor axis and the ellipticity which define the size and the shape of the orbit in its plane
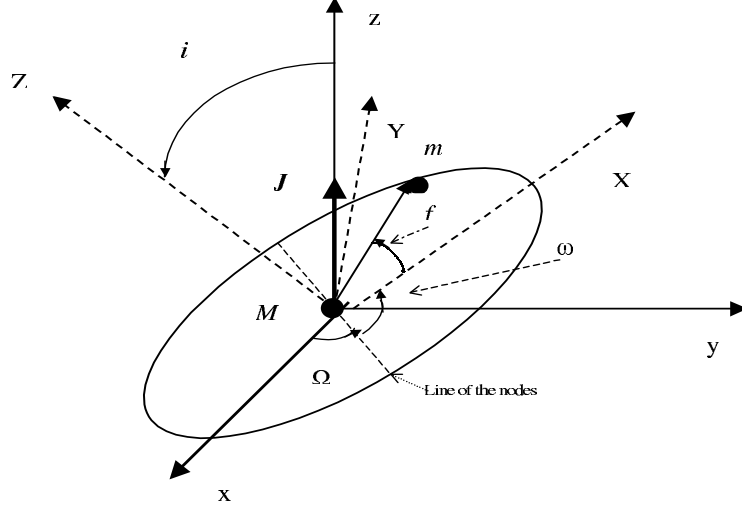
Fig. 1. – Orbital elements for a general Keplerian osculating ellipse.

- Ω, i, the longitude of the ascending node and the inclination which fix the orientation of the orbit in the space, i.e. of K' with respect to K. The longitude of the ascending node Ω is the angle in the equatorial plane of $K\{x,\ y,\ z\}$ between the x axis and the line of nodes in which the orbital plane intersects the equatorial plane. The inclination i is the angle between the z and Z axis
- ω, $\mathcal{M}$, the argument of pericenter and the mean anomaly. The argument of pericenter ω is the angle in the orbital plane between the line of nodes and the X axis; it defines the orientation of the orbit in its plane. The mean anomaly $\mathcal{M}$ specifies the motion of the test particle on its orbit. It is related to the mean motion $n = (GM)^{1/2}a^{-3/2}$, where M is the mass of the gravitating central source, through $\mathcal{M} = n(t - t_p)$ in which t_p is the time of pericenter passage

It is customary to define also

- $\varpi = \Omega + \omega$, the longitude of pericenter
- $u = \omega + f$, the argument of latitude where f is the angle, called true anomaly, which in the orbital plane determines the position of the test particle with respect to the pericenter
- $\varepsilon = \varpi + n(t_0 - t_p)$, the mean longitude at the epoch t_0. If $t_0 = 0$, it is customary to write ε as $L_0 = \varpi - nt_p$.

The matrix $\mathbf{R}_{xX}$ for the change of coordinates from K' to K is [1]

$$(16)\begin{pmatrix} \cos\Omega\cos\omega - \sin\Omega\cos i\sin\omega & -\cos\Omega\sin\omega - \sin\Omega\cos i\cos\omega & \sin\Omega\sin i \\ \sin\Omega\cos\omega + \cos\Omega\cos i\sin\omega & -\sin\Omega\sin\omega + \cos\Omega\cos i\cos\omega & -\cos\Omega\sin i \\ \sin i\sin\omega & \sin i\cos\omega & \cos i \end{pmatrix}.$$

Using eq. (16) and $X = r\cos f$, $Y = r\sin f$, $Z = 0$ it is possible to express the geocentric rectangular Cartesian coordinates of the orbiter in terms of its Keplerian

elements

$$(17) \qquad \begin{cases} x = r(\cos u \cos \Omega - \sin u \cos i \sin \Omega) \\ y = r(\cos u \sin \Omega + \sin u \cos i \cos \Omega) \\ z = r \sin u \sin i. \end{cases}$$

Redefining suitably the origin of the angle Ω so that $\cos \Omega = 1$, $\sin \Omega = 0$, the previous equations become

$$(18) \qquad \begin{cases} x = r \cos u \\ y = r \sin u \cos i \\ z = r \sin u \sin i. \end{cases}$$

Considering for the test particle the total mechanical energy with the sign reversed, according to [27], $\mathcal{F} \equiv -\mathcal{E}_{tot} = -(\mathcal{T} + \mathcal{U})$, where $\mathcal{T}$ and $\mathcal{U}$ are the kinetic and potential energies per unit mass, it is possible to work out the analytical expressions for the rate of changes of a, e, i, Ω, ω, $\mathcal{M}$ due to any non-central gravitational contribution. To this aim it is useful to isolate in $\mathcal{U}$ the central part $-\mathcal{C}$ of the gravitational field from the terms $-\mathcal{R}$ which may cause the Keplerian orbital elements to change in time: $\mathcal{U} = -\mathcal{C} - \mathcal{R}$. For a spherically symmetric body, $\mathcal{F}$ becomes

$$(19) \qquad \mathcal{F} = \frac{GM}{r} + \mathcal{R} - \mathcal{T} = \frac{GM}{2a} + \mathcal{R}.$$

Concerning the perturbative scheme to be employed, the well known Lagrange planetary equations are adopted. At first order, they are

$$(20) \qquad \frac{da}{dt} = \frac{2}{na} \frac{\partial \mathcal{R}}{\partial \mathcal{M}},$$

$$(21) \qquad \frac{de}{dt} = \frac{1-e^2}{na^2 e} \frac{\partial \mathcal{R}}{\partial \mathcal{M}} - \frac{(1-e^2)^{1/2}}{na^2 e} \frac{\partial \mathcal{R}}{\partial \omega},$$

$$(22) \qquad \frac{di}{dt} = \cos i \frac{1}{na^2(1-e^2)^{1/2} \sin i} \frac{\partial \mathcal{R}}{\partial \omega} - \frac{1}{na^2(1-e^2)^{1/2} \sin i} \frac{\partial \mathcal{R}}{\partial \Omega},$$

$$(23) \qquad \frac{d\Omega}{dt} = \frac{1}{na^2(1-e^2)^{1/2} \sin i} \frac{\partial \mathcal{R}}{\partial i},$$

$$(24) \qquad \frac{d\omega}{dt} = -\cos i \frac{1}{na^2(1-e^2)^{1/2} \sin i} \frac{\partial \mathcal{R}}{\partial i} + \frac{(1-e^2)^{1/2}}{na^2 e} \frac{\partial \mathcal{R}}{\partial e},$$

$$(25) \qquad \frac{d\mathcal{M}}{dt} = n - \frac{1-e^2}{na^2 e} \frac{\partial \mathcal{R}}{\partial e} - \frac{2}{na} \frac{\partial \mathcal{R}}{\partial a}.$$

The idea consists of using $\mathcal{L}_{gm}$ to obtain a suitable non-central term $\mathcal{R}_{gm}$ to be employed in these equations. This can be done considering the Hamiltonian for the test particle

$$(26) \qquad \mathcal{H} = \mathbf{p} \cdot \mathbf{v} - \mathcal{L}.$$

Inserting eq. (13) in eq. (26) one has

$$(27) \qquad \mathcal{H} = \mathcal{H}^{(0)} + \mathcal{H}_{gm},$$

with $\mathcal{H}_{gm} = -\frac{m}{c}(\mathbf{A}_g \cdot \mathbf{v})$. So it can be posed

$$(28) \qquad \mathcal{R}_{gm} = -\frac{\mathcal{H}_{gm}}{m} = \frac{(\mathbf{A}_g \cdot \mathbf{v})}{c}.$$

Now it is useful to express eq. (28) in terms of the Keplerian elements. Referring to eq. (9), eq. (18), and recalling that in the frame $K\{x,\ y,\ z\}$ $\mathbf{J} = (0,\ 0,\ J)$ and that for an unperturbed Keplerian motion

$$(29) \qquad \frac{1}{r} = \frac{(1 + e\cos f)}{a(1 - e^2)},$$

it is possible to obtain, for a perfectly spherical central body

$$(30) \qquad \mathcal{R}_{gm} = -\frac{2G}{c^2}\frac{J\cos i}{r}\dot{u} = -\frac{2GJ\cos i}{c^2}\frac{(1 + e\cos f)}{a(1 - e^2)}\dot{u}.$$

In eq. (30) $\dot{u} \simeq \dot{f}$ is assumed due to the fact that the osculating element ω may be retained almost constant on the temporal scale of variation of the true anomaly of the test body.

2˙4. *Secular gravitomagnetic effects on the Keplerian orbital elements.* – The secular effects can be worked out by adopting the same strategy followed, e.g., in [27] for a similar kind of perturbing functions. By using averaging we implicitly make several assumptions about the system that may restrict the validity and applicability of our result. Averaging is generally applied to systems where the perturbing force is sufficiently small so that, over one orbital period, the deviations of the true trajectory from the Keplerian trajectory are relatively small. This perturbation can generally be related to the magnitude of the perturbing acceleration as compared to the central-body attraction. In this case, clearly, we can view the application of the averaging approach as valid. When eq. (30) is mediated over one orbital period of the test body, $a,\ e,\ i,\ \Omega$ and ω are to be considered constant

$$(31) \qquad \langle \mathcal{R} \rangle_{2\pi} = -\frac{1}{P}\int_0^P \frac{G}{c^2}\frac{2J}{r}\cos i\, du = -n\frac{G}{c^2}\frac{2J\cos i}{2\pi}\int_0^{2\pi}\frac{df}{r} = -n\frac{G}{c^2}\frac{2J\cos i}{a(1 - e^2)}.$$

The relation $du = d\omega + df = df$ has been used in eq. (31). Eq. (31) can now be used in determining the secular changes of the Keplerian orbital elements of the test body. From it one gets

$$(32) \qquad \frac{\partial \langle \mathcal{R} \rangle_{2\pi}}{\partial \mathcal{M}} = 0,$$

$$(33) \qquad \frac{\partial \langle \mathcal{R} \rangle_{2\pi}}{\partial \omega} = 0,$$

$$(34) \qquad \frac{\partial \langle \mathcal{R} \rangle_{2\pi}}{\partial \Omega} = 0,$$

$$(35) \qquad \frac{\partial \langle \mathcal{R} \rangle_{2\pi}}{\partial i} = \frac{G}{c^2}\frac{2nJ\sin i}{a(1 - e^2)},$$

$$(36) \qquad \frac{\partial \langle \mathcal{R} \rangle_{2\pi}}{\partial e} = -\frac{G}{c^2}\frac{4nJe\cos i}{a(1 - e^2)^2}.$$

A particular care is needed for the treatment of n when the derivative of $\langle \mathcal{R} \rangle_{2\pi}$ with respect to a is taken; indeed, it must be posed as

$$(37) \qquad \frac{\partial \langle \mathcal{R} \rangle_{2\pi}}{\partial a} = \frac{\partial \langle \mathcal{R} \rangle_{2\pi}}{\partial a} \bigg|_{n} + \frac{\partial \langle \mathcal{R} \rangle_{2\pi}}{\partial n} \bigg|_{a} \frac{\partial n}{\partial a}.$$

In eq. (37)

$$(38) \qquad \frac{\partial \langle \mathcal{R} \rangle_{2\pi}}{\partial a} \bigg|_{n} = \frac{G}{c^2} \frac{2nJ \cos i}{a^2 (1 - e^2)},$$

and

$$(39) \qquad \frac{\partial \langle \mathcal{R} \rangle_{2\pi}}{\partial n} \bigg|_{a} \frac{\partial n}{\partial a} = \frac{G}{c^2} \frac{3nJ \cos i}{a^2 (1 - e^2)}.$$

From eq. (20) and eq. (32) it appears that there are no secular changes in the semimajor axis([4]), and so the orbital period of the test body, related to the mean motion by $P = 2\pi/n$, can be considered constant. So in eq. (37) only eq. (38) must be retained. Using eqs. (32)-(37) in eqs. (20)-(25) one obtains for the averaged rates

$$(40) \qquad \frac{da}{dt} \bigg|_{\text{LT}} = 0,$$

$$(41) \qquad \frac{de}{dt} \bigg|_{\text{LT}} = 0,$$

$$(42) \qquad \frac{di}{dt} \bigg|_{\text{LT}} = 0,$$

$$(43) \qquad \frac{d\Omega}{dt} \bigg|_{\text{LT}} = \frac{G}{c^2} \frac{2J}{a^3 (1 - e^2)^{3/2}},$$

$$(44) \qquad \frac{d\omega}{dt} \bigg|_{\text{LT}} = -\frac{G}{c^2} \frac{6J \cos i}{a^3 (1 - e^2)^{3/2}},$$

$$(45) \qquad \frac{d\mathcal{M}}{dt} \bigg|_{\text{LT}} = 0.$$

They are the well known Lense-Thirring equations [7, 8, 25]. In deriving them it has been assumed that the spatial average over f yields the same results for the time average [33, 34, 2].

The effects of the quadrupole mass moments of the source are treated in [25]: it turns out that they are negligible in the context of the LAGEOS Lense–Thirring experiment.

3. – Orbital perturbations induced by solid Earth and ocean tides

3 $^{.}$1. *Introduction*. – In this section the problem of calculating the gravitational time-dependent perturbations induced by solid Earth and ocean tides on the Keplerian orbital

---

([4]) Here only the effect of the off-diagonal gravitomagnetic components of the metric tensor is considered, neglecting any other physical influence of gravitational and non gravitational origin.

RECENT DEVELOPMENTS IN TESTING GENERAL RELATIVITY WITH SATELLITE LASER RANGING**11**

elements of LAGEOS and LAGEOS II is addressed. The focus of the analysis is on the nodes of LAGEOS and LAGEOS II and the perigee of LAGEOS II in view of their close connection to the measurement of the Lense-Thirring effect. The perturbative scheme adopted is that based on the Lagrange' s planetary equations [1, 35, 36, 37].

An evaluation from first principles of the amplitudes, the periods and the initial phases of the tidal perturbations on the nodes of LAGEOS and LAGEOS II and the perigee of LAGEOS II is useful, in the present context, for the following reasons.

• It allows one to point out which tidal constituents the Lense-Thirring shift is mainly sensitive to, so that people can focus the researches on them

• It allows one to get insight in how to update the orbit determination softwares. In this way the impact on the time series of those tidal constituents which will turn out to be more effective could be reduced along with the number of the parameters to be included in the least-squares solution

• For a given observational time span T_{obs} it allows one to find those constituents whose periods are longer than it and consequently may act like superimposed bias (e.g. the 18.6-year and 9.3-year zonal tides and the K_1 $l = 3$ $p = 1$ $q = -1$ ocean diurnal tide on the perigee of LAGEOS II) corrupting the detection of the gravitomagnetic shift. In these cases, if we know their amplitudes, periods and initial phases we could fit and remove them from the time series[5] or, at least, it should be possible to assess the mismodelling level induced by them on the detection of the Lense-Thirring trend. So, also these estimates can be included in the final error budget. (See section 4)

• It can be used as starting point for numerical simulations of the combined residual data in order to check, e. g., the impact of the diurnal (m=1) and semidiurnal (m=2) tidal perturbations (not cancelled out by the Ciufolini' s observable), as done in section 4

The section is organized as follows. In subsect. 2 the essential features of the tide generating potential, from which the tidal forces are traditionally derived, are reviewed.

The solid Earth tidal perturbations are worked out in subsect. 3. An evaluation of their mismodelling and a comparison with the Lense-Thirring perturbations on the nodes of LAGEOS and LAGEOS II and the perigee of LAGEOS II over 4 years are also presented.

Subsect. 4-5 are devoted to the orbital perturbations due to the ocean tides and their mismodelling in connection with the Lense-Thirring drag. They are treated in detail because the ocean tides are known less accurately than the solid ones, so that the impact of their mismodelling on the gravitomagnetic trend is more relevant.

Subsect. 6 is devoted to the conclusions.

3˙2. *The tide generating potential*. – On the scale of the Earth's dimensions the gravitational field of any not too far astronomical body B cannot be considered uniform so that the various points of our planet are acted upon by a differential gravitational pull in the external field of B. This is the origin of the Earth's solid, ocean and atmospheric tides, mainly due to the Moon and the Sun. It is customary to derive the tidal forces acting on a point on the Earth' s surface from the so called tide generating potential

---

[5] If the period of the disturbing harmonic, assumed to be known, is shorter than the time series length the perturbation can be viewed as an empirically fit quantity. But if its period is longer than the time series length it is not possible to fit and remove the harmonic from the data without removing also the true trend, unless we know the initial phase.

which, in its most general form, for a perturbing body B can be written as [38, 39, 20]

$$\Phi_B = \frac{GM_B}{d_B} \sum_{l=2}^{\infty} \left(\frac{r}{d_B}\right)^l P_l(\cos z) =$$

$$(46) \qquad = \frac{3}{4} GM_B \frac{R^2}{c_B^3} \left(\frac{r}{R}\right)^2 \left(\frac{c_B}{d_B}\right)^3 \left[\frac{4}{3} P_2(\cos z) + \frac{4}{3}\frac{r}{d_B} P_3(\cos z) + ... \right].$$

In eq. (46) the following quantities appear
  • R mean Earth' s equatorial radius
  • M_B mass of the perturbing body
  • d_B instantaneous distance between the Earth and the perturbing body B
  • r distance between the center of mass of the Earth and a point on its surface
  • $P_l(x)$ Legendre polynomials of degree l

$$(47) \qquad P_l(x) = \frac{(-1)^l}{l!2^l} \frac{d^l}{dx^l}(1 - x^2)^l$$

  • z geocentric zenithal distance of the perturbing body
  • c_B mean distance between the Earth and the perturbing body
  The factor

$$(48) \qquad \frac{3}{4} GM_B \frac{R^2}{c_B^3} \left(\frac{r}{R}\right)^2$$

is often rewritten as

$$(49) \qquad D_B(r) = \frac{M_B}{M_M} \frac{c_M^3}{c_B^3} D(r),$$

with

$$(50) \qquad D(r) = \frac{3}{4} GM_M \frac{R^2}{c_M^3} \left(\frac{r}{R}\right)^2 = D_1 \left(\frac{r}{R}\right)^2$$

in which

$$(51) \qquad D_1 = \frac{3}{4} GM_M \frac{R^2}{c_M^3}$$

is the Doodson constant for the Moon, having the dimension of an energy per unit mass, and M_M is the Moon's mass. Thus the tide generating potential outside of the Earth Φ_B^l is a harmonic function of degree l and can be written in the form $\Phi_B^l = r^l Y_l(\phi, \lambda)$ where $Y_l(\phi, \lambda)$ is a surface harmonic, with ϕ and λ the terrestrial latitude and East longitude. At the Earth's surface it becomes $\Phi_B^l(\mathbf{R}) = (R/r)^l \Phi_B^l(\mathbf{r})$.

   It is useful to express eq. (46) in terms of the geocentric equatorial coordinates $\{\phi, \delta_B, H_B\}$ of an Earth-fixed frame where
  • δ_B declination of the perturbing body
  • H_B hour angle of the perturbing body

This can be done by means of the following spherical trigonometric formula

$$(52) \qquad \cos z = \sin \phi \sin \delta_B + \cos \phi \cos \delta_B \cos H_B.$$

The result is the Laplace's tidal development: it consists of a sum of terms each of which is the product of a factor depending only on the latitude of a given place on the Earth (the geodetic coefficient) and a time-dependent factor which depends on the astronomical coordinates δ_B and H_B of the perturbing body. E.g., the term of degree $l = 2$ becomes

$$\Phi_B^2 = D_B(r) \left(\frac{c_B}{d_B} \right)^3 \left[\left(\frac{1 - 3\sin^2 \phi}{2} \right) \left(\frac{1}{3} - \sin^2 \delta_B \right) + \right.$$

$$(53) \qquad \left. + \sin 2\phi \sin 2\delta_B \cos H_B + \cos^2 \phi \cos^2 \delta_B \cos 2H_B \right].$$

In this sum the quantities c_B/d_B, δ_B, H_B exhibit a very complex behavior in time due to the astronomical motions of the perturbing body B. They must be carefully expanded in periodic components in order to obtain an expression for the tidal potential as a sum of harmonic terms. This can be done by using the ephemerides tables for the perturbing bodies. Obviously, the most relevant are the Moon and the Sun. Since the ephemerides refer to the ecliptic and not to the celestial equator, it is necessary to express δ_B and H_B in terms of ecliptical coordinates. Spherical trigonometry gives

$$(54) \qquad \sin \delta_B = \sin \varepsilon \cos \beta_B \sin \lambda_B + \cos \varepsilon \sin \lambda_B,$$

$$(55) \quad \cos \delta_B \cos H_B = \cos \beta_B \cos \lambda_B \cos \theta + (\cos \varepsilon \cos \beta_B \sin \lambda_B - \sin \varepsilon \sin \beta_B) \sin \theta,$$

where
- ε inclination of the ecliptic to the celestial equator
- λ_B, β_B ecliptical longitude and latitude of the perturbing body, respectively
- θ sidereal time

The lunar and solar ephemerides express d_B, λ_B, β_B in terms of time-dependent series of sines and cosines whose arguments are linear combinations of the mean Lunar time τ and other astronomical quantities of the Moon and the Sun ([6]). Among them the most useful are the mean ecliptical lunisolar variables s, h, p, N', p_s [38]. They are
- s mean ecliptical longitude of the Moon with period $P_s = 27.32$ days
- h mean ecliptical longitude of the Sun with period $P_h = 365.2422$ days
- p mean ecliptical longitude of the Moon's perigee with period $P_p = 3,232$ days (8.84 years)
- $N' = -N$ mean ecliptical longitude of the Moon's node with the sign reversed, with period $P_N = 6,798.38$ days (18.61 years). The lunar node, moving in the Earth-fixed frame from East to West counterclockwise, is retrograde with respect to the other lunisolar longitudes
- p_s mean ecliptical longitude of the perihelion with period $P_{p_s} = 7.65 \times 10^6$ days (20,953 years)

([6]) The most recent developments take in account also the influence of other planets like Venus and Jupiter [47].

Putting eqs. (54)-(55) in the Laplace' s tidal development, with the ephemerides expansions for d_B, λ_B, β_B, allows one to obtain the harmonic expansion of the tide generating potential Φ_B [40, 41, 42, 43, 44, 45, 46, 47]. It consists of a sum of terms, the constituents, with sinusoidal time dependence where the sines and cosines have arguments involving linear combinations σt of the previously defined orbital longitudes of the Sun and the Moon

$$(56) \qquad \sigma t = j_1 \tau + j_2 s + j_3 h + j_4 p + j_5 N^{'} + j_6 p_s.$$

The circular frequency of the tidal bulge generated by the corresponding constituent, viewed in the terrestrial frame, is then given by

$$(57) \qquad \sigma \equiv 2\pi f = j_1 \dot{\tau} + j_2 \dot{s} + j_3 \dot{h} + j_4 \dot{p} + j_5 \dot{N}^{'} + j_6 \dot{p}_s;$$

by considering that $\tau = \theta - s$, eq. (57) becomes

$$(58) \qquad \sigma = j_1 \dot{\theta} + (j_2 - j_1)\dot{s} + j_3 \dot{h} + j_4 \dot{p} + j_5 \dot{N}^{'} + j_6 \dot{p}_s.$$

The coefficients j_k, $k = 1, ..., 6$ are small integers which can assume negative, positive or null values. The advantage of using such lunisolar ecliptical variables relies in the fact that they, over an interval of a century or so, are practically linear increasing with time. This feature will reveal itself very useful in integrating the equations for the orbital perturbations. Each tidal constituent is identified by the set of the six integers j_k, $k = 1, ..., 6$ arranged in the so called Doodson number

$$(59) \qquad j_1 (j_2 + 5)(j_3 + 5).(j_4 + 5)(j_5 + 5)(j_6 + 5).$$

In it the integer j_1 classifies the tides in long period or zonal ($j_1 = 0$), diurnal or tesseral ($j_1 = 1$) and semidiurnal or sectorial ($j_1 = 2$).

The tide generating potential is the cornerstone for every calculation of tidal perturbations on the satellites' Keplerian orbital elements. Indeed, if the Earth, globally modeled as a nonrigid body, is acted upon by a tidal potential Φ_l harmonic in degree, it deforms itself giving rise, among other things, to a periodic redistribution of the masses within its volume. This deformation acts upon a point in the external space surrounding the Earth by means of an additional potential [48]

$$(60) \qquad \phi_l(\mathbf{r}) = k_l \left(\frac{R}{r}\right)^{l+1} \Phi_l(R) = k_l \left(\frac{R}{r}\right)^{2l+1} \Phi_l(r)$$

where k_l is one of the so called Love numbers (they will be defined precisely in the following sections). A close orbiting satellite is perturbed by such an additional potential and senses the global effect of the solid and fluid mass redistribution in the Earth. This means that if one wish to employ a pool of satellites in order to recover the tidal parameters, like the Love numbers, entering the tidal perturbations and wants to use the so obtained values to predict the perturbations on some particular satellite, he or she must be very careful. Indeed, such values are aliased by the whole of the effects sensed by the measuring satellites; it is as if they would be "tailored" for the satellites used in their recovery. So, these "effective" tidal parameters neither can be directly compared to those measured on the Earth's surface or predicted by any theoretical model and

related to the physical properties of the Earth, nor can be used in calculating *a priori* the tidal perturbations on the satellites of interest for some particular application, as is the case for the detection of the Lense-Thirring effect. Differently stated, when the tidal perturbations are to be predicted for a given satellite, it is incorrect to use for it the "effective" values of the geophysical parameters recovered by other satellites. It is so customary to split the analytical expressions of the tidal perturbations into a part due to the solid Earth tides and another one which accounts for the effects of the oceans [49]. After this step, their effects on the satellite of interest must be analytically predicted using for the various parameters the values theoretically calculated or measured in such a way that they reflect the effective Earth's properties.

3˙3. *Solid Earth tidal perturbations*. – Concerning the solid Earth tides [50], as in [35, 51], the starting point is the frequency-dependent model of [52]. It is based on the assumption of a perfectly elastic, hydrostatically prestressed, ellipsoidal rotating Earth acted upon by the lunisolar tidal potential. The interior of our planet is thought to be made of a solid inner core, a fluid outer core, and a solid mantle capped by a thin continental crust, without oceans and atmosphere. Substantially, the Earth is thought as a set of coupled harmonic oscillators showing a variety of resonant frequencies, the normal modes, which can be excited by the external forcing constituents of the tide generating potential [53].

The expansion adopted for it is that of Cartwrigt and Tayler in [41] in terms of harmonic constituents of degree l, order m and circular frequency σ

$$(61) \qquad \Phi = g \sum_{l=2}^{\infty} \sum_{m=0}^{l} \left(\frac{r}{R}\right)^l Y_l^m(\phi, \lambda) \sum_f H_l^m(f) e^{i(\sigma t + c_{lm})}.$$

Only the real part of eq. (61) has to be retained. The quantities entering eq. (61) are
- Y_l^m spherical harmonics

$$(62) \qquad Y_l^m(\phi, \lambda) = \sqrt{\frac{2l+1}{4\pi} \frac{(l-m)!}{(l+m)!}} P_l^m(\sin \phi) e^{im\lambda},$$

in which the Condon-Shortley phase factor $(-1)^m$ has been neglected in order to compare our results to those of [51]
- $H_l^m(f)$ coefficients of the harmonic expansion. They contain the lunisolar ephemerides information and define the modulus of the vertical shift V/g in the equipotential surface at the Earth's surface for $r = R_\oplus$ with respect to the case in which only proper Earth's gravity is considered. The values used in the present calculation are those recently released in [47] using the ELP2000-85 series for the ecliptical coordinates of the Moon [54] and the VSOP87 series for those of the Sun [55]. Their accuracy is of the order of 10^{-7} m. In order to use them in place of the coefficients of [42], which have a different normalization, a multiplication for a suitable conversion factor [56] has been performed. Due to the extreme smallness of the $H_l^m(f)$ for $l \geq 3$, in the following summations only the term of degree $l = 2$ are to be considered
- c_{lm} additive constant. It is equal to $-\pi/2$ in order to generate sines for the $l - m$ odd constituents, while it is equal to 0 in order to yield cosines for the $l - m$ even constituents.

The Earth free space potential under the action of the tidal constituent of degree l, order m and circular frequency σ, dropping the time dependence due to $e^{i\sigma t}$, can be written as

$$(63) \qquad \phi_l^m = Re\ gH_l^m \left[k_{lm}^{(0)} \left(\frac{R}{r} \right)^{l+1} Y_l^m + k_{lm}^+ \left(\frac{R}{r} \right)^{l+3} Y_{l+2}^m \right],$$

in which

• r distance from the Earth's center of mass and a point in the space outside of the Earth

• The parameter

$$(64) \qquad k_{lm}^{(0)}(f) = \sqrt{k_{lm}^R(f)^2 + k_{lm}^I(f)^2},$$

is the modulus of the Love number k [48, 57] for a static, spherical Earth. In general, it is defined as the ratio of the free space gravitational potential $\phi(\mathbf{r})$, evaluated at the Earth's equator, and the tide generating potential $\Phi(\mathbf{r})$ calculated at the mean equatorial radius. If the rotation and non-sphericity of the Earth are accounted for, there are different values of k for any l, m and f. In general, they are evaluated by convolving, in the frequency domain, the tide generating potential with the transfer function for a non rigid Earth [58, 59]. There are several theoretical calculations for the Love numbers k [52, 60, 57, 56, 61]. They differ in the choice of the Earth's interior models [77, 63] adopted for the calculation of the transfer function and the departure from elasticity of the mantle's behavior. Particularly important is also if they account for, or not, the normal modes in the diurnal band. In eq. (64) the IERS conventions [56] have been used for $k_{lm}^{(0)}(f)$

$$(65) \qquad k_{lm}^I(f) = Im\ k_{lm} + \delta k_f^{anel},$$

$$(66) \qquad k_{lm}^R(f) = Re\ k_{lm} + \delta k_f^{el},$$

where $Im\ k_{lm}$ and $Re\ k_{lm}$ are the frequency-independent parts of Love numbers, and δk_f^{anel}, δk_f^{el} are the frequency-dependent corrections. They are important in the diurnal band, through δk_f^{el}, and in the zonal band with δk_f^{anel} due to the anelasticity of the mantle. The $k_{lm}^+(f)$ account for the rotation and ellipticity of our planet. In the present analysis for the latitude dependent Love numbers $k_{lm}^+(f)$ the values quoted in [61] have been adopted.

Neglecting, in this first step, their tiny contribution, the free space potential by means of which the Earth responds to the forcing lunisolar tidal potential can be written, in the time domain, as

$$(67) = \frac{GM}{R} \sum_{l=2}^{\infty} \sum_{m=0}^{l} \sqrt{\frac{2l+1}{4\pi} \frac{(l-m)!}{(l+m)!}} \frac{1}{r} \left(\frac{R}{r} \right)^l \times \sum_f k_{lm}^{(0)} H_l^m P_l^m(\sin\phi) \begin{bmatrix} \cos(\sigma t + m\lambda) \\ \sin(\sigma t + m\lambda) \end{bmatrix}.$$

Here and in the following, the upper expressions refer to $l - m$ even while the lower ones

refer to $l - m$ odd. Eq. (67) can be put into the form

$$(68) \qquad \phi = \frac{GM}{R} \sum_{l=2}^{\infty} \sum_{m=0}^{l} \frac{1}{r} \left(\frac{R}{r}\right)^l (C_{lm} \cos m\lambda + S_{lm} \sin m\lambda) P_l^m(\sin \phi),$$

in which, assuming temporarily for the sake of simplicity that the Love numbers are not frequency-dependent, the coefficients C_{lm} and S_{lm} are

$$(69) \qquad C_{lm} = A_{lm} k_{lm}^{(0)} \sum_{f} H_l^m \begin{bmatrix} \cos \sigma t \\ \sin \sigma t \end{bmatrix},$$

$$(70) \qquad S_{lm} = A_{lm} k_{lm}^{(0)} \sum_{f} H_l^m \begin{bmatrix} -\sin \sigma t \\ \cos \sigma t \end{bmatrix},$$

with

$$(71) \qquad A_{lm} = \sqrt{\frac{2l+1}{4\pi} \frac{(l-m)!}{(l+m)!}}.$$

The C_{lm} and S_{lm} have the dimensions of lengths. Eq. (68) is formally equal to the well known expression of the static geopotential worked out by Kaula in ref.[1]

$$(72) \qquad \phi = \frac{GM}{r} \left\{ 1 + \sum_{l=2}^{\infty} \sum_{m=0}^{l} \left(\frac{R}{r}\right)^l P_{lm}(\sin \phi)[C_{lm} \cos m\lambda + S_{lm} \sin m\lambda] \right\}.$$

By means of the transformation

$$(73) \qquad \frac{1}{r} \left(\frac{R}{r}\right)^l P_l^m(\sin \phi) e^{im\lambda} = \frac{1}{a} \left(\frac{R}{a}\right)^l \sum_{p=0}^{l} F_{lmp}(i) \sum_{q=-\infty}^{+\infty} G_{lpq}(e) \begin{bmatrix} e^{i\psi_{lmpq}} \\ -ie^{i\psi_{lmpq}} \end{bmatrix},$$

with

$$(74) \qquad \psi_{lmpq} = (l - 2p)\omega + (l - 2p + q)\mathcal{M} + m(\Omega - \theta),$$

it can be cast into the familiar form

$$(75) \qquad \phi = \frac{GM}{R} \sum_{l=2}^{\infty} \sum_{m=0}^{l} \frac{1}{a} \left(\frac{R}{a}\right)^l \sum_{p=0}^{l} \sum_{q=-\infty}^{+\infty} F_{lmp}(i) \, G_{lpq}(e) S_{lmpq}(\omega, \, \Omega, \mathcal{M}, \, \theta),$$

where $F_{lmp}(i)$ and $G_{lpq}(e)$ are the inclination and eccentricity functions respectively [1]. The S_{lmpq} is given by

$$(76) \qquad S_{lmpq} = \begin{bmatrix} C_{lm} \\ -S_{lm} \end{bmatrix} \cos \psi_{lmpq} + \begin{bmatrix} S_{lm} \\ C_{lm} \end{bmatrix} \sin \psi_{lmpq}.$$

Eq. (76) in our case becomes

$$(77) \qquad S_{lmpq} = A_{lm} k_{lm}^{(0)} \sum_f H_l^m \cos(\sigma t + \psi_{lmpq}).$$

It is worthwhile noting that eq. (73) expresses a transformation of coordinates from the geocentric equatorial frame rotating with the Earth to the geocentric inertial frame $K\{x, \ y, \ z\}$. This fact will reveal itself of paramount importance in evaluating the frequencies of the tidal perturbations on the Keplerian elements.

Up to now the response of the Earth to the forcing tidal potential has been considered as perfectly elastic; if it had been so, there would be no delay between the Earth's tidal bulge and the Moon in the sense that when the latter passes at the observer's meridian, say, at A the tidal bulge reaches A at exactly the same time. The reality is quite different since complicated mechanisms of energy dissipation in the interior of the Earth [64] makes its response to depart from the perfectly elastic behavior previously sketched. A phase lag with respect to the external lunisolar potential must be introduced in the sense that the tidal bulge reaches the observer's meridian at A after a certain time Δt with respect to the passage at A of Moon. It is generally assumed that it is the Earth's mantle to exhibit an anelastic behavior at the various frequencies of the tide generating potential; this topic is not yet well understood, but if one wants to account for the phase lag introduced by it, he or she has to adopt complex frequency-dependent Love numbers [57]. In order to give a quantitative estimation also of the lag angle it has been decided to adopt the values of ref.[57] quoted in ref.[56]; indeed, the authors of ref.[61] do not quote the imaginary part of $k_{lm}^{(0)}(f)$ and the discrepancies with their values for $\left| k_{lm}^{(0)}(f) \right|$ amount to only 0.1 %. Moreover, concerning the effects of mantle's anelasticity, the results of ref.[61] are not less uncertain than the other ones.

An equivalent form of eq. (69) and eq. (70), for a single constituent of frequency σ, which reveals useful in handling with complex quantities is

$$(78) \qquad C_{lmf} - iS_{lmf} = \eta A_{lm} k_{lm}^{(0)} H_l^m(f) e^{i\sigma t},$$

with $\eta = -i$ if $l - m$ is odd and $\eta = 1$ if $l - m$ is even. If the anelasticity of the Earth's mantle is to be accounted for writing $k_{lm}^{(0)}(f) = k_{lm}^R(f) + ik_{lm}^I(f)$, eq. (78) becomes

$$C_{lmf} - iS_{lmf} = \eta A_{lm} H_l^m(f) \times \left[(k_{lm}^R \cos\sigma t - k_{lm}^I \sin\sigma t) + \right.$$

$$(79) \qquad \left. + i(k_{lm}^R \sin\sigma t + k_{lm}^I \cos\sigma t) \right],$$

or

$$(80) \qquad C_{lm} = A_{lm} \sum_f H_l^m \begin{bmatrix} k_{lm}^R \cos\sigma t - k_{lm}^I \sin\sigma t \\ k_{lm}^R \sin\sigma t + k_{lm}^I \cos\sigma t \end{bmatrix},$$

$$(81) \qquad S_{lm} = A_{lm} \sum_f H_l^m \begin{bmatrix} -k_{lm}^R \sin\sigma t - k_{lm}^I \cos\sigma t \\ k_{lm}^R \cos\sigma t - k_{lm}^I \sin\sigma t \end{bmatrix},$$

If eq. (80) and eq. (81) are put into eq. (76), it is straightforward to obtain for it

$$(82) \qquad S_{lmpq} = A_{lm} \sum_f H_l^m k_{lm}^{(0)}(f) \cos(\sigma t + \psi_{lmpq} - \delta_{lmf}),$$

with

$$(83) \qquad k_{lm}^{(0)}(f) = \sqrt{k_{lm}^R(f)^2 + k_{lm}^I(f)^2},$$

$$(84) \qquad \tan \delta_{lmf} = \frac{k_{lm}^I(f)}{k_{lm}^R(f)}.$$

The factor δ_{lmf} is the phase lag of the response of the solid Earth with respect to the tidal constituent of degree l, order m and circular frequency σ induced by the anelasticity in the mantle: notice that if $k_{lm}^I(f) = 0$, also $\tan \delta_{lmf} = 0$. An inspection of the values quoted in [56] shows that, at the low frequencies of the zonal constituents of the tide generating potential, the role played by the mantle's anelasticity is more relevant than in the diurnal and semidiurnal bands. Indeed, while for the tesseral and sectorial tides one finds $k_{21}^I = -0.00144$ and $k_{22}^I = -0.00130$ for all the frequencies, in the zonal band $k_{20}^I(f)$ varies from -0.00541 to -0.00192.

Eq. (75), with the S_{lmpq} given by eq. (82), is the dynamical, non-central part of the geopotential due to the response of the solid Earth to the forcing lunisolar tidal action. In the linear Lagrange equations of perturbation theory for the rates of change of the Keplerian elements it can play the role of the perturbative term $\mathcal{R}$. It is an observed fact that the secular motions are the dominant perturbation in the elements ω, Ω, $\mathcal{M}$ of geodetically useful satellites. So, taking as constants a, e, i and consider as linearly variable in time ω, Ω, $\mathcal{M}$ and θ, apart from σt, the following expressions, at first order, may be worked out

$$\Delta \Omega_f = \frac{g}{na^2 \sqrt{1 - e^2} \sin i} \sum_{l=0}^{\infty} \sum_{m=0}^{l} \left(\frac{R}{r}\right)^{l+1} \times$$

$$(85) \qquad \times A_{lm} \sum_{p=0}^{l} \sum_{q=-\infty}^{+\infty} \frac{dF_{lmp}}{di} G_{lpq} \frac{1}{f_p} k_{lm}^{(0)} H_l^m \sin \gamma_{flmpq},$$

$$\Delta \omega_f = \frac{g}{na^2 \sqrt{1 - e^2}} \sum_{l=0}^{\infty} \sum_{m=0}^{l} \left(\frac{R}{r}\right)^{l+1} \times$$

$$(86) \quad \times A_{lm} \sum_{p=0}^{l} \sum_{q=-\infty}^{+\infty} \left[\frac{1 - e^2}{e} F_{lmp} \frac{dG_{lpq}}{de} - \frac{\cos i}{\sin i} \frac{dF_{lmp}}{di} G_{lpq}\right] \frac{1}{f_p} k_{lm}^{(0)} H_l^m \sin \gamma_{flmpq},$$

with

$$(87) \qquad \gamma_{flmpq} = (l - 2p)\omega + (l - 2p + q)\mathcal{M} + m(\Omega - \theta) + \sigma t - \delta_{lmf},$$

(88) $$f_p = (l - 2p)\dot{\omega} + (l - 2p + q)\dot{\mathcal{M}} + m(\dot{\Omega} - \dot{\theta}) + \sigma.$$

The indirect, second order effects due to the oblateness of the Earth [65] have been neglected in this section. Due to the secular trend of the Lense-Thirring effect, only the perturbations whose periods are much longer than those of the orbital satellites motions, which, typically, amount to a few hours, are to be considered. This implies that in such terms the rate of the mean anomaly does not appear and the condition

(89) $$l - 2p + q = 0$$

must hold. Moreover, if the effect of Earth's diurnal rotation, which could introduce periodicities of the order of 24 hours, is to be neglected, one must retain only those terms in which the non-negative multiplicative coefficient j_1 of the Greenwich sidereal time in σt coincides to the order m of the tidal constituent considered: in this way in f_p the contributions of $\dot{\theta}$ are equal and opposite, and cancel out. With these bounds on l, m, p and q the circular frequencies of the perturbations of interest become

(90) $$f_p = \dot{\Gamma}_f + (l - 2p)\dot{\omega} + m\dot{\Omega}$$

in which

(91) $$\dot{\Gamma}_f = (j_2 - m)\dot{s} + j_3\dot{h} + j_4\dot{p} + j_5\dot{N}' + j_6\dot{p}_s.$$

In the performed calculation only the degree $l = 2$ constituents have been considered due to the smallness of the $k_{3m}^{(0)}$ and $H_3^m(f)$. For $l = 2$, p runs from 0 to 2, and so, in virtue of the condition $l - 2p + q = 0$, q assumes the values -2, 0, 2. From an inspection of the table of the eccentricity functions $G_{lpq}(e)$ in [1] it turns out that $G_{20-2} = G_{222} = 0$, while $G_{210} = (1 - e^2)^{-3/2}$. For this combination of l, p and q the condition $l - 2p = 0$ holds: the frequencies of the perturbations are, in this case, given by

(92) $$f_p = \dot{\Gamma}_f + m\dot{\Omega}.$$

Passing from σ to $\dot{\Gamma}_f + m\dot{\Omega}$, as previously noticed, is equivalent to leaving the Earth-fixed frame of reference for the inertial one, in which the relevant physical feature is the orientation of the tidal bulges with respect to the orbital plane of satellite. Indeed, $\dot{\Gamma}_f + m\dot{\Omega}$ could be considered as the relative frequency of motions of the tidal bulge and the orbital plane, both viewed in the inertial frame. $\dot{\Gamma}_f$ is the opposite of the inertial rate of the tidal bulge obtained from the Earth-fixed one subtracting the Earth's rotation rate $\dot{\theta}$ times m in order to account for the symmetry of the bulges. The periodicities introduced in the perturbations by eq. (92) are, in general, much longer that the ones present in the tidal potential because, while the latter are dominated by $j_1\dot{\theta}$ due to the rotation of the Earth-fixed frame, the former are mainly determined by the precessional rates $m\dot{\Omega}$ of the orbital frames of the different satellites in the inertial frame. This explain the major variety of periodicities in the orbital elements' perturbations of the near-Earth's satellites with respect to the tides sensed by an observer on the Earth surface which are mainly concentrated in the diurnal and semidiurnal bands. In eqs. (85)-(86) it is worthwhile noting that the amplitudes of the perturbations are inversely proportional to the frequency of the perturbation f_p. This implies that some tidal constituent which in the Earth-fixed frame has an high frequency, in the inertial frame may induce relevant

perturbations because its frequency greatly decreases; this fact could compensate an eventual small value of its coefficient in the harmonic expansion of the tide generating potential (calculated in the terrestrial frame). In other words, constituents which on the Earth's surface would produce small tides may become important in perturbing the orbits of near-Earth' s satellites due to the changes in their frequencies when viewed in the inertial frame.

3˙4. *Discussion of the numerical results.* – In view of their direct implication in eq. (5), in the following we shall focus our attention to the nodes of LAGEOS and LAGEOS II and the perigee of LAGEOS II. In Table I, Table II, and Table III the results for them are shown; since the observable quantity for ω is $ea\dot\omega$ [14], the calculation for the perigee of LAGEOS, due to the notable smallness of the eccentricity of its orbit, have not been performed.

TABLE I. – *Perturbative amplitudes on the node Ω of LAGEOS due to solid Earth tides for $l = 2$, $p = 1$, $q = 0$. In the first column the Doodson number of each constituent is quoted followed by the Darwin's name, when it is present. The tidal lines are listed in order of decreasing periods. The coefficients $H_l^m(f)$ are those recently calculated by Roosbeek and multiplied by suitable normalization factors (IERS standards) in order to make possible a comparison with those of Cartwright and Edden. $\tan\delta_{lmf}$ expresses the phase lag of the solid Earth response with respect to the tidal potential due to the anelasticity in the mantle. The periods are in days, the amplitudes in mas and the $H_l^m(f)$ in meters.*

Tide	Period	Amplitude	k_2 Love number	$H_l^m(f)$	$\tan\delta_{lmf}$
055.565	6,798.38	-1,079.38	0.315	0.02792	-0.01715
055.575	3,399.19	5.23	0.313	0.000272	-0.015584
056.554 S_a	365.27	9.96	0.307	-0.00492	-0.01135
057.555 S_{sa}	182.62	31.21	0.305	-0.03099	-0.01029
065.455 M_m	27.55	5.28	0.302	-0.03518	-0.00782
075.555 M_f	13.66	4.94	0.301	-0.06659	-0.007059
165.545	1232.94	-41.15	0.259	-0.007295	-0.00554
165.555 K_1	1,043.67	1,744.38	0.257	0.3687012	-0.0055933
165.565	904.77	203.02	0.254	0.050028	-0.005653
163.555 P_1	-221.35	136.44	0.286	-0.12198	-0.005017
145.555 O_1	-13.84	19	0.297	-0.26214	-0.00484
135.655 Q_1	-9.21	2.42	0.297	-0.05019	-0.00483
274.556	-1,217.55	1.68	0.301	0.000625	-0.00431
274.554	-1,216.73	-6.63	0.301	-0.00246	-0.00431
275.555 K_2	521.835	-92.37	0.301	0.0799155	-0.00431
273.555 S_2	-280.93	182.96	0.301	0.2940	-0.00431
272.556 T_2	-158.80	6.04	0.301	0.0171884	-0.00431
255.555 M_2	-14.02	19.63	0.301	0.6319	-0.00431
245.655 N_2	-9.29	2.49	0.301	0.12099	-0.00431

TABLE II. – *Perturbative amplitudes on the node Ω of LAGEOS II due to solid Earth tides for $l = 2$, $p = 1$, $q = 0$. In the first column the Doodson number of each constituent is quoted followed by the Darwin's name, when it is present. The tidal lines are listed in order of decreasing periods. The coefficients $H_l^m(f)$ are those recently calculated by Roosbeek and multiplied by suitable normalization factors (IERS standards) in order to make possible a comparison with those of Cartwright and Edden. $\tan \delta_{lmf}$ expresses the phase lag of the solid Earth response with respect to the tidal potential due to the anelasticity in the mantle. The periods are in days, the amplitudes in mas and the $H_l^m(f)$ in meters.*

Tide	Period	Amplitude	k_2 Love number	$H_l^m(f)$	$\tan \delta_{lmf}$
055.565	6,798.38	1,982.16	0.315	0.02792	-0.01715
055.575	3,399.19	-9.61	0.313	-0.000272	-0.015584
056.554 S_a	365.27	-18.28	0.307	-0.00492	-0.01135
057.555 S_{sa}	182.62	-57.31	0.305	-0.03099	-0.01029
065.455 M_m	27.55	-9.71	0.302	-0.03518	-0.00782
075.555 M_f	13.66	-9,08	0.301	-0.06659	-0.007059
165.565	-621.22	-58.31	0.254	0.050028	-0.005653
165.555 K_1	-569.21	-398	0.257	0.3687012	-0.0055933
165.545	-525.23	7.33	0.259	-0.007295	-0.005541
163.555 P_1	-138.26	35.65	0.286	-0.1219	-0.005017
145.555 O_1	-13.33	7.66	0.297	-0.26214	-0.00484
135.655 Q_1	-8.98	0.98	0.297	-0.05019	-0.00483
275.555 K_2	-284.6	-92.51	0.301	0.079915	-0.004318
274.556	-159.96	-0.40	0.301	0.000625	-0.00431
274.554	-159.95	1.6	0.301	-0.00246	-0.0043
273.555 S_2	-111.24	-133.04	0.301	0.29402	-0.00431
272.556 T_2	-85.27	-5.96	0.301	0.017188	-0.00431
255.555 M_2	-13.03	-33.05	0.301	0.6319	-0.004318
245.655 N_2	-8.84	-4.35	0.301	0.12099	-0.00431

TABLE III. – *Perturbative amplitudes on the perigee ω of LAGEOS II due to solid Earth tides for $l = 2$, $p = 1$, $q = 0$. In the first column the Doodson number of each constituent is quoted followed by the Darwin's name, when it is present. The tidal lines are listed in order of decreasing periods. The coefficients $H_l^m(f)$ are those recently calculated by Roosbeek and multiplied by suitable normalization factors (IERS standards) in order to make possible a comparison with those of Cartwright and Edden. $\tan\delta_{lmf}$ expresses the phase lag of the solid Earth response with respect to the tidal potential due to the anelasticity in the mantle. The periods are in days, the amplitudes in mas and the $H_l^m(f)$ in meters.*

Tide	Period	Amplitude	k_2 Love number	$H_l^m(f)$	$\tan\delta_{lmf}$
055.565	6,798.38	-1,375.58	0.315	0.02792	-0.01715
055.575	3,399.19	6.66	0.313	-0.000272	-0.015584
056.554 S_a	365.27	12.69	0.307	-0.00492	-0.01135
057.555 S_{sa}	182.62	39.77	0.305	-0.03099	-0.01029
065.455 M_m	27.55	6.74	0.302	-0.03518	-0.00782
075.555 M_f	13.66	6.30	0.301	-0.06659	-0.007059
165.565	-621.22	290.43	0.254	0.050028	-0.005653
165.555 K_1	-569.21	1,982.14	0.257	0.3687012	-0.0055933
165.545	-525.23	-36.52	0.259	-0.007295	-0.005541
163.555 P_1	-138.26	-177.56	0.286	-0.1219	-0.005017
145.555 O_1	-13.33	-38.16	0.297	-0.26214	-0.00484
135.655 Q_1	-8.98	-4.92	0.297	-0.05019	-0.00483
275.555 K_2	-284.6	-88.19	0.301	0.079915	-0.004318
274.556	-159.96	-0.38	0.301	0.000625	-0.00431
274.554	-159.95	1.52	0.301	-0.00246	-0.0043
273.555 S_2	-111.24	-126.83	0.301	0.29402	-0.00431
272.556 T_2	-85.27	-5.68	0.301	0.017188	-0.00431
255.555 M_2	-13.03	-31.9	0.301	0.6319	-0.004318
245.655 N_2	-8.84	-4.15	0.301	0.12099	-0.00431

The tidal lines for which the analysis was performed have been chosen also in order to make a comparison with the perturbative amplitudes of the ocean tides based on the results of EGM96 gravity model [19] which will be shown in the next sections. It is interesting to notice that the periods of many of these tidal perturbations are almost equal to or longer than an year, a time interval in which their effect may alias the Lense-Thirring effect, if the observations are taken on a such temporal scale; indeed, only if the data were acquired on time intervals of the order of many years it should be possible to clearly resolve the action of these tidal lines with respect to the secular Lense-Thirring trend. And also in this case, it could remain the aliasing effect of the 18.6-year and 9.3-year tides. Up to now, in refs.[66, 15] the authors have analyzed the data acquired on a 4 years interval for a suitable combination of residuals showing that many tidal signals with periods shorter than it can be resolved by means of suitable fits.

The results presented in Table I, Table II and Table III can be compared to those of [35, 51]. See also [67]. In doing so it must be kept in mind that both these authors have neglected not only the contribution of k_{lm}^+ but also the anelasticity and the frequency dependence of the Love numbers $k_{lm}^{(0)}$. Moreover, Dow includes in his analysis also the indirect influences of the oblateness of the Earth for O_1, Q_1, M_2 and N_2. Obviously,

in their analyses the LAGEOS II is not present since it was launched only in 1992. Another important factor to be considered is the actual sensitivity in measurements of Ω and ω, in the sense that the eventual discrepancies between the present results and the other ones must be not smaller than the experimental error in the Keplerian elements if one wish to check the theoretical assumptions behind the different models adopted. Carpino has analyzed the inclination and the node of LAGEOS only. His value for the important zonal 18.6-year tide is -1087.24 mas, while Table I gives $-1,079.38$ mas; the difference amounts to 7.86 mas, the 0.72 % of the "elastic", frequency-independent Carpino's value. Considering that for the node Ω of LAGEOS the present accuracy is of the order of the mas, 7.86 mas could be in principle detected, allowing for a discrimination between the different models adopted in the calculation. For the K_1 tide, one of the most powerful constituent in perturbing the satellites' orbits, Table I quotes $1,744.38$ mas against 2144.46 mas of Carpino's result; the gap is 400.08 mas, the 18.6 % of Carpino. In the sectorial band, the present analysis quotes for the K_2 -92.37 mas and Carpino -97.54 mas; there is a difference of 5.17 mas, the 5.3 % of the Carpino's value. It must pointed out that there are other tidal lines for which the difference falls below the mas level, as is the case for the 9.3-year tide. As it could be expected, the major differences between the present "anelastic", frequency-dependent calculations and the other ones based on a single, real value for the Love number k_2 lie in the diurnal band: in it the contribution of anelasticity is not particularly relevant, but, as already pointed out, the elastic part of $k_{21}^{(0)}$ is strongly dependent on frequencies of the tidal spectrum. May be interesting to notice that when the calculation have been repeated with the same value $k_2 = 0.317$ adopted by Carpino, his results have been obtained again.

Another feature which characterizes this study is the calculation of the phase lag of the solid Earth' s response with respect to the tide generating potential. In Table I, Table II and Table III $\tan \delta_{lmf}$ is always negative and does not exceed 10^{-2} in absolute value showing that the response of the Earth is slightly retarded with respect to the forcing lunisolar tidal potential. In absolute value, $\tan \delta_{20f}$ is greater than $\tan \delta_{21f}$ and $\tan \delta_{22f}$ of one order of magnitude, confirming that the behavior of the solid Earth's response is more influenced by the anelasticity in the zonal band that in the diurnal and semidiurnal ones.

Up to now the effects induced by the Earth's flattening and the Earth's rotation have been neglected. If they have to be analyzed it is necessary to take in eq. (63) the part

$$(93) \qquad Re \; g \sum_{l=2}^{\infty} \sum_{m=0}^{l} \sum_{f} H_l^m(f) \left(\frac{R}{r}\right)^{l+3} k_{lm}^+(f) Y_{l+2}^m(\phi, \lambda)$$

and work out it in the same manner as done for the spherical non-rotating Earth's contribution. In applying the transformation to the orbital elements given by eq. (73) one has to substitute everywhere l with $l + 2$. So the equations for the perturbations on the node and the perigee become

$$\Delta\Omega_f^+ = \frac{g}{na^2\sqrt{1-e^2}\sin i} \sum_{l=0}^{\infty} \sum_{m=0}^{l} \left(\frac{R}{r}\right)^{l+3} A_{l+2\ m} H_l^m \times$$

$$(94) \qquad \times k_{lm}^+ \frac{1}{f_p} \sum_{p=0}^{l} \sum_{q=-\infty}^{+\infty} \frac{dF_{l+2\ mp}}{di} G_{l+2\ pq} \sin \gamma_{fl+2\ mpq},$$

$$\Delta \omega_f^+ = \frac{g}{na^2 \sqrt{1-e^2}} \sum_{l=0}^{\infty} \sum_{m=0}^{l} \left(\frac{R}{r} \right)^{l+3} A_{l+2\ m} k_{lm}^+ H_l^m \frac{1}{f_p} \times$$

$$(95) \quad \times \sum_{p=0}^{l} \sum_{q=-\infty}^{+\infty} \left[\frac{1-e^2}{e} F_{l+2\ mp} \frac{dG_{l+2\ pq}}{de} - \frac{\cos i}{\sin i} \frac{dF_{l+2\ mp}}{di} G_{l+2\ pq} \right] \sin \gamma_{fl+2\ mpq}.$$

The corrections induced by the Earth's flattening and rotation, due to the smallness of k_{lm}^+, have been calculated only for those tidal lines which turned out to be the most effective in perturbing the node and the perigee of LAGEOS and LAGEOS II, i.e. the zonal 18.6-year tide and the K_1. Adopting the values quoted in ref.[61] for k_{lm}^+ and eqs. (94)-(95) it is possible to obtain the results summarized in Table IV. The quoted values,

TABLE IV. – *Corrections, in mas, to the Earth solid tidal perturbations on the nodes of LAGEOS and the perigee of LAGEOS II due to the Earth's flattening and Earth's rotation for $l = 2$, $p = 2$, $q = 0$. The values adopted for k_{2m}^+ are those quoted in ref.[61].*

Tide	$\Delta\Omega_{\text{LAGEOS}}$	$\Delta\Omega_{\text{LAGEOS II}}$	$\Delta\omega_{\text{LAGEOS II}}$	k_{2m}^+
055.565	0.43	1.28	0.19	-0.00094
165.555 K_1	-0.97	-9.49	0.85	-0.00074

with the exception of the node of LAGEOS II, fall below the mas level turning out, at the present, undetectable.

3˙5. *The mismodelling in the nodes and the perigee.* – Concerning the errors in the values released in Table I, Table II, and Table III, the major source of uncertainty in the perturbative amplitudes lies in the Love numbers $k_{2m}^{(0)}(f)$. and the orbital injection errors δi affecting the inclination i.

About the latter, by assuming $\delta i = 0.5$ mas [68], we have calculated $\left| \frac{\partial A(\Omega)}{\partial i} \right| \delta i$ and $\left| \frac{\partial A(\omega)}{\partial i} \right| \delta i$ for 055.565, K_1, and S_2 which are the most powerful tidal constituents in perturbing LAGEOS and LAGEOS II orbits. The results are of the order of 10^{-6} mas, so that we can neglect the effect of uncertainties in the inclination determination.

Concerning the Love numbers $k_{2m}^{(0)}(f)$, from a preliminary point of view, theoreticians claim that they are able to compute them with an accuracy of 10^{-4} using the specified Earth model. But the Earth models may differ. Probably uncertainty in Earth models may bring errors in computation of the Love numbers of the second order about 10^{-3} (L. Petrov, private communication, 1999). First of all, this means that the level of accuracy of 1 mas, i.e. 10^{-9} rad, on Ω and ω given by eq. (85) and eq. (86) can be well reached, since the uncertainty in $H_l^m(f)$ amounts to 10^{-7} m. Second, assuming a mean value of 0.3 for k_2, it can be stated that the uncertainty in the solid Earth tidal perturbation due to a single tide generating potential's constituent amount to almost 0.3 % for Ω and ω.

More specifically, we have assessed the uncertainties in them by calculating for certain tidal constituents the factor $\delta k_2/k_2$; k_2 is the average on the values released by the most reliable models and δk_2 is its standard deviation. According to the recommendations of the Working Group of Theoretical Tidal Model of the Earth Tide Commission (**http://www.astro.oma.be/D1/EARTH_TIDES/wgtide.html**), in the diurnal band we have chosen the values released in refs.[57, 56] and the two sets of ref.[61]. For the zonal and sectorial bands we have included also the results of ref.[60]. The uncertainties calculated in the Love numbers k_2 span from 0.5% to 1.5% for the tides of interest. However, it must be noticed that the worst known Love numbers are those related to the zonal band of the tidal spectrum due to the uncertainties in the anelasticity of the Earth' s mantle. These results have been obtained in order to calculate the mismodelled amplitudes of the solid tidal perturbations $\delta\Omega^{\mathrm{I}}$, $\delta\Omega^{\mathrm{II}}$ and $\delta\omega^{\mathrm{II}}$ for the nodes of LAGEOS and LAGEOS II and the perigee of LAGEOS II; they have been subsequently compared with the gravitomagnetic precessions over 4 years $\Delta\Omega^{\mathrm{I}}_{\mathrm{LT}} = 124$ mas, $\Delta\Omega^{\mathrm{II}}_{\mathrm{LT}} = 126$ mas and $\Delta\omega^{\mathrm{II}}_{\mathrm{LT}} = -228$ mas. In Table V we have quoted only those tidal lines whose mismodelled perturbative amplitudes are greater than 1% of the gravitomagnetic perturbations. It turns out that only 055.565 18.6-year and K_1 exceed this cutoff.

TABLE V. – *Mismodeled solid tidal perturbations on the nodes Ω of LAGEOS and LAGEOS II and the perigee ω of LAGEOS II compared to their gravitomagnetic precessions over 4 years $\Delta\Omega^{\mathrm{I}}_{\mathrm{LT}} = 124$ mas $\Delta\Omega^{\mathrm{II}}_{\mathrm{LT}} = 126$ mas $\Delta\omega^{\mathrm{II}}_{\mathrm{LT}} = -228$ mas. Only those constituents which exceed the 1 % cutoff have been quoted. The ratios are in percent and the δX in mas.*

Tide	$\frac{\delta k_2}{k_2}$	$\delta\Omega^{\mathrm{I}}$	$\frac{\delta\Omega^{\mathrm{I}}}{\Delta\Omega^{\mathrm{I}}_{\mathrm{LT}}}$	$\delta\Omega^{\mathrm{II}}$	$\frac{\delta\Omega^{\mathrm{II}}}{\Delta\Omega^{\mathrm{II}}_{\mathrm{LT}}}$	$\delta\omega^{\mathrm{II}}$	$\frac{\delta\omega^{\mathrm{II}}}{\Delta\omega^{\mathrm{II}}_{\mathrm{LT}}}$
055.565	1.5	-16.5	13.3	30.3	24	-21	9.2
165.555 K_1	0.5	9	7.2	-2	1.6	10.2	4.4

3˙6. *Gravitational potential of the ocean Earth tides*. – One of the early attempts to explain the phenomenon of fluid tides [69] in its globality is the equilibrium theory [70, 20] by Newton. It is based on the assumption that at every time the free water surface of the oceans coincides exactly with the spheroidal equipotential surface at $r = R$ due to the combined action of the Earth's proper gravity and the lunisolar tidal potential. Differently stated, the oceanic tidal bulge at every instant coincides exactly with the envelope of the forces produced by the tide generating potential at the Earth's surface. At every tidal constituents $\Phi(f)$ corresponds an equilibrium partial tide η_f. Referring to eq. (61) it can be write

$$(96) \qquad \eta_f = \frac{\Phi_f(R)}{g} = A_{lm}H_l^m P_l^m(\sin\phi)\cos(\sigma t + m\lambda + c_{lm}).$$

For $l = 2$ and $m = 0$ eq. (96) represents a standing wave which crests at $t = 0$, while for $l = 2$ and $m = 1, 2$ it refers to running waves around the oceans from East to West. If the equilibrium theory had been valid, it would mean that the water masses acted upon by the tidal potential are deprived almost entirely of their inertia in the sense that they would adapt instantaneously to their equilibrium positions on the equipotential surface which, in fact, changes in time at the frequencies of the lunisolar tidal potential. The

reality is quite different, because of the complex hydrodynamical behavior of the oceans; at every equilibrium partial tide η_f corresponds an effective partial tide [71]

$$(97) \qquad \zeta_f = \xi_f(\vartheta, \lambda) \cos \left[\sigma t - \delta_f(\vartheta, \lambda) \right],$$

where $\xi_f(\vartheta, \lambda)$ and $\delta_f(\vartheta, \lambda)$ [72] are defined as harmonic constants: $\xi_f(\vartheta, \lambda)$ is half the difference between high water and low water for a given place while $\delta_f(\vartheta, \lambda)$ is the phase lag of the ocean tide with respect to the equilibrium one when the phase of the latter is calculated at Greenwich meridian $\lambda = 0$: the delay at any other meridian is obtained simply adding $m\lambda$ to $\delta_f(\vartheta, \lambda)$. Moreover, ζ_f at every time $\bar{t}$ crests on the "cotidal" line $\sigma\bar{t} = \delta_f(\vartheta, \lambda)$; in general, referring to a given point (ϑ, λ), e.g., on the shoreline, the cotidal lines related to two consecutive instants may depart from the shore into the sea or vice versa, giving rise to outcoming and incoming waves with respect to that place.

Such departures from the equilibrium theory are due to several reasons. First of all, the fluid elements can freely flow and once they had been put in motion, their notable inertia prevent them to change instantaneously their state of motion making them stop at the equipotential surface. Second, dissipative phenomena and non-linear interactions among the various partial tides and other ocean currents must be taken in account. This implies that the response of the water masses to the forcing lunisolar potential presents a phase lag with respect to it: the sea surface is not an equipotential one so that tangential forces acts on the water particles generating tidal currents. The equilibrium theory may be considered an almost good approximation to the reality only at very low frequencies of the tidal potential, like as the Moon and the Sun would remain fix in the space with respect to the Earth.

The equations of motion governing the complex hydrodynamics of the tidal currents are the so called Lagrange Tidal Equations (LTE) [73, 74, 75, 76, 77], which, in general, are not linear. The simplest form for them is obtained considering a spherical, rotating Earth entirely covered by an ocean made of a perfect and incompressible fluid; if only the tangential motion is considered, neglecting the squares and the cross products of the velocity field's components, it is possible to obtain the following linearized LTE

$$(98) \qquad \frac{\partial v_\vartheta}{\partial t} = +2\omega_\oplus v_\lambda \cos \vartheta - \frac{g}{R} \frac{\partial(\zeta - \eta)}{\partial \vartheta},$$

$$(99) \qquad \frac{\partial v_\lambda}{\partial t} = -2\omega_\oplus v_\vartheta \cos \vartheta - \frac{g}{R \sin \vartheta} \frac{\partial(\zeta - \eta)}{\partial \lambda},$$

$$(100) \qquad \frac{\partial \zeta}{\partial t} = -\frac{1}{R \sin \vartheta} \left[\frac{\partial(h v_\lambda)}{\partial \lambda} + \frac{\partial(h \sin \vartheta \; v_\vartheta)}{\partial \vartheta} \right],$$

in which
ϑ terrestrial colatitude.
h depth of the ocean, $h = h(\vartheta, \lambda)$, m.
ζ non-equilibrium, ocean partial tide, m.
v_ϑ and v_λ tangential components of the water's velocity field.
The LTE are linear, and so each ocean partial tide ζ_f can be treated independently of the other ones. The fundamental problem of the ocean tides consists of the determination of the harmonic constants for every place on the Earth: this can be obtained, in principle, resolving the LTE for a given constituent, but this task is in many cases prohibitive due to the great calculational complexity needed to obtain realistic results. Another strategy consists of employing geodetic artificial satellites, as is done in the realization of the

various Earth Gravity Model of the Goddard Space Flight Center among which EGM96 [19] is the most recent, or in altimetric measurements [78].

In order to calculate the gravitational effect of the water masses raised by the tidal forces of a given constituent $\Phi_l^m(f)$ it can be considered a spherical layer with radius R endowed with a bidimensional surface mass density $\mu_f(\vartheta, \lambda) = \rho\zeta_f(\vartheta, \lambda)$, where ρ is the volumetric ocean water density assumed constant, and calculate its potential as

$$(101) \qquad U_f = G \int \frac{\mu_f(\vartheta', \lambda')}{|\mathbf{r} - \mathbf{r}'|} d\Sigma' = G \int \frac{\rho\zeta_f(\vartheta', \lambda')}{|\mathbf{r} - \mathbf{r}'|} d\Sigma'.$$

In eq. (101) the geodetic convention for the potential is used [1]: in it U is the potential usually defined in physics with the sign reversed. Let us rewrite ζ_f as

$$(102) \qquad \zeta_f = \xi_f \cos(\sigma t - \delta_f) = \xi_f \cos\delta_f \cos\sigma t + \xi_f \sin\delta_f \sin\sigma t.$$

The following step consists of expanding eq. (102) in spherical harmonics [35, 36]

$$(103) \qquad \xi_f \cos\delta_f = \sum_{l=0}^{\infty} \sum_{m=0}^{l} (a_{lmf} \cos m\lambda + b_{lmf} \sin m\lambda) P_l^m(\sin\phi),$$

$$(104) \qquad \xi_f \sin\delta_f = \sum_{l=0}^{\infty} \sum_{m=0}^{l} (c_{lmf} \cos m\lambda + d_{lmf} \sin m\lambda) P_l^m(\sin\phi).$$

The coefficients of the harmonic expansion, which have the dimension of lengths, can be calculated if the harmonic constants are known by means of the following formulas

$$(105) \qquad a_{lmf} = \frac{(2l+1)(2-\delta_{0m})}{4\pi} \frac{(l-m)!}{(l+m)!} \times \int \xi_f \cos\delta_f \cos m\lambda P_l^m(\sin\phi) d\Sigma,$$

$$(106) \qquad b_{lmf} = \frac{(2l+1)(2-\delta_{0m})}{4\pi} \frac{(l-m)!}{(l+m)!} \times \int \xi_f \cos\delta_f \sin m\lambda P_l^m(\sin\phi) d\Sigma,$$

$$(107) \qquad c_{lmf} = \frac{(2l+1)(2-\delta_{0m})}{4\pi} \frac{(l-m)!}{(l+m)!} \times \int \xi_f \sin\delta_f \cos m\lambda P_l^m(\sin\phi) d\Sigma,$$

$$(108) \qquad d_{lmf} = \frac{(2l+1)(2-\delta_{0m})}{4\pi} \frac{(l-m)!}{(l+m)!} \times \int \xi_f \sin\delta_f \sin m\lambda P_l^m(\sin\phi) d\Sigma.$$

Eqs. (105)-(108) are the connection between the harmonic constants obtained through oceanographic models and the data acquired by geodetic satellites, in the sense that if the coefficients a_{lmf}, b_{lmf}, c_{lmf}, d_{lmf}, for a given tidal line, are known from orbital analysis, by means of eq. (105)-eq. (108), the essential features of that partial tide may be recovered. With eqs. (103)-(104) eq. (102) becomes

$$(109) \qquad \zeta_f = \sum_{l=0}^{\infty} \sum_{m=0}^{l} (C_{lmf} \cos m\lambda + S_{lmf} \sin m\lambda) P_l^m(\sin\phi)$$

in which

$$(110) \qquad C_{lmf} = a_{lmf} \cos\sigma t + c_{lmf} \sin\sigma t,$$
$$(111) \qquad S_{lmf} = b_{lmf} \cos\sigma t + d_{lmf} \sin\sigma t.$$

By inserting eq. (109) in eq. (101) and expanding in spherical harmonics also the term $1/\left| \mathbf{r} - \mathbf{r}' \right|$, it can be obtained

$$(112)\ U_f = 4\pi GR\rho \sum_{l=0}^{\infty} \sum_{m=0}^{l} \frac{1}{2l+1} \left(\frac{R}{r} \right)^{l+1} (C_{lmf} \cos m\lambda + S_{lmf} \sin m\lambda) P_l^m (\sin \phi).$$

In eq. (112), using eq. (110)-eq. (111), one can further expand $(C_{lmf} \cos m\lambda + S_{lmf} \sin m\lambda)$ by introducing the prograde (westwards) and retrograde waves [72]

$$(113)\ C_{lmf} \cos m\lambda + S_{lmf} \sin m\lambda = \sum_{+}^{-} K_{lmf}^{\pm} \cos (m\lambda \pm \sigma t) \pm S_{lmf}^{\pm} \sin (m\lambda \pm \sigma t).$$

In eq. (113) and in the following, expressions like $\sum_{+}^{-} A^{\pm} \cos (a \pm b)$ must be interpreted as $A^{+} \cos (a + b) + A^{-} \cos (a - b)$. The sign $+$ refers to the progressive (westwards) waves while the sign $-$ is for the waves moving from West to East. From eqs. (110)-(111) and eq. (113) one has

$$(114) \qquad\qquad a_{flm} = K_{flm}^{+} + K_{flm}^{-},$$

$$(115) \qquad\qquad b_{flm} = S_{flm}^{+} - S_{flm}^{-},$$

$$(116) \qquad\qquad c_{flm} = S_{flm}^{+} + S_{flm}^{-},$$

$$(117) \qquad\qquad d_{flm} = -K_{flm}^{+} + K_{flm}^{-}.$$

From these equations, by defining

$$(118) \qquad\qquad K_{lmf}^{\pm} = C_{lmf}^{\pm} \cos \varepsilon_{flm}^{\pm},$$

$$(119) \qquad\qquad S_{lmf}^{\pm} = C_{lmf}^{\pm} \sin \varepsilon_{flm}^{\pm},$$

it is possible to express the coefficients of the expansion of the harmonic constants a_{lmf}, b_{lmf}, c_{lmf}, d_{lmf} in terms of $C_{lmf}^{\pm}$, $\varepsilon_{lmf}^{\pm}$ which can be recovered by geodetic satellites

$$(120) \qquad\qquad C_{lmf}^{+} \cos \varepsilon_{lmf}^{+} = \frac{a_{lmf} - d_{lmf}}{2},$$

$$(121) \qquad\qquad C_{lmf}^{-} \cos \varepsilon_{lmf}^{-} = \frac{a_{lmf} + d_{lmf}}{2},$$

$$(122) \qquad\qquad C_{lmf}^{+} \sin \varepsilon_{lmf}^{+} = \frac{c_{lmf} + b_{lmf}}{2},$$

$$(123) \qquad\qquad C_{lmf}^{-} \sin \varepsilon_{lmf}^{-} = \frac{-b_{lmf} + c_{lmf}}{2}.$$

Eq. (106) and eq. (108) show that, for $m = 0$, it turns out $b_{l0f} = d_{l0f} = 0$ identically; this implies through eqs. (120)-(123) that

$$(124) \qquad\qquad C_{l0f}^{+} = C_{l0f}^{-},$$

(125)
$$\varepsilon_{l0f}^{+} = \varepsilon_{l0f}^{-}.$$

Eqs. (124)-(125) will be used in the next section. It is interesting to notice that eqs. (120)-(123), or also eqs. (114)-(117), show that if it were $c_{lmf} = d_{lmf} = 0$, the distinction between the prograde and retrograde waves would disappear and only one kind of waves would remain, as in the equilibrium theory. Indeed, eqs. (107)-(108) point out that $c_{lmf} = d_{lmf} = 0$ if and only if $\delta_f = 0$, where δ_f is the phase lag of the ocean response with respect to the lunisolar tidal constituent due to the ocean hydrodynamics.

Eq. (112), with eq. (113) and eqs. (118)-(119), becomes

(126) $\quad U_f = 4\pi G R \rho \sum_{l=0}^{\infty} \sum_{m=0}^{l} \sum_{+}^{-} \left(\frac{R}{r}\right)^{l+1} \frac{C_{lmf}^{\pm}}{2l+1} \cos\left(\sigma t \pm m\lambda - \varepsilon_{lmf}^{\pm}\right) P_l^m(\sin\phi).$

Eq. (126) expresses the gravitational potential of the Earth's ocean waters, thought as a spherical layer of mass $\rho\zeta_f$ raised by the action of a given lunisolar tidal constituent of circular frequency σ.

But these enormous water masses act upon the sea floor and the whole of the solid Earth which are deformed and attracted by them. This effect has also to be considered. It can be done according to eq. (60) and introducing the so called load Love numbers k_l' [79, 35, 80]. The global response of the Earth oceans to the forcing tidal constituent of frequency σ can be written as

$$U_f = U_{\text{oc}} + U_{\text{load}} = 4\pi G R \rho \sum_{l=0}^{\infty} \sum_{m=0}^{l} \sum_{+}^{-} \left(\frac{R}{r}\right)^{l+1} \frac{(1+k_l')}{2l+1} \times$$

(127)
$$\times C_{lmf}^{\pm} \cos\left(\sigma t \pm m\lambda - \varepsilon_{lmf}^{\pm}\right) P_l^m(\sin\phi),$$

with $U_f < U_{\text{oc}}$, i.e. $k' < 0$. This fact can be intuitively guessed by thinking about U in terms of shift of the equipotential surfaces $h = U/g$: if the sea floor is raised by the tidally driven water masses the total shift is smaller than it would be if we considered the solid Earth as completely rigid.

3˙7. *Ocean tidal orbital perturbations*. – Eq. (127) can be fruitfully rewritten in a form more suitable for calculating the perturbations induced on the Keplerian orbital elements of artificial satellites [81, 82]. To this aim the following quantities are defined

(128)
$$A_{lmf}^{\pm} = 4\pi G R \rho \frac{(1+k_l')}{2l+1} C_{lmf}^{\pm},$$

(129)
$$\mathcal{C}_{lmf}^{\pm} = A_{lmf}^{\pm} \cos\left(\mp\sigma t \pm \varepsilon_{lmf}^{\pm}\right),$$

(130)
$$\mathcal{S}_{lmf}^{\pm} = A_{lmf}^{\pm} \sin\left(\mp\sigma t \pm \varepsilon_{lmf}^{\pm}\right).$$

U_f becomes

(131)
$$U_f = \sum_{l=0}^{\infty} \sum_{m=0}^{l} \sum_{+}^{-} \left(\frac{R}{r}\right)^{l+1} \left(\mathcal{C}_{lmf}^{\pm} \cos m\lambda + \mathcal{S}_{lmf}^{\pm} \sin m\lambda\right) P_l^m(\sin\phi).$$

Eq. (131) is formally equal to the expression of the static gravitational potential of the Earth worked out by Kaula. So, with the same mathematical menagerie used for the geopotential in ref.[1], it is possible to write eq. (131) in terms of the Keplerian orbital elements of a test body in the field of the Earth as

$$(132) \quad U_f = \sum_{l=0}^{\infty} \sum_{m=0}^{l} \sum_{+}^{-} \left(\frac{R}{r}\right)^{l+1} A^{\pm}_{lmf} \sum_{p=0}^{l} \sum_{q=-\infty}^{+\infty} F_{lmp}(i)G_{lpq}(e) \begin{bmatrix} \cos \gamma^{\pm}_{flmpq} \\ \sin \gamma^{\pm}_{flmpq} \end{bmatrix},$$

in which

$$(133) \qquad \gamma^{\pm}_{flmpq} = (l-2p)\omega + (l-2p+q)\mathcal{M} + m(\Omega - \theta) \pm (\sigma t - \varepsilon^{\pm}_{lmf}).$$

The equations for the tidal ocean perturbations may be worked out as already done for the solid Earth tides in subsect. 4. At first order, one obtains

$$\Delta\Omega_f = \frac{1}{na^2\sqrt{1-e^2}\sin i} \sum_{l=0}^{\infty} \sum_{m=0}^{l} \sum_{+}^{-} \left(\frac{R}{r}\right)^{l+1} A^{\pm}_{lmf} \times$$

$$(134) \qquad \times \sum_{p=0}^{l} \sum_{q=-\infty}^{+\infty} \frac{dF_{lmp}}{di}G_{lpq}\frac{1}{f_p}\begin{bmatrix} \sin \gamma^{\pm}_{flmpq} \\ -\cos \gamma^{\pm}_{flmpq} \end{bmatrix}^{l-m \text{ even}}_{l-m \text{ odd}},$$

$$\Delta\omega_f = \frac{1}{na^2\sqrt{1-e^2}} \sum_{l=0}^{\infty} \sum_{m=0}^{l} \sum_{+}^{-} \left(\frac{R}{r}\right)^{l+1} A^{\pm}_{lmf} \times$$

$$(135) \times \sum_{p=0}^{l} \sum_{q=-\infty}^{+\infty} \left[\frac{1-e^2}{e}F_{lmp}\frac{dG_{lpq}}{de} - \frac{\cos i}{\sin i}\frac{dF_{lmp}}{di}G_{lpq}\right]\frac{1}{f_p}\begin{bmatrix} \sin \gamma^{\pm}_{flmpq} \\ -\cos \gamma^{\pm}_{flmpq} \end{bmatrix}^{l-m \text{ even}}_{l-m \text{ odd}},$$

in which

$$(136) \qquad f_p = (l-2p)\dot\omega + (l-2p+q)\dot{\mathcal{M}} + m(\dot\Omega - \dot\theta) \pm \sigma.$$

It should be noticed that the frequencies of the perturbations given by eq. (136) are different, in general, from the frequencies of the solid Earth tidal perturbations given by eq. (88). While for the solid tides the diurnal modulation due to $\dot\theta$ cancels out automatically if one considers those terms in which $j_1 = m$, for the ocean tides, in general, this does not happen because of the presence of the Eastwards waves due to the non-equilibrium pattern of the ocean tidal bulge.

Long periodicities can be obtained considering those combinations of l, p and q for which $l - 2p + q = 0$ holds and retaining the Westward prograde terms with $j_1 = m$. Only in this way in eq. (136) the contributions of $\dot\theta$ are equal and opposite, and cancel out. With these bounds on l, m, p and q the frequencies of the perturbations of interest become

$$(137) \qquad f_p = \dot\Gamma_f + (l-2p)\dot\omega + m\dot\Omega.$$

It is worthwhile noting that the frequencies f_p are identical to those of solid tidal perturbations [35, 51], so that the satellites cannot distinguish one effect from the other, a feature which will turn out to be important in the recovery of the coefficients $C_{lmf}^{\pm}$.

For $l = 2$, as for the solid tides, $l - 2p = 0$ holds. The frequencies of the perturbations are, in this case, given by

$$(138) \qquad f_p = \dot{\Gamma}_f + m\dot{\Omega}.$$

If l is odd the situation is different because now all the terms with p running from 0 to l must be considered and q is different from zero: $q = 2p - l$. So, the rates of the perturbations include the contribute of $\dot{\omega}$.

Up to now the prograde wave terms only have been considered in order to deal with long period perturbations. Yet, there is a case in which also the retrograde terms fit into this scheme; it is possible to show that for l even and $m = 0$ the frequencies of prograde and retrograde terms coincide, in absolute values, and the perturbation amplitudes are twice the amplitudes of the prograde terms only. Indeed, according to eqs. (134)-(135), $\Delta\Omega_f$, $\Delta\omega_f$ are proportional to

$$(139) \qquad \sum_{+}^{-} A_{flm}^{\pm} \frac{1}{f_p} \left[\begin{array}{c} \sin\gamma_{flmpq}^{\pm} \\ -\cos\gamma_{flmpq}^{\pm} \end{array} \right];$$

in this case $l - m$ is even and retaining only those terms for which $l - 2p = 0$ one has

$$(140) \qquad \gamma_{fl0\frac{l}{2}0}^{\pm} = \pm(\sigma t - \varepsilon_{fl0}^{\pm}),$$

$$(141) \qquad f_p = \pm\sigma.$$

Expanding eq. (139) it can be obtained

$$A_{fl0}^{+} \frac{1}{\sigma} \sin(\sigma t - \varepsilon_{fl0}^{+}) + A_{fl0}^{-} \frac{1}{-\sigma} \sin[-(\sigma t - \varepsilon_{fl0}^{-})] =$$

$$(142) \qquad = A_{fl0}^{+} \frac{1}{\sigma} \sin(\sigma t - \varepsilon_{fl0}^{+}) + A_{fl0}^{-} \frac{1}{\sigma} \sin(\sigma t - \varepsilon_{fl0}^{-}).$$

Since $A_{fl0}^{+} = A_{fl0}^{-}$ and $\varepsilon_{fl0}^{+} = \varepsilon_{fl0}^{-}$, as shown by eq. (124) and eq. (125), eq. (142) becomes

$$(143) \qquad \frac{2A_{fl0}^{+}}{\sigma} \sin(\sigma t - \varepsilon_{fl0}^{+}).$$

Eqs. (134)-(135) have been adopted in order to compute the amplitudes of the ocean tidal perturbations on the Keplerian elements Ω for LAGEOS and LAGEOS II and ω for LAGEOS II which pertain directly the Lense-Thirring experiment. Also in this section the perturbations of second order [65] due to the oblateness of the Earth have not been considered, as already done for the solid tides. The inclination and eccentricity functions used are those quoted in [1]. For the numerical values of the various geophysical parameters which figure in eqs. (134)-(135) the IERS standards [56] have been used, while

the EGM96 gravity model [19] has been adopted for the choice of the tidal constituents and their coefficients $C_{lm}^{\pm}$ in the ocean tidal potential U_f. The calculation have been performed, considering only the progressive waves, for the following tidal lines
- M_m (065.455), S_a (056.554), M_f (075.555), S_{sa} (057.555);
- K_1 (165.555), O_1 (145.555), P_1 (163.555), Q_1 (135.655);
- K_2 (275.555), M_2 (255.555), S_2 (273.555), N_2 (245.655), T_2 (272.556).

For each of these tidal constituents the following terms have been calculated
$l = 2$, $p = 1$, $q = 0$ because the eccentricity functions $G_{lpq}(e)$ for $p = 0$, $q = -2$ and $p = 2$, $q = 2$ vanish.
$l = 3$, $p = 1$, $q = -1$ and $l = 3$, $p = 2$, $q = 1$ because G_{30-3} and G_{333} are not quoted in [1] due to their smallness: indeed, the $G_{lpq}(e)$ are proportional to $e^{|q|}$.
$l = 4$, $p = 2$, $q = 0$ because the other admissible combinations of l, p and q give rise to negligible eccentricity functions. So, also for $l = 4$ the condition $l - 2p = 0$, in practice, holds and the constituents of degree $l = 2$ and $l = 4$ generate detectable perturbations with identical periods.

Similar analysis can be found in [67, 35]. It should be noticed that when Christodoulidis performed his study, which is relative to only five constituents, neither the LAGEOS nor the LAGEOS II were in orbit, while Dow has sampled the tidal spectrum for LAGEOS in a poorer manner with respect to this study in the sense that, for each constituent, only the terms of degree $l = 2$ have been considered with the exception of the K_1 whose $l = 4$ contribution has been also analyzed. Moreover, when these works have been realized there were a few coefficients C_{lmf}^{+} available with relevant associated errors.

Some explanations are needed about the determination of the coefficients $C_{lmf}^{\pm}$. In EGM96 the geopotential is recovered through both altimeter and surface gravity information, and satellites data. The pool of near-Earth satellites employed, in general, are not perceptibly perturbed by the entire tidal spectrum, but they are sensitive only to some certain tidal lines, depending on the features of their orbits. Moreover, on a large enough temporal scale they cannot distinguish between solid and prograde ocean tidal perturbations because their frequencies are the same. Finally, there are also other periodic physical phenomena different from the tides that affect the orbits of the geodetic satellites; in many cases their periodicities are similar to that of the tides, particularly in the zonal band. These facts imply that in the analytical expressions of the perturbations it is necessary to assume as known *a priori* from various reliable models some solid or ocean tidal terms and consider variable the other ones in order to adjust them by means of the experimentally determined values of the perturbations; all the constituents considered, both those held fixed and the other recovered, must be capable to influence perceptibly the satellites employed. The strategy followed in EGM96 has consisted in adopting the frequency-dependent Wahr model for the solid tides [52] with its values for the Love numbers and the $H_l^m(f)$ of Cartwright and Edden, calculating a certain number of ocean tidal terms by means of oceanographic models, when it has been possible to solve the LTE, or by means of other algorithms [37], considering also the retrograde waves, and choosing the 13 ocean tidal terms listed above to be adjusted. The values recovered for the coefficients C_{20f}^{+} account for also the retrograde terms because, as previously noticed, their periods are equal to those of prograde ones. The terms whose value has been considered given *a priori* constitute the so called background; it necessarily contains terms up to sixth degree because the attenuation due to altitude makes the near-Earth satellites almost insensitive to larger degree terms: indeed, in eqs. (134)-(135) the $A_{lmf}^{\pm}$

are proportional to

$$(144) \qquad \left(\frac{R}{r}\right)^{l+1} \frac{1}{2l+1}.$$

The values obtained for the coefficients C^+_{lmf} are, in general, biased by the effects of the anelasticity of the solid Earth's mantle and by all other phenomena which have not been explicitly modeled in the background. For example, in the values recovered for the S_a are included climatological effects which have not gravitational origin; in the S_2 coefficients are also included the variations of the atmospheric pressure due to the atmospheric tides.

3˙8. *Discussion of the numerical results.* – In Table VI, Table VII and Table VIII the present results for the nodes Ω of LAGEOS and LAGEOS II, and the argument of perigee ω for LAGEOS II are quoted.

TABLE VI. – *Perturbative amplitudes on the node Ω of LAGEOS due to ocean tides. P indicates the periods in days, A the amplitudes in mas and E the percent error in the C^+_{lmf}. The values employed for them and the related errors are those quoted in EGM96 model.*

Tide	$l=2,\ p=1,\ q=0$			$l=3,\ p=1,\ q=-1$			$l=3,\ p=2,\ q=1$			$l=4,\ p=2,\ q=0$		
	P	A	E	P	A	E	P	A	E	P	A	E
065.455 M_m	27.55	-0.54	14.4	28	-10^{-4}	66.6	27.11	10^{-4}	66.6	-	-	-
056.554 S_a	365.27	-20.55	6.7	464.67	-10^{-2}	10	300.91	10^{-2}	10	-	-	-
075.555 M_f	13.66	-0.62	7.8	13.77	-10^{-4}	112	13.55	10^{-4}	112	-	-	-
057.555 S_{sa}	182.62	-5.98	9.4	204.5	-10^{-3}	27.2	164.9	10^{-3}	27.2	-	-	-
165.555 K_1	1,043.67	156.55	3.8	2,684.2	-0.36	5.2	647.76	10^{-2}	5.2	1,043.67	4.63	3.9
163.555 P_1	-221.35	-11.49	8.1	-195.95	10^{-3}	18.5	-254.3	-10^{-3}	18.5	-221.35	-0.32	8
145.555 O_1	-13.84	-2	2.9	-13.72	10^{-3}	3.2	-13.95	10^{-4}	3.2	-13.84	10^{-2}	5.7
135.655 $Q1$	-9.21	-0.28	13.5	-9.16	10^{-4}	25	-9.26	10^{-5}	25	-9.21	-10^{-3}	20
275.555 K_2	521.83	-6.24	11.1	751.5	-10^{-2}	5.5	399.7	10^{-2}	5.5	521.83	-9.58	15.4
273.555 S_2	-280.93	9.45	3.9	-241.24	10^{-3}	7.1	-336.25	-10^{-2}	7.1	-280.93	15.08	5.2
272.556 T_2	-158.8	0.28	75	-145.3	10^{-4}	50	-175	-10^{-3}	50	-158.8	0.44	100
255.555 M_2	-14.02	2.03	0.9	-13.9	-10^{-4}	7.4	-14.14	10^{-3}	7.4	-14.02	2.08	2.8
245.655 N_2	-9.29	0.3	4.6	-9.2	10^{-5}	12.5	-9.3	10^{-4}	12.5	-9.29	0.3	8.3

From an accurate inspection of Table VI, Table VII it is possible to notice that, for the nodes Ω, only the even degree terms give an appreciable contribute; the $l=3$ terms are totally negligible. This so because $\Delta\Omega_f$ is proportional to the $G_{lpq}(e)$ functions which, in turn, are, in general, proportional to $e^{|q|}$: in this case the eccentricity functions are $G(e)_{31-1} = e(1-e^2)^{-5/2} = G(e)_{321}$ and the eccentricities of LAGEOSsatellites are of the order of 10^{-2} or less.

Among the long period zonal tides, the Solar annual tide S_a (056.554) exerts the most relevant action on the nodes, with an associated percent error in the amplitudes of 6.7 %. It is interesting to compare for this tidal line the ocean tidal perturbations of degree $l=2$ $A^{\text{ocean}}_{\text{LAGEOS}}(\Omega) = -20.55$ mas, $A^{\text{ocean}}_{\text{LAGEOS II}}(\Omega) = 37.7$ mas, with those due to the solid Earth tides $A^{\text{solid}}_{\text{LAGEOS}}(\Omega) = 9.96$ mas, $A^{\text{solid}}_{\text{LAGEOS II}}(\Omega) = -18.28$ mas. The ocean amplitudes amount to 204 % of the solid ones, while for the other zonal constituents they vary from 9.9 % for the M_m to the 18.5 % of the S_{sa}. This seems to point toward that the recovered value of C^+_{20f} for the S_a is biased by other climatological effects than the tides; indeed, for all the other tidal lines, zonal or not, the ocean tidal perturbations of degree $l=2$ amount to almost 10 % of the solid Earth tides perturbations.

TABLE VII. – *Perturbative amplitudes on the node Ω of LAGEOS II due to ocean tides. P indicates the periods in days, A the amplitudes in mas and E the percent error in the C_{lmf}^{+}. The values employed for them and the related errors are those quoted in EGM96 model.*

Tide	$l=2,\ p=1,\ q=0$			$l=3,\ p=1,\ q=-1$			$l=3,\ p=2,\ q=1$			$l=4,\ p=2,\ q=0$		
	P	A	E	P	A	E	P	A	E	P	A	E
065.455 M_m	27.55	1	14.4	26.65	10^{-3}	66.6	28.5	-10^{-3}	66.6	-	-	-
056.554 S_a	365.27	37.71	6.7	252.8	0.13	10	657.5	-0.35	10	-	-	-
075.555 M_f	13.6	1.13	7.8	13.43	10^{-4}	112	13.89	-10^{-4}	112	-	-	-
057.555 S_{sa}	182.62	10.98	9.4	149.41	10^{-2}	27.2	234.8	-10^{-2}	27.2	-	-	-
165.555 K_1	-569.21	-35.69	3.8	-1,851.9	-1.02	5.2	-336.3	-10^{-3}	5.2	-569.21	41.58	3.9
163.555 P_1	-138.26	-3	8.1	-166.23	-10^{-2}	18.5	-118.35	-10^{-4}	18.5	-138.26	3.29	8
145.555 O_1	-13.3	-0.8	2.9	-13.5	-10^{-2}	3.2	-13.12	-10^{-4}	3.2	-13.3	0.7	5.7
135.655 Q_1	-8.98	-0.11	13.5	-9.08	-10^{-3}	25	-8.89	10^{-5}	25	-8.98	0.11	20
275.555 K_2	-284.6	-6.24	11.1	-435.38	-0.13	5.5	-211.4	10^{-2}	5.5	-284.6	-5.95	15.4
273.555 $S2$	-111.2	-6.87	3.9	-128.6	-10^{-2}	7.1	-97.9	10^{-2}	7.1	-111.2	-6.79	5.2
272.556 T_2	-85.27	-0.277	75	-95.14	-10^{-3}	50	-77.25	10^{-3}	50	-85.27	-0.274	100
255.555 M_2	-13.03	-3.46	0.9	-13.2	-10^{-3}	7.4	-12.83	10^{-3}	7.4	-13.03	-2.2	2.8
245.655 N_2	-8.8	-0.46	4.6	-8.9	-10^{-3}	12.5	-8.7	10^{-4}	12.5	-8.8	-0.34	8.3

TABLE VIII. – *Perturbative amplitudes on the perigee ω of LAGEOS II due to ocean tides. P indicates the periods in days, A the amplitudes in mas and E the percent error in the C_{lmf}^{+}. The values employed for them and the related errors are those quoted in EGM96 model.*

Tide	$l=2,\ p=1,\ q=0$			$l=3,\ p=1,\ q=-1$			$l=3,\ p=2,\ q=1$			$l=4,\ p=2,\ q=0$		
	P	A	E	P	A	E	P	A	E	P	A	E
065.455 M_m	27.55	-0.69	14.4	26.65	-1.53	66.6	28.5	1.64	66.6	-	-	-
056.554 S_a	365.27	-26.17	6.7	252.8	-114.35	10	657.55	297.34	10	-	-	-
075.555 M_f	13.66	-0.78	7.8	13.43	-0.58	112	13.89	0.60	112	-	-	-
057.555 S_{sa}	182.6	-7.62	9.4	149.41	-22.95	27.2	234.8	36.07	27.2	-	-	-
165.555 K_1	-569.21	177.76	3.8	-1,851.9	-1,136	5.2	-336.28	346.6	5.2	-569.21	-3.95	3.9
163.555 P_1	-138.26	14.95	8.1	-166.2	-28.97	18.5	-118.35	34.67	18.5	-138.2	-0.31	8
145.555 O_1	-13.3	4	2.9	-13.55	-13.7	3.2	-13.12	22.3	3.2	-13.3	-10^{-2}	5.7
135.655 Q_1	-8.98	0.58	13.5	-9.08	-1.17	25	-8.89	1.92	25	-8.98	-10^{-2}	20
275.555 K_2	-284.6	-5.95	11.1	-435.3	214.23	5.5	-211.4	87.3	5.5	-284.6	-2.49	15.3
273.555 S_2	-111.2	-6.55	3.9	-128.6	98.47	7.1	-97.9	62.9	7.1	-111.2	-2.85	5.2
272.556 T_2	-85.2	-0.26	75	-95.1	5.2	50	-77.2	3.54	50	-85.2	-0.11	100
255.555 M_2	-13.03	-3.3	0.9	-13.2	9.7	7.4	-12.83	7.9	7.4	-13.03	-0.92	2.8
245.655 N_2	-8.48	-0.44	4.6	-8.94	1.95	12.5	-8.75	1.6	12.5	-8.84	-0.14	8.3

The terms of degree $l=2$ of the tesseral tides K_1 (165.555) and O_1 (145.555) induce very large perturbations on the node of LAGEOS and, to a lesser extent, of LAGEOS II; Table VI and Table VII quote 156.55 mas, 151.02 mas for the former and -35.69 mas, -34.43 mas for the latter. The associated percent errors are 3.8 % and 2.9 %, respectively. For the terms of degree $l=4$, which have the same periods of those of degree $l=2$, the situation is reversed: Table VI and Table VII quote 4.63 mas and 3.54 mas for LAGEOS and 41.58 and 31.81 mas for LAGEOS II. The percent errors associated with K_1 and O_1, for $l=4$, are 3.9 % and 5.7 % respectively. For all the tesseral lines investigated the ocean tidal perturbations of degree $l=2$ are, in general, the 10 % of the solid tidal perturbations.

Among the sectorial tides, the most relevant in perturbing the nodes of LAGEOS satellites, on large temporal scales, is the M_2 (255.555): Table VI and Table VII quote -75.59 mas ($l=2$) and -77.40 mas ($l=4$) for LAGEOS, and -75.65 mas ($l=2$) and -48.07 mas ($l=4$) for LAGEOS II. The associated percent errors are 0.9 % for $l=2$

and 42.8 % for $l = 4$. The M_2 ocean perturbation of degree $l = 2$ amounts to 10.3 % of the corresponding solid tide. The same holds for the other sectorial tides of degree $l = 2$.

About the periodicities of these perturbations in relation to the detection of Lense-Thirring effect, the same considerations already exposed for the solid tides hold also in this case. Moreover, it must be pointed out the aliasing role played by the zonal 18.6-year and 9.3-year tides in the extracting any secular effect, like the gravitomagnetic precession, from a record whose duration is shorter than their very long periods. Recently both Starlette and LAGEOS SLR satellites passed their 19th year in orbit and this span of time is now adequate to get reliable information about these tides [83, 84] due to their slow frequencies they can be correctly modelled in terms of the equilibrium theory through the H_l^m coefficients and a complex Love number accounting for the anelasticity of the mantle. So, concerning them the results quoted for the solid tides can be considered adequately representative. In Table VIII the amplitudes of the perturbations on the argument of perigee ω for LAGEOS II are quoted. For this orbital element the factor

(145)
$$\frac{1 - e^2}{e} F_{lmp} \frac{dG_{lpq}}{de} - \frac{\cos i}{\sin i} \frac{dF_{lmp}}{di} G_{lpq}$$

to which $\Delta\omega_f$ is proportional makes the contributions of the $l = 3$ terms not negligible. For the even degree terms the situation is quite similar to that of Ω in the sense that the most influent tidal lines are the S_a, K_1, O_1 and M_2.

Once again, among the long period tides the S_a exhibits a characteristic behavior. Indeed, its $l = 3$ contributions are much stronger than those of the other zonal tides. This fact could be connected to the large values obtained in its C_{30f}^+ coefficient and people believe that it partially represents north to south hemisphere mass transport effects with an annual cycle nontidal in origin. The $l = 3$ terms present, in general, for the perigee of LAGEOS II a very interesting spectrum also for the tesseral and sectorial bands: for LAGEOS II there are lots of tidal lines which induce, on large temporal scales, very relevant perturbations on ω, with periods of the order of an year or more. In particular, it must be quoted the effect of K_1 line for $p = 1$, $q = -1$: the perturbation induced amount to -1,136 mas with period of -1,851.9 days. These values are comparable to the effects induced by the solid Earth tidal constituent of degree $l = 2$ on the node Ω of LAGEOS. Comparing the degree $l = 2$ terms with those of the solid tides, it can be noticed that also for the perigee the proportions are the same already seen for the nodes.

3'9. *The mismodelling in the nodes and the perigee.* – Concerning the mismodelling on the ocean tidal perturbations, the main source of uncertainties in them is represented by the load Love numbers k_l' and the coefficients C_{lmf}^+. In regard to the ocean loading, the first calculations of the load Love numbers k_l' can be found in refs.[79]. Pagiatakis, in ref.[80], in a first step has recalculated k_l' for an elastic, isotropic and non-rotating Earth: for $l < 800$ he claims that his estimates differ from those by Farrell in ref.[79], calculated with the same hypotheses, of less than 1%. Subsequently, he added to the equations, one at a time, the effects of anisotropy, rotation and dissipation; for low values of l their effects on the results of the calculations amount to less than 1%. It has been decided to calculate $\left| \frac{\partial A(\omega)}{\partial k_l'} \right| \delta k_l'$ of the perigee of LAGEOS II for K_1 $l = 3$ $p = 1$ which turns out to be the most powerful ocean tidal constituent acting upon this orbital element. First, we have calculated mean and standard deviation of the values for k_3' by Farrell and Pagiatakis obtaining $\delta k_3'/k_3' = 0.9\%$, in according to the estimates by Pagiatakis.

Then, by assuming in a pessimistic way that the global effect of the departures from these symmetric models yield to a total $\delta k_3^{'}/k_3^{'} = 2\%$, we have obtained $\delta\omega^{\mathrm{II}} = 5.5$ mas which corresponds to 2% of $\Delta\omega_{\mathrm{LT}}^{\mathrm{II}}$ over 4 years. Subsequently, for this constituent and for all other tidal lines we have calculated the effect of the mismodelling of C_{lmf}^{+} as quoted in EGM96 [19]. In Table IX we compare the so obtained mismodelled ocean tidal perturbations to those generated over 4 years by the Lense-Thirring effect. It turns

TABLE IX. – *Mismodeled ocean tidal perturbations on the nodes Ω of LAGEOS and LAGEOS II and the perigee ω of LAGEOS II compared to their gravitomagnetic precessions over 4 years $\Delta\Omega_{\mathrm{LT}}^{\mathrm{I}} = 124$ mas $\Delta\Omega_{\mathrm{LT}}^{\mathrm{II}} = 126$ mas $\Delta\omega_{\mathrm{LT}}^{\mathrm{II}} = -228$ mas. The effect of the ocean loading has been neglected. When the 1% cutoff has not been reached a - has been inserted. The values quoted for K_1 $l=3$ $p=1$ includes also the mismodelling in the ocean loading coefficient $k_3^{'}$ assumed equal to 2%. The ratios are in percent and the mismodelled amplitudes δX in mas.*

Tide	$\frac{\delta C^{+}}{C^{+}}$	$\delta\Omega^{\mathrm{I}}$	$\frac{\delta\Omega^{\mathrm{I}}}{\Delta\Omega_{\mathrm{LT}}^{\mathrm{I}}}$	$\delta\Omega^{\mathrm{II}}$	$\frac{\delta\Omega^{\mathrm{II}}}{\Delta\Omega_{\mathrm{LT}}^{\mathrm{II}}}$	$\delta\omega^{\mathrm{II}}$	$\frac{\delta\omega^{\mathrm{II}}}{\Delta\omega_{\mathrm{LT}}^{\mathrm{II}}}$
S_a $l=2$ $p=1$ $q=0$	6.7	1.37	1.1	2.5	1.9	-	-
S_a $l=3$ $p=1$ $q=-1$	10	-	-	-	-	11.4	5
S_a $l=3$ $p=2$ $q=1$	10	-	-	-	-	29.7	13
S_{sa} $l=3$ $p=1$ $q=-1$	27.2	-	-	-	-	6.2	2.7
K_1 $l=2$ $p=1$ $q=0$	3.8	5.9	4.7	1.3	1	6.75	2.9
K_1 $l=3$ $p=1$ $q=-1$	5.2	-	-	-	-	64.5	28.3
K_1 $l=3$ $p=2$ $q=1$	5.2	-	-	-	-	18	7.9
K_1 $l=4$ $p=2$ $q=0$	3.9	-	-	1.6	1.2	-	-
P_1 $l=3$ $p=1$ $q=-1$	18.5	-	-	-	-	5.3	2.3
P_1 $l=3$ $p=2$ $q=1$	18.5	-	-	-	-	6.4	2.8
K_2 $l=3$ $p=1$ $q=-1$	5.5	-	-	-	-	11.7	5
K_2 $l=3$ $p=2$ $q=1$	5.5	-	-	-	-	4.8	2
S_2 $l=3$ $p=1$ $q=-1$	7.1	-	-	-	-	6.9	3
S_2 $l=3$ $p=2$ $q=1$	7.1	-	-	-	-	4.4	1.9
T_2 $l=3$ $p=1$ $q=-1$	50	-	-	-	-	2.6	1.1

out that the perigee of LAGEOS II is more sensitive to the mismodelling of the ocean part of the Earth response to the tide generating potential. In particular, the effect of K_1 $l=3$ $p=1$ $q=-1$ is relevant with a total $\delta\omega = \left| \frac{\partial A(\omega)}{\partial C_{lmf}^{+}} \right| \delta C_{lmf}^{+} + \left| \frac{\partial A(\omega)}{\partial k_l^{'}} \right| \delta k_l^{'}$ of 64.5 mas amounting to 28.3 % of $\Delta\omega_{\mathrm{LT}}^{\mathrm{II}}$ over 4 years.

3˙10. *Conclusions*. – Concerning the orbital tidal perturbations on LAGEOS and LAGEOS II the following improvements with respect to the previous works have been reached
- The node and the perigee have been considered
- The analysis has been extended also to LAGEOS II, launched in 1992
- Concerning the solid tides, the most recent available frequency-dependent Love numbers k_2 have been used instead of a single-valued Love number $k_2 = 0.317$. Moreover,

the latitude-dependence of the Love number k^+ has been considered for some selected tidal lines

• About the ocean tides, their orbital perturbations have been extensively calculated for $l = 2, 3, 4$ by using the most recent available model EGM96. Interesting are the results obtained for the K_1, $l = 3$ $m = 1$ $p = 1$ $q = -1$ oceanic constituent. Indeed it induces on the perigee of LAGEOS II perturbations whose amplitudes are of the order of thousands of mas and the periods amounts to some years as the solid tidal perturbations

• An evaluation of the mismodelling on such orbital perturbations, for certain tidal constituents, have been performed

The calculations performed here have a general validity because they can be extended to any artificial satellite. The results presented here for the LAGEOS can be used, from one hand, in improving the modelling of their orbital perturbations and, from another hand, for the correct evaluation of the error budget in any space-based experiment devoted to the measurement of some particular feature of the Earth's gravitational field.

In the context of the general relativistic Lense-Thirring experiment, the calculations performed here have been used, in view of a refinement of the error budget, in order to check preliminarily which tidal constituents are really important in perturbing the combined residuals so to fit and remove them from the data, if possible, or, at least, to evaluate the systematic error induced by them. Table eq. (V) and Table eq. (IX) show that, over a 4 years time span the nodes of the two LAGEOS are sensitive to the even components of the 18.6-year line, the K_1 and the S_a at a 1% level at least. Moreover, the perigee of LAGEOS II turns out to be very sensitive to the $l = 3$ part of the ocean tidal spectrum.

The results obtained in this section for the nodes of LAGEOS and LAGEOS II and the perigee of LAGEOS II will be the starting point for the numerical simulations with MATLAB, described in section 4 and section 6, performed to assess quantitatively the direct impact of the tidal perturbations on the gravitomagnetic Lense-Thirring experiment, currently implemented, and on the proposed gravitoelectric experiment.

4. – The impact of the Earth tides on the determination of the Lense-Thirring effect

4˙1. *Introduction.* – According to [14], the Lense-Thirring effect could be detected, in the field of the Earth, by analyzing the orbits of the two laser-ranged LAGEOS and LAGEOS II satellites. The observable adopted is the combination of orbital residuals of eq. (5): the determination of the scaling parameter μ_{LT}, 1 in General Relativity and 0 in Newtonian mechanics, is influenced by a great number of gravitational and non-gravitational perturbations acting upon LAGEOS and LAGEOS II. Among the perturbations of gravitational origin a primary role is played by the solid Earth and ocean tides. Their effects on the orbital elements of LAGEOS and LAGEOS II has been extensively analyzed in section 3.

In [14] it is claimed the combined residuals $y \equiv \delta\Omega_{\mathrm{exp}}^{\mathrm{I}} + c_1 \delta\Omega_{\mathrm{exp}}^{\mathrm{II}} + c_2 \delta\omega_{\mathrm{exp}}^{\mathrm{II}}$ allow one to cancel out the static and dynamical perturbations of degree $l = 2, 4$ and order $m = 0$ of the terrestrial gravitational field; however, this is not so for the tesseral ($m = 1$) and sectorial ($m = 2$) tides. This section aims to assess quantitatively how the solid and ocean Earth tides of order $m = 0, 1, 2$ affect the recovery of μ_{LT} in view of a refinement of the error budget of the gravitomagnetic LAGEOS experiment.

Concerning the zonal tides, the results obtained in section 3 for the amplitudes of their perturbations have been used directly in eq. (5) in order to test in a preliminary way if

the $l = 2, 4$ $m = 0$ tidal perturbations really cancel out. In regard to the tesseral and sectorial tides the analysis of their impact on the Lense-Thirring measurement has been done by simulating the real residual curve and analyzing it. The T_{obs} chosen span ranges from 4 years to 8 years. This is so because 4 years is the length of the latest time series actually analyzed in [15] and 8 years is the maximum length obtainable today (Summer 2000) because LAGEOS II has been launched in 1992. The analysis includes also the long-period signals due to solar radiation pressure and the J_3 geopotential zonal harmonic acting on the perigee of LAGEOS II. In our case we have a signal built up with the secular Lense-Thirring trend(^{7}) and a certain number of long-period harmonics, i.e. the tesseral and sectorial tidal perturbations and the other signals with known periodicities.

The part of interest for us is the secular trend while the harmonic part represents the noise. We address the problem of how the harmonics affect the recovery of the secular trend on given time spans T_{obs} and various samplings Δt.

Among the long-period perturbations we distinguish between those signals whose periods are shorter than T_{obs} and those signals with periods longer than T_{obs}. While the former average out if T_{obs} is an integer multiple of their periods, the action of the latter is more subtle since they could resemble a trend over temporal intervals too short with respect to their periods. They must be considered as biases on the Lense-Thirring determination affecting its recovery by means of their mismodelling. Thus, it is of the utmost importance that we reliably assess their effect on the determination of the trend of the gravitomagnetic effect. It would be useful to direct the efforts of the community (geophysicists, astronomers and space geodesists) towards the improvement of our knowledge of those tidal constituents to which μ_{LT} turns out to be particularly sensitive (for the LAGEOS orbits).

This investigation will quantify unambiguously what one means with statements like: $\Delta\mu_{\mathrm{tides}} \leq X\%\mu_{\mathrm{LT}}$. In this section we shall try to put forward a simple and meaningful approach. It must be pointed out though that it is not a straightforward application of any exact or rigorously proven method; on the contrary, it is, at a certain level, heuristic and intuitive, but it has the merit of yielding reasonable and simple answers and allowing for their critical discussion.

The section is organized as follows. In subsect. 2 the effects of the $l = 2, 4$ $m = 0$ tidal constituents on the combined residuals is examined; it turns out that, not only they affect it at a level $\ll 1\%$, but this feature also extends, within certain limits, to the $l = 3$, $m = 0$ part of the tidal spectrum. In subsect. 3 the features of the simulation procedure of the observable curve are outlined. In subsect. 4 the effects of the harmonics of the order $m = 1, 2$ with period shorter than 4 years are examined by comparing the least squares fitted values of μ_{LT} in two different scenarios: in the first one the simulated curve is complete and the fitting model contains all the most relevant signals plus a straight line, while in the second one some selected harmonics are removed from the simulated curve which is fitted by means of the straight line only. Subsect. 5 addresses the topic of the harmonics with periods longer than 4 years. Subsect. 6 is devoted to the conclusions.

(^{7}) In fact, the combined residuals are affected also by the secular contribution due to $l = 6, 8, ..$ zonal terms of the geopotential. Their effect amounts to almost 13% of the Lense-Thirring trend [15]. See also Appendix A.

4'2. *Systematic error due to the zonal tides.* – The combined residuals by Ciufolini are useful since they should vanish if calculated for the even zonal contributions C_{20} and C_{40} of the geopotential [14]. More precisely, the right side of eq. (5) should become equal to zero if the left side were calculated for any of these two even zonal contributions, both of static and dynamical origin; the nearer to zero is the right side, the smaller is the systematic uncertainty in μ_{LT} due to the contribution considered.

In order to test this important feature for the case of tides, in a very conservative way the results obtained in section 3, Table I, Table II, Table III for the solid Earth tides and Table VI, Table VII, Table VIII for the ocean tides, have been used in eq. (5) by assuming, for the sake of clarity and in order to make easier the comparison with ref.[66], an observational period of 1 year and the nominal values of the calculated tidal perturbative amplitudes, as if the zonal solid and ocean tides were not at all included in the GEODYN II dynamical models so that the residuals should account entirely for them.

The results are released in Table X and Table XI.

TABLE X. – *Contribution of the even zonal solid tidal constituents to* $\Delta\mu_{LT}$ *by means of the formula* $\delta\dot\Omega^{I} + \delta\dot\Omega^{II} \times 0.295 - \delta\dot\omega^{II} \times 0.35 = 60.2 \times \mu_{LT}$ *for* $l = 2, \ m = 0, \ p = 1, \ q = 0$.

Tide	$A(\Omega_{I})$ (mas)	$A(\Omega_{II})$ (mas)	$A(\omega_{II})$ (mas)	$\Delta\mu_{LT}$
055.565	-1,079.38	1,982.16	-1,375.58	-0.219
055.575	5.23	-9.61	6.66	1.06×10^{-3}
056.554 S_a	9.95	-18.28	12.69	2.02×10^{-3}
057.555 S_{sa}	31.21	-57.31	39.77	6.33×10^{-3}
065.455 M_m	5.28	-9.71	6.74	1.07×10^{-3}
075.555 M_f	4.94	-9.08	6.3	1×10^{-3}

TABLE XI. – *Contribution of the even zonal ocean tidal constituents to* $\Delta\mu_{LT}$ *by means of the formula* $\delta\dot\Omega^{I} + \delta\dot\Omega^{II} \times 0.295 - \delta\dot\omega^{II} \times 0.35 = 60.2 \times \mu_{LT}$ *for* $l = 2, \ m = 0, \ p = 1, \ q = 0$.

Tide	$A(\Omega_{I})$ (mas)	$A(\Omega_{II})$ (mas)	$A(\omega_{II})$ (mas)	$\Delta\mu_{LT}$
056.554 S_a	-20.55	37.71	-26.17	-3.68×10^{-3}
057.555 S_{sa}	-5.98	10.98	-7.62	-1.28×10^{-3}
065.455 M_m	-0.54	1	-0.69	-8.78×10^{-5}
075.555 M_f	-0.62	1.13	-0.78	-1.73×10^{-4}

The values of $\Delta\mu_{LT}$ quoted there for the various zonal tidal lines may be considered as the systematic error in μ_{LT} due to the chosen constituents, if considered one at a time by neglecting any possible reciprocal correlation among the other tidal lines. Table X and Table XI show that the percent error in the general relativistic value of μ_{LT} due to the 18.6-year tide, the most insidious one in recovering the LT since it superimposes to the gravitomagnetic trend over time spans of a few year, amounts to 21.9 %, while for all the other zonal tides it decreases to 0.1 % or less. This means that, even if neglected in the satellite orbit determination models, the $l = 2$ $m = 0$ tides, with the exception of the 18.6-year tide, do not affect the recovery of μ_{LT} by means of the combined residuals.

It is interesting to compare the present results to those released in ref.[66] for the 18.6-year tide. The value -0.219 due to the solid component for μ_{LT} quoted in Table X must be compared to -0.361 in ref.[66], with an improvement of 39.3 %. In the cited work there is no reference to any estimate of the mismodelling of the 18.6-year tide, so that we have used the nominal tidal perturbative amplitudes released in it: $A(\Omega^{I}) = -997$ mas, $A(\Omega^{II}) = 1,805$ mas and $A(\omega^{II}) = -1,265$ mas. These figures for the perturbative amplitudes due to the solid Earth tide of 18.6-year are notably different from those quoted in the present study. In ref.[66] the theoretical framework in which they have been calculated (F. Vespe, private communication, 1999) is based on the assumption of a spherical, static, elastic Earth with a single nominal value of $k_2 = 0.317$ used for the entire tidal spectrum. The inclusion of the tiny corrections due to the Earth's flattening and rotation on the perturbative amplitudes of Ω and ω for the 18.6-year tide could allow one to slightly improve the related uncertainty in μ_{LT}; it would amount to 20.6 %. But since the present-day accuracy in laser ranging measurements could hardly allow one to detect these small effects, their utilization in eq. (5) is debatable.

Remember that the result quoted for the 18.6-year tide is obtained in the worst possible case, i.e. a time span of only 1 year and the assumption that the residuals have been built up by neglecting completely the zonal tides in the dynamical models used. If, more realistically, we calculate eq. (5) with the mismodelled amplitudes quoted in the first row of Table V for the 18.6-year tide we obtain, over 1 year, $\Delta\mu = -3.51\times10^{-3}$. This strongly highlights that many efforts, either theoretical or experimental, must be done in order to modelling as accurately as possible such a constituent, so that it can be included in the nominal background of the orbital determination softwares like GEODYN II at a satisfactory level of accuracy. The calculations performed here point toward this goal in the sense that, if we put our values for the perturbative amplitudes due to the 18.6-year tide in the models of, e.g., GEODYN II and subsequently build up the orbital residuals, we expect that the contribution of such semisecular constituent to $\Delta\mu_{LT}$ amounts to the value quoted here.

Even though a cancellation is not expected as for the first two even zonal constituents, by calculating the left hand side of eq. (5) for the other tides yields, at least, an order of magnitude of their effect on μ_{LT}. An interesting, unpredicted feature stands out for the odd zonal ocean tides. The contribution of $l = 3$ zonal ocean tidal nominal perturbations over 1 year to $\Delta\mu_{LT}$ can be found in Table XII and Table XIII.

TABLE XII. – *Contribution of the odd zonal ocean tidal constituents to $\Delta\mu_{LT}$ by means of the formula $\delta\dot{\Omega}_I + \delta\dot{\Omega}^{II} \times 0.295 - \delta\dot{\omega}^{II} \times 0.35 = 60.2 \times \mu_{LT}$ for $l = 3$, $m = 0$, $p = 1$, $q = -1$.*

Tide	$A(\Omega_I)$ (mas)	$A(\Omega_{II})$ (mas)	$A(\omega_{II})$ (mas)	$\Delta\mu_{LT}$
056.554 S_a	-0.063	0.13	-114.35	0.66
057.555 S_{sa}	-9×10^{-3}	0.028	-22.95	0.133
065.455 M_m	-4×10^{-4}	1×10^{-3}	-1.53	-8.93×10^{-3}
075.555 M_f	-1×10^{-4}	7×10^{-4}	-0.58	3.41×10^{-3}

By inspecting them it is clear that the sensitivity of perigee of LAGEOS II to the $l = 3$ part of the ocean tidal spectrum may affect the recovery of the Lense-Thirring parameter μ_{LT} by means of the proposed combined residuals, especially as far as S_a and S_{sa} are concerned. This fact agrees with the results of Table IX which tells us that

TABLE XIII. – *Contribution of the odd zonal ocean tidal constituents to $\Delta\mu_{\mathrm{LT}}$ by means of the formula $\delta\dot{\Omega}^{\mathrm{I}} + \delta\dot{\Omega}^{\mathrm{II}} \times 0.295 - \delta\dot{\omega}^{\mathrm{II}} \times 0.35 = 60.2 \times \mu_{\mathrm{LT}}$ for $l = 3,\ m = 0,\ p = 2,\ q = 1$.*

Tide	$A(\Omega_{\mathrm{I}})$ (mas)	$A(\Omega_{\mathrm{II}})$ (mas)	$A(\omega_{\mathrm{II}})$ (mas)	$\Delta\mu_{\mathrm{LT}}$
056.554 S_a	0.047	-0.36	297.34	-1.72
057.555 S_{sa}	7×10^{-3}	-0.044	36.07	-0.209
065.455 M_m	4×10^{-4}	-2×10^{-3}	1.642	-9.55×10^{-3}
075.555 M_f	1.79×10^{-4}	-7×10^{-4}	-0.60	-3.52×10^{-3}

the mismodelled parts of S_a and S_{sa} are not negligible fractions of $\Delta\omega_{\mathrm{LT}}^{\mathrm{II}}$. However, if the mismodelled amplitudes are employed in eq. (5) it can be seen that, over 1 year, a cancellation of the order of 10^{-1} ($S_a\ l = 3\ p = 2$) and 10^{-2} ($S_a\ l = 3\ p = 1$; $S_{sa}\ l = 3\ p = 1, 2$) takes place. The contributions of the mismodelling on M_m and M_f are completely negligible. So, we can conclude that also the $l = 3$ part of the zonal ocean tidal spectrum may not affect the combined residuals in a notable manner if the $l = 3$ part of S_a and S_{sa} is properly accounted for.

4˙3. *The simulated residual signal.* – The first step of our strategy was to generate with MATLAB a time series which simulates, at the same length and resolution, the real residual curve obtainable from $y = \delta\Omega_{\mathrm{exp}}^{\mathrm{I}} + c_1\delta\Omega_{\mathrm{exp}}^{\mathrm{II}} + c_2\delta\omega_{\mathrm{exp}}^{\mathrm{II}}$ through, e.g., GEODYN. This simulated curve ("Input Model" - IM in the following) was constructed with

• The secular Lense-Thirring trend as predicted by the General Relativity[8]

• A certain number of sinusoids of the form $\delta A_k \cos\left(\frac{2\pi}{P_k}t + \phi_k\right)$ with known periods $P_k,\ k = 1, ..N$ simulating the mismodelled tides and other long-period signals which, to the level of assumed mismodelling, affect the combined residuals

• A noise of given amplitude which simulates the experimental errors in the laser-ranged measurements and, depending on the characteristics chosen for it, some other physical forces.

In a nutshell

$$(140) \quad \mathrm{IM} = \mathrm{LT} + [\text{mismodelled tides}] + [\text{other mismodelled long period signals}] + [\text{noise}].$$

The harmonics included in the IM are the following
• $K_1,\ l = 2$ solid and ocean; node of LAGEOS (P=1,043.67 days)
• $K_1,\ l = 2$ solid and ocean; node and perigee of LAGEOS II (P=-569.21 days)
• $K_1,\ l = 3,\ p = 1$ ocean; perigee of LAGEOS II (P=-1,851.9 days)
• $K_1,\ l = 3,\ p = 2$ ocean; perigee of LAGEOS II (P=-336.28 days)
• $K_2,\ l = 3,\ p = 1$ ocean; perigee of LAGEOS II (P=-435.3 days)
• $K_2,\ l = 3,\ p = 2$ ocean; perigee of LAGEOS II (P=-211.4 days)
• 165.565, $l = 2$ solid; node of LAGEOS (P=904.77 days)
• 165.565, $l = 2$ solid; node and perigee of LAGEOS II (P=-621.22 days)
• $S_2,\ l = 2$ solid and ocean; node of LAGEOS (P=-280.93 days)
• $S_2,\ l = 2$ solid and ocean; node and perigee of LAGEOS II (P=-111.24 days)

---

[8] Remember that in the dynamical models of GEODYN II it was set purposely equal to 0 so that the residuals absorbed (contained) entirely the relativistic effect [66].

- S_2, $l = 3$, $p = 1$ ocean; perigee of LAGEOS II (P=-128.6 days)
- S_2, $l = 3$, $p = 2$ ocean; perigee of LAGEOS II (P=-97.9 days)
- P_1, $l = 2$ solid and ocean; node of LAGEOS (P=-221.35 days)
- P_1, $l = 2$ solid and ocean; node and perigee of LAGEOS II (P=-138.26 days)
- P_1, $l = 3$, $p = 1$ ocean; perigee of LAGEOS II (P=-166.2 days)
- P_1, $l = 3$, $p = 2$ ocean; perigee of LAGEOS II (P=-118.35 days)
- Solar Radiation Pressure, perigee of LAGEOS II (P=-4,241 days)
- Solar Radiation Pressure, perigee of LAGEOS II (P=657 days)
- perigee odd zonal C_{30}, perigee of LAGEOS II (P=821.79)

In the following the signals due to solar radiation pressure will be denoted as SRP(P) where P is their period; the effects of the eclipses and Earth penumbra have not been accounted for. Many of the periodicities listed above have been actually found in the Fourier spectrum of the real residual curve [66]. Concerning K_1 $l = 3$ $p = 1$ and SRP(4,241), see subsect. 5.

When the real data are collected they refer to a unique, unrepeatable situation characterized by certain starting and ending dates for T_{obs}. This means that each analysis which could be carried out in the real world necessarily refers to a given set of initial phases and noise for the residual curve corresponding to the chosen observational period; if the data are collected over the same T_{obs} shifted backward or forward in time, in general, such features of the curve will change. We neither know a priori when the next real experiment will be performed, nor which will be the set of initial phases and the level of experimental errors accounted for by the noise. Moreover, maybe the dynamical models of the orbit determination software employed are out of date in regard to the perturbations acting upon satellites' orbits or do not include some of them at all. Consequently, it would be incorrect to work with a single simulated curve, fixed by an arbitrary set of δA_k, ϕ_k and noise, because it could refer to a situation different from that in which, in the real world, the residuals will actually correspond.

The need for great flexibility in generating the IM becomes apparent: to account for the entire spectrum of possibilities occurring when the real analysis will be carried out. We therefore decided to build into the MATLAB routine the capability to vary randomly the initial phases ϕ_k, the noise and the amplitude errors δA_k. Concerning the error amplitudes of the harmonics, they can be randomly varied so that δA_k spans $[0, \ \delta A_k^{\mathrm{nom}}]$ where $\delta A_k^{\mathrm{nom}}$ is the nominal mismodelled amplitude calculated taking into account Table V and Table IX; it means that we assume they are reliable estimates of the differences between the real data and the dynamical models of the orbital determination softwares, i.e. of the residuals. The MATLAB routine allows also the user to decide which harmonic is to be included in the IM; it is also possible to choose the length of the time series T_{obs}, the sampling step Δt and the amplitude of the noise.

In order to assess quantitatively this feature we proceeded as follows. First, over a time span of 3.1 years, we fitted the IM with a straight line only, finding for a choice of random phases and noise which qualitatively reproduces the curve shown in ref.[66], the value of 38.25 mas for the root mean square of the post fit IM. The value quoted in ref.[66]is 43 mas. Second, as done in the cited paper, we fitted the complete IM with the LT plus a set of long-period signals (see subsect. 4) and then we subtracted the so adjusted harmonics from the original IM obtaining a "residual" simulated signal curve. The latter was subsequently fitted with a straight line only, finding a rms post fit of 12.3 mas (it is nearly independent of the random phases and the noise) versus 13 mas quoted in [66]. A uniformly distributed noise with nonzero average and amplitude of 50 mas was used (see subsect. 4). These considerations suggest that the simulation procedure

adopted is reliable, replicates the real world satisfactorily and yields a good starting point for conducting our sensitivity analysis.

4˙4. *Sensitivity analysis*. – A preliminary analysis was carried out in order to evaluate the importance of the mismodelled solid tides on the recovery of $\mu_{\rm LT}$. We calculated the average

$$(147) \qquad\qquad\qquad \frac{1}{T_{\rm obs}} \int_0^{T_{\rm obs}} [\text{solid tides}] dt,$$

where [solid tides] denotes the analytical expressions of the mismodelled solid tidal perturbations as given by eqs. (85)-(86). Subsequently, we compared it to the value of the gravitomagnetic trend for the same $T_{\rm obs}$. The tests were repeated by varying Δt, $T_{\rm obs}$ and the initial phases. They have shown that the mismodelled part of the solid Earth tidal spectrum is entirely negligible with respect to the LT signal, falling always below 1% of the gravitomagnetic shift of the combined residuals accumulated over the examined $T_{\rm obs}$.

For the ocean tides and the other long-period signals the problem was addressed in a different way. First, for a given Δt and different time series lengths, we included in the IM the effects of LT, the noise and the solid tides only: subsequently we fitted it simply by means of a straight line. In a second step we have simultaneously added, both to the IM and the fitting model (FM hereafter), all the ocean tides, the solar radiation pressure SRP(657) signal and the odd zonal geopotential harmonic. We then compared the fitted values of $\mu_{\rm LT}$ and $\delta\mu_{\rm LT}$ recovered from both cases in order to evaluate $\Delta\mu_{\rm LT}$ and $\Delta\delta\mu_{\rm LT}$. The least squares fits [85, 86] were performed by means of the MATLAB routine "nlleasqr" (see, e.g., **http://www.ill.fr/tas/matlab/doc/mfit.html**); as $\delta\mu_{\rm LT}$ we have assumed the square root of the diagonal covariance matrix element relative to the slope parameter. It simulates the formal experimental error which, in the context of the gravitomagnetic LAGEOS experiment, is far smaller than the systematic errors which, consequently, must be carefully assessed. Notice that the SRP(4,241) has never been included in the FM (See section 5), while K_1 $l = 3$ $p = 1$ has been included for $T_{\rm obs} > 5$ years. For both of the described scenarios we have taken the average for $\mu_{\rm LT}$ and $\delta\mu_{\rm LT}$ over 1,500 runs performed by varying randomly the initial phases, the noise and the amplitudes of the mismodelled signals in order to account for all possible situations occurring in the real world, as pointed out in the previous section. The large number of repetitions was chosen in order to avoid that statistical fluctuations in the results could "leak" into $\Delta\overline{\mu_{\rm LT}}$ and $\Delta\overline{\delta\mu_{\rm LT}}$ and corrupt them at the level of 1%. With 1,500 runs the standard deviations on $\overline{\mu_{\rm LT}}$ and $\overline{\delta\mu_{\rm LT}}$ are of the order of 10^{-3} or less, so that we can reliably use the results of such averages for our comparisons of $\overline{\mu_{\rm LT}}$(no tides) vs $\overline{\mu_{\rm LT}}$(all tides).

Before implementing such strategy for different $T_{\rm obs}$, Δt and noise we carefully analyzed the $\Delta t = 15$ days, $T_{\rm obs}$=4 years experiment considered in [15] by trying to obtain the quantitative features outlined there, so that we start from a firm and reliable basis. This goal was achieved by proceeding as outlined in the previous section and adopting a uniformly distributed random noise with an amplitude of 35 mas.

Fig. 2 shows the results for $\Delta\overline{\mu_{\rm LT}}$ obtained with $\Delta t = 15$ days and a uniform random noise with amplitudes of 50 mas and 35 mas corresponding to the characteristics of the real curves in [66, 15]. Notice that our estimates for the case $T_{\rm obs} = 4$ years almost coincide with those in [15] who claim $\Delta\mu_{\rm tides} \leq 4\%$. Notice that for $T_{\rm obs} > 7$ years the
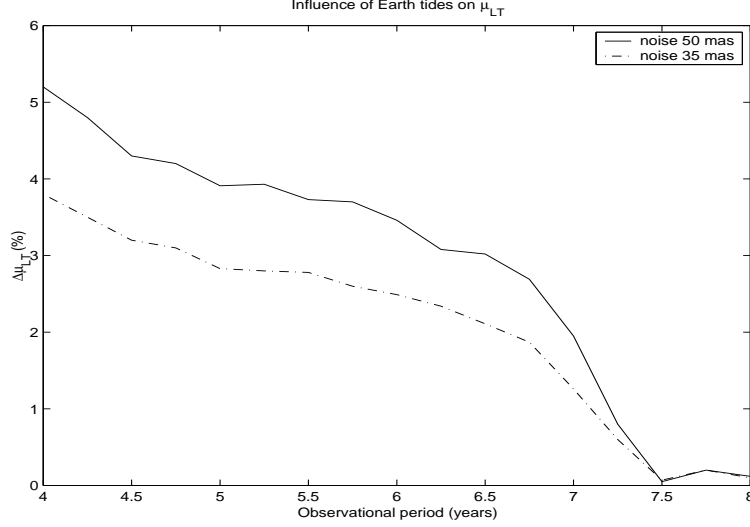
Fig. 2. – Effects of the long period signals on the recovery of μ_{LT} for Δt=15 days and different choice of uniform random noise. Each point in the curves represents an average over 1,500 runs performed by varying randomly the initial phases and the noise' s pattern. $\Delta\mu_{\mathrm{LT}}$ is the difference between the least squares fitted value of μ_{LT} when both the IM and the FM includes the LT plus all the harmonics and that obtained without any harmonic both in the IM and in the FM.

effect of tidal perturbations errors falls around 2%. By choosing different Δt does not introduce appreciable modifications to the results presented here. This fact was tested by repeating the set of runs with $\Delta t = 7$ and 22 days.

Up to this point we dealt with the entire set of long-period signals affecting the combined residuals; now we ask if it is possible to assess individually the influence of each tide on the recovery of LT. We shall focus our attention on the case $\Delta t = 15$ days, T_{obs}=4 years.

In order to evaluate the influence of each tidal constituent on the recovery of μ_{LT} two complementary approaches could be followed in principle. The first one consists of starting without any long-period signal either in the IM or in the FM, and subsequently adding to them one harmonic at a time, while neglecting all the others. In doing so it is implicitly assumed that each constituent is mutually uncorrelated with any other one present in the signal. In fact, the matter is quite different since if for the complete model case we consider the covariance and correlation matrices of the FM adjusted parameters it turns out that the LT is strongly correlated, at a level of $|\ Corr(i,j)|\ > 0.9$, with certain harmonics, which happen to be mutually correlated too. These are
• $K_1,\ l = 2$ (P=1,043.67 days; 1.39 cycles completed)
• $K_1,\ l = 2$ (P=-569.21 days; 2.56 cycles completed)
• $K_1,\ l = 3,\ p = 2$ (P=-336.28 days; 4.34 cycles completed)
• $K_2,\ l = 3,\ p = 1$ (P=-435.3 days; 3.35 cycles completed)
• Solar Radiation Pressure, (P=657 days; 2.22 cycles completed)
• perigee odd zonal C_{30}, (P=821.79; 1.77 cycles completed)
Their FM parameters are indeterminate in the sense that the values estimated are smaller

than the relative uncertainties assumed to be $\sqrt{Cov(i,i)}$. On the contrary, there are other signals which are poorly correlated to the LT and whose reciprocal correlation too is very low and that are well determined. These are

- K_2, $l = 3$, $p = 2$ (P=-211.4 days; 6.91 cycles completed)
- S_2, $l = 3$, $p = 1$ (P=-128.6 days; 11.3 cycles completed)
- S_2, $l = 3$, $p = 2$ (P=-97.9 days; 14.9 cycles completed)
- P_1, $l = 3$, $p = 1$ (P=-166.2 days; 8.78 cycles completed)
- P_1, $l = 3$, $p = 2$ (P=-118.35 days; 12.3 cycles completed)

It is interesting to notice that over $T_{\rm obs} = 4$ years the signals uncorrelated with the LT have in general described many complete cycles, contrary to these correlated with LT. This means that the signals that average out over $T_{\rm obs}$ decorrelate with LT, allowing the gravitomagnetic trend to emerge clearly against the background, almost not affecting the LT recovery. This feature has been tested as follows. In a first step, all the uncorrelated tides have been removed from both the IM (50 mas uniform random noise) and the FM, leaving only the correlated tides in. The runs were then repeated, all other things being equal, the following values were recorded: $\overline{\mu_{\rm LT}} = 1.2104$, $\overline{\delta\mu_{\rm LT}} = 0.1006$ with a variation with respect to the complete model case ($\overline{\mu_{\rm LT}} = 1.2073$, $\overline{\delta\mu_{\rm LT}} = 0.1295$) of: $\Delta\overline{\mu_{\rm LT}} \simeq 0.3\%$, $\Delta\overline{\delta\mu_{\rm LT}} \simeq 2.9\%$. Conversely, if all the signals with strong correlation are removed from the simulated data and from the FM, leaving only the uncorrelated ones in, we obtain: $\overline{\mu_{\rm LT}} = 1.1587$, $\overline{\delta\mu_{\rm LT}} = 0.0186$ with $\Delta\overline{\mu_{\rm LT}} \simeq 4.8\%$, $\Delta\overline{\delta\mu_{\rm LT}} \simeq 11\%$. Notice that the sum of both contributions for $\Delta\overline{\mu_{\rm LT}}$ yields exactly the overall value $\Delta\overline{\mu_{\rm LT}} = 5.2\%$ as obtained in the previous analysis (cf. fig. 2 for $T_{\rm obs} = 4$ years). This highlights the importance of certain long period signals in affecting the recovery of LT and justify the choice of treating them simultaneously as it was done in obtaining fig. 2. Moreover, it clearly indicates that the efforts of the scientific community should be focused on the improvement of the knowledge of these tidal constituents. It has been tested that for $T_{\rm obs} = 8$ years all such "geometrical" correlations among the LT and the harmonics nearly disappear, as it would be intuitively expected.

4˙5. *The effect of the very long periodic harmonics.* – In this section we shall deal with those signals whose periods are longer than 4 years which could corrupt the recovery of LT resembling superimposed trends if their periods are considerably longer than the adopted time series length.

In section 3 we have shown the existence of a very long periodic ocean tidal perturbation acting upon the perigee of LAGEOS II. It is the K_1 $l = 3$ $p = 1$ $q = -1$ constituent with period $P = 1,851.9$ days (5.07 years) and nominal amplitudes of $-1,136$ mas. In ref.[87], for the effect of the direct solar radiation pressure on the perigee of LAGEOS II, it has been explicitly calculated, by neglecting the effects of the eclipses, a signal SRP(4,241) with $P = 4,241$ days (11.6 years) and nominal amplitude of 6400 mas. The mismodelling on these harmonics, both of the form $\delta A \sin\left(\frac{2\pi}{P}t + \phi\right)$, amounts to 64.5 mas for the tidal constituent, as shown in section 3.6, and to 32 mas for SRP(4,241), according to ref.[87].

About the actual presence of such semisecular harmonics in the spectrum of the real combined residuals, it must be pointed out that, over $T_{\rm obs} = 3.1$ years [66], it is not possible that so low frequencies could be resolved by Fourier analysis. Indeed, according to refs.[88, 89], when a signal is sampled over a finite time interval $T_{\rm obs}$ it induces a

sampling also in the spectrum. The lowest frequency that can be resolved is

$$(148) \qquad f_{\min} = \frac{1}{2T_{\text{obs}}},$$

i.e. a harmonic must describe, at least, half a cycle over T_{obs} in order to be detected in the spectrum. $f_{\min}$ is called elementary frequency band and it also represents the minimum separation between two frequencies in order to be resolved. For our two signals we have $f(K_1) = 5.39 \times 10^{-4}$ cycles per day (cpd) and $f(\text{SRP}) = 2.35 \times 10^{-4}$ cpd; over 3.1 years $f_{\min} = 4.41 \times 10^{-4}$ cpd. This means that the two harmonics neither can be resolved as distinct nor they can be found in the spectrum at all. In order to resolve them we should wait for $T_{\text{obs}} = 4.5$ years which corresponds to their separation $\Delta f = 3.04 \times 10^{-4}$ cpd, according to eq. (148). In view of the potentially large aliasing effect of these two harmonics on the LT it was decided to include both K_1 $l = 3$ $p = 1$ and SRP(4,241) in the simulated residual curve at the level of mismodelling claimed before.

In order to obtain an upper bound of their contribution to the systematic uncertainty in μ_{LT} we proceeded as follows. First, we calculated the temporal average of the perturbations induced on the combined residuals by the two harmonics over different T_{obs} according to

$$(149) \quad I = \frac{1}{T_{\text{obs}}} \int_0^{T_{\text{obs}}} c_2 \delta A \sin\left(\frac{2\pi}{P}t + \phi\right)dt = c_2 \frac{\delta A}{\tau}(\cos\phi + \sin\phi\sin\tau - \cos\phi\cos\tau),$$

with $\tau = 2\pi\frac{T_{\text{obs}}}{P}$. It turns out that, for given T_{obs}, the averages are periodic functions of the initial phases ϕ with period 2π. Since the gravitomagnetic trend is positive and growing in time, we shall consider only the positive values of the temporal averages corresponding to those portions of sinusoid which are themselves positive. Moreover, notice that, in this case, one should consider if the perturbation's arc is rising or falling over the considered T_{obs}: indeed, even though the corresponding averages could be equal, it is only in the first case that the sinusoid has an aliasing effect on the LT trend. The values of ϕ which maximize the averages were found numerically and for such values the maxima of the averages were calculated. Subsequently, these results in mas were compared to the amount of the predicted gravitomagnetic shift accumulated over the chosen T_{obs} by the combined residuals $y_{\text{LT}} = 60.2$ (mas/y)$\times T_{\text{obs}}$ (y). The results are shown in Table XIV and Table XV and, as previously outlined, represent a pessimistic estimate.

TABLE XIV. – *Effect of the averaged mismodelled harmonic K_1 $l = 3$ $p = 1$ on the Lense-Thirring trend for different T_{obs}. In order to obtain upper limits the maximum value for the average of the tidal constituent has been taken, while for the gravitomagnetic effect it has been simply taken the value $\dot{y}_{\text{LT}} \times T_{\text{obs}}$.*

T_{obs} (years)	max $c_2 \left\langle \delta\omega^{\text{II}} \right\rangle$ (mas)	y_{LT} (mas)	max $c_2 \left\langle \delta\omega^{\text{II}} \right\rangle / y_{\text{LT}}$ (%)
4	5.6	240.8	2.3
5	0.3	301	0.09
6	3.3	361.2	0.9
7	4.8	421.4	1.1

TABLE XV. – *Effect of the averaged mismodelled harmonic* SRP(4, 241) *on the Lense-Thirring trend for different* T_{obs}. *In order to obtain upper limits the maximum value for the average of the radiative harmonic has been taken, while for the gravitomagnetic effect it has been simply taken the value* $\dot{y}_{LT} \times T_{obs}$.

T_{obs} (years)	max $c_2 \left\langle \delta\omega^{II} \right\rangle$ (mas)	y_{LT} (mas)	max $c_2 \left\langle \delta\omega^{II} \right\rangle / y_{LT}$ (%)
4	9.1	240.8	3.7
5	8	301	2.6
6	6.8	361.2	1.8
7	5.6	421.4	1.3

It is interesting to notice that an analysis over $T_{obs} = 5$ years, that should not be much more demanding than the already performed works, could cancel out the effect of the K_1 $l = 3$ $p = 1$ tide; in this scenario the effect of SRP(4,241) should amount, at most to 2.6% of the LT effect. Notice also that for $T_{obs} = 7$ years, a time span sufficient for the LT to emerge on the background of most of the other tidal perturbations, the estimates of fig. 2 are compatible with those of Table XIV and Table XV which predict an upper contribution of 1.1% from the K_1 $l = 3$ $p = 1$ and 1.3% from SRP(4,241) on the LT parameter μ_{LT}.

An approach, similar to that used in [90] in order to assess the influence of the eclipses and Earth penumbra effects on the perigee of LAGEOS II has been applied also to our case. It consists of fitting with a straight line only the mismodelled perturbation to be considered and, subsequently, comparing the slope of such fits to that due to gravitomagnetism which is equal to 1 in units of 60.2 mas/y. We have applied this method to K_1 $l = 3$ $p = 1$ and SRP(4,241) with the already cited mismodelled amplitudes and by varying randomly the initial phases ϕ within $[-2\pi, \ 2\pi]$. The mean value of the fit's slope, in units of 60.2 mas/y, over 1,500 runs is very close to zero. Concerning the upper limits of $\Delta\mu_{LT}$ derived from these runs, they agree with those released in Table XIV and Table XV up to 1-2 %.

The method of temporal averages can be successfully applied also for the $l = 2$ $m = 0$ 18.6-year tide. It is a very long period zonal tidal perturbation which could potentially reveal itself as the most dangerous in aliasing the results for μ_{LT} since its nominal amplitude is very large and its period is much longer than the T_{obs} which could be adopted for real analysis. Ciufolini in ref.[14] claims that the combined residuals have the merit of cancelling out all the static and dynamical geopotential's contributions of degree $l = 2, 4$ and order $m = 0$, so that the 18.6-year tide would not create problems. This topic was quantitatively addressed in a preliminary way. Indeed, in order to make comparisons with other works, we have simply calculated for $T_{obs} = 1$ year the combined residuals with only the mismodelled amplitudes of the 18.6-year tidal perturbations on the nodes of LAGEOS and LAGEOS II and the perigee of LAGEOS II. This means that the dynamical pattern over the time span of such important tidal perturbation was not investigated. We did this by calculating the average over different T_{obs}. The results show clearly that the 18.6-year tide does not affect at all the estimation of μ_{LT} if we adopt as observable the combined residuals proposed by Ciufolini. Indeed, for $T_{obs} = 4$ years, it turns out that the average effect will reach, at most, 0.08% of the gravitomagnetic shift over the same time span.

This feature of the 18.6-year tide is confirmed also by fitting with a straight line only the sinusoid of this perturbation on the combined residual: the adjusted slope amounts, at most, to less than 1% of the gravitomagnetic effect for different $T_{\rm obs}$.

4˙6. *Conclusions.* – The detection of the Lense-Thirring effect can be achieved by means of the eq. (5). Ciufolini in ref.[14] claims that the static and dynamical terms of degree $l = 2, 4$ and order $m = 0$ of the geopotential do not affect his proposed combined residuals.

In this section we have tested this statement in regard not only to the $l = 2, 4$ $m = 0$ solid and ocean Earth tides, but also to the $m = 1, 2$ ones and to the other long-period perturbations which affect the combined residuals.

Concerning the zonal tides, in order to compare our results to those released in [66], we have preliminarily used the nominal perturbative amplitudes by calculating eq. (5) on a time span of 1 year. As far as the $l = 2$ $m = 0$ tides are concerned, the 18.6-year tide cancels out at a level of 10^{-1} only. But if we repeat the calculations with the mismodelled amplitudes over 1 year the accuracy of the cancellation grows to 10^{-3}. This shows that the more accurate the dynamical models employed in building up the orbital residuals are, the more accurate the recovery of the Lense-Thirring becomes. The $l = 4$ zonal tides do not create problems. Also the $l = 3$ $m = 0$ tides, and this is an unpredicted feature, although at a lesser extent, cancel out at a level ranging from 10^{-1}-10^{-2} if they are properly accounted in the residuals' construction. This points towards a better understanding, from both a theoretical and experimental point of view, of the $l = 3$, $m = 0$ part of the tidal spectrum. The results presented in this section not only confirm the usefulness of the formula by Ciufolini for the $l = 2, 4$ $m = 0$ tides, but also extend its validity to the $l = 3$ $m = 0$ part of the tidal response spectrum.

In regard to the tesseral and sectorial tides, on one hand, by simulating the real residual curve in order to reproduce as closely as possible the results obtained for the $\Delta t = 15$ days $T_{\rm obs} = 4$ years scenario published in [15] it has been possible to refine and detail the estimates for it. On the other hand, this procedure also extends them to longer observational periods in view of new, more sophisticated analysis to be completed in the near future based on real data analyzed with the orbit determination software GEODYN II in collaboration with the teams from the Joint Center for Earth Systems Technology at NASA Goddard Space Flight Center and at the University of Rome La Sapienza. Since such numerical analysis is very demanding in terms of both time employed and results analysis burden, it should be very useful to have a priori estimates which could better direct the work. This could be done, e.g., by identifying which tidal constituents $\mu_{\rm LT}$ is more or less sensitive to in order to seek improved dynamical models for use in GEODYN.

As far as the perturbations generated by the solid Earth tides, the high level of accuracy with which they are known has yielded a contribution to the systematic errors in $\mu_{\rm LT}$ which falls well below 1%, so that they are of no concern at present.

Concerning the ocean tidal perturbations and the other long-period harmonics, for those whose periods are shorter than 4 years, the role played by $T_{\rm obs}$, Δt and the noise has been investigated. It turned out that Δt has no discernible effect on the adjusted value of $\mu_{\rm LT}$, while $T_{\rm obs}$ is very important and so is the noise. The main results for these are summarized in fig. 2, which tells us that the entire set of long-period signals, if properly accounted for in building up the residuals, affect the recovery of the Lense-Thirring effect at a level not worse than $4\% - 5\%$ for $T_{\rm obs} = 4$ years; the error contribution diminishes to about 2% after 7 years of observations.

We have also shown which tides are strongly anticorrelated and correlated with the gravitomagnetic trend over 4 years of observations. The experimental and theoretical efforts should concentrate on improving these constituents in particular. This geometrical correlation tends to diminish as T_{obs} grows. This can be intuitively recognized by noting that the longer T_{obs} is, the larger the number of cycles these periodic signals are sampled over and cleaner the way in which the secular Lense-Thirring trend emerges against the background "noise".

The ocean tide constituents K_1 $l = 3$ $p = 1$ and the solar radiation pressure harmonic SRP(4,241) generate perturbations on the perigee of LAGEOS II with periods of 5.07 years and 11.6 years respectively, so that they act on the Lense-Thirring effect as biases and corrupt its determination with the related mismodelling: indeed they may resemble trends if T_{obs} is shorter than their periods. They were included in the simulated residual curve and their effect was evaluated in different ways with respect to the other tides. An upper bound was calculated for their action and it turns out that they contribute to the systematic uncertainty in the recovery of μ_{LT} at a level of less than 4% depending on T_{obs} and the initial phases ϕ. The results are summarized in Table XIV and Table XV. An observational period of 5 years, which seems to be a reasonable choice in terms of time scale and computational burden, allows one to average out the effect of the K_1 $l = 3$ $p = 1$.

The strategy followed for the latter harmonics has been extended also to the $l = 2$ $m = 0$ zonal 18.6-year tide. The obtained results confirm the claim in [14] that it does not affect the combined residuals.

In conclusion, the strategy presented here could be used as follows. Starting from a simulated residual curve based on the state of art of the real analysis performed until now, it provides helpful indications in order to improve the force models of the orbit determination software as far as tidal perturbations are concerned and to perform new analysis with real residuals. Moreover, when real data will be collected for a given scenario it will be possible to use them in our software in order to adapt the simulation procedure to the new situation; e.g. it is expected that the noise level in the near future will diminish in view of improvements in laser ranging technology and modelling. Thus, we shall repeat our analysis for $\Delta\mu_{\text{tides}}$ when these new results become available.

5. – Measuring the gravitoelectric perigee advance with LAGEOS and LAGEOS II

In order to test general relativity versus alternative metric theories of gravitation, following a method introduced by Eddington (1922), Robertson (1962) and Schiff (1967), one can expand the spacetime metric (which describes the gravitational interaction) at the order beyond Newtonian theory (post-Newtonian) and then multiply each post-Newtonian term by a dimensionless parameter, the PPN parameters, to be experimentally determined. Using this method, Nordtvedt and Will have developed the PPN (Parameterized-Post-Newtonian) formalism [91], a powerful and useful tool for testing general relativity and alternative metric theories. Therefore, the PPN formalism is a post–Newtonian parameterized expansion of the metric tensor **g** and of the energy-momentum tensor **T** in terms of small known classical potentials.

In the slow-motion and weak-field approximation, at the so-called post-Newtonian limit, the structure of known metric theories of gravity is identical apart from the numerical values of the PPN parameters which appear in the expansion of the metric coefficients [91, 8, 92]. Especially meaningful are the parameters β and γ, i.e the usual

Eddington-Robertson-Schiff parameters used to describe the "classical" tests of General Relativity. γ measures how much space curvature is produced by unit rest mass and in the standard parameterized post-Newtonian gauge β accounts for the level of nonlinearity in the superposition law for gravity [32]. In general relativity $\beta = 1$ and $\gamma = 1$.

To-day a very accurate measurement of γ was performed by using the Viking time delay [93]: the results was $\gamma = 1.000 \pm 2 \times 10^{-3}$. The quoted uncertainty allows for possible systematic errors. Other recent measurements exploit the gravitational bending of the electromagnetic waves at various wavelength [94] obtaining an uncertainty of the order of 10^{-3}; e.g., according to the VLBI radio analysis by [95] $\gamma = 0.9996 \pm 1.7 \times 10^{-3}$, while in ref.[94] $\gamma = 0.997 \pm 3 \times 10^{-3}$ is quoted based on the astrometric observations of the electromagnetic waves deflection in the visible. An improvement in the accuracy of two orders of magnitude [94] is expected from the future GAIA astrometric mission [96]. Lunar laser ranging (LLR) measurements of the geodetic precession yields for γ an accuracy of 10^{-2} [97]. However a careful discussion of the different terms in the lunar motion yields eventually $\gamma = 1.000 \pm 5 \times 10^{-3}$ as the present LLR result [94].

The value of the parameter β, which cannot be measured independently, can be obtained from the measured values of γ and of some combinations of γ and β: $\eta = 4\beta - \gamma - 3$ and $\frac{2+2\gamma-\beta}{3}$ are the most accurately determined. General relativity predicts $\eta = 0$ and $\frac{2+2\gamma-\beta}{3} = 1$. For β in ref.[98] by using LLR data $\delta\beta = 4.7 \times 10^{-4}$ is reported.

The combination η measures the possible violation of the strong equivalence principle, i.e. the so-called Nordvedt effect [99]. η has been measured by analyzing the motion of the Moon via LLR data analyses [100, 97, 98]. The most recent determination of η by LLR is $\eta = 0.0002 \pm 8 \times 10^{-4}$ [98].

The combination $\frac{2+2\gamma-\beta}{3}$ is related to the well known pericenter shift of a test body induced by the Schwarzschild's gravioelectric part of the metric for a static, spherically symmetric distribution of mass-energy [32, 8]. This effect has been accurately measured for the Mercury perihelion shift in the field of the Sun by means of the echo delays of radar signals transmitted from Earth to Mercury [101] yielding $\frac{2+2\gamma-\beta}{3} = 1.005 \pm 7 \times 10^{-3}$. Inclusion of the probable contribution of systematic errors raises the uncertainty to about 2×10^{-2}. In this case the major sources of systematic error are the poorly-known variation in topography on the planet's surface and the uncertainties in the radar scattering law [102, 103].

It should be considered that the interpretation of the perihelion advance of Mercury as a test of general relativity must cope with the uncertainty in the mass quadrupole moment of the Sun which also contributes to the perihelion advance. From the expression of the perihelion precession and from the 1976 experimental uncertainties in $\dot\omega$, one can easily calculate that for Mercury orbiting the Sun, any value of $J_{2\odot}$ larger than about 3×10^{-6} would disagree with the general relativistic prediction of 42.98 arcseconds/century; indeed, according to some authors measured values of $J_{2\odot}$ may be as large as $\sim 5.5 \times 10^{-6}$ (for a comprehensive discussion see refs.[8, 104]). Laboratory experiments have been also proposed [105] to measure the solar mode $l = 1$, to get information on the rotation of the core of the Sun from the $l = 1$ rotational frequency splitting. Nevertheless, according to more recent determinations of $J_{2\odot}$ using the analysis of the Sun's pressure modes, both from the ground-based network of observatories and the space based SOHO, $J_{2\odot} = (2.3 \pm 0.1) \times 10^{-7}$ [106]; in ref.[107] a theoretical estimate of $J_{2\odot} = (2.0 \pm 0.4) \times 10^{-7}$ is reported. Thus, according to these values of $J_{2\odot}$ the observed perihelion advance of Mercury is well in agreement with the general relativistic predictions.

In order to measure $J_{2\odot}$, among other astrodynamical and relativistic parameters,

several space missions have been proposed using a variety of techniques: the most recent and promising are SORT, IPLR and ASTROD [108]. In [109] a measurement of the LAGEOS laser ranged satellite perigee shift in the field of the Earth is quoted, but the accuracy amounts only to 2×10^{-1}. More accurate measurements of $\frac{2+2\gamma-\beta}{3}$ might be performed in the future by means of an ESA Mercury orbiter [110, 111].

In this section we explore the possibility of performing a complementary measurement of $\frac{2+2\gamma-\beta}{3}$ in the gravitational field of the Earth by using some suitable combinations of the orbital residuals of the presently (or proposed) existing spherical geodetic laser ranged satellites with particular emphasis to LAGEOS and LAGEOS II in order to exploit the relevant experience obtained with the gravitomagnetic measurements in [112, 66, 15]. Moreover, as a secondary outcome of the proposed experiment, by combining the accurate determinations of the Nordtvedt parameter η and of $\frac{2+2\gamma-\beta}{3}$ from SLR it would be possible to obtain independent values for γ and β.

This section is organized as follows. In subsect. 1 we compare the present experimental accuracy in satellite laser-ranging measurements with the relativistic expressions of the perigee shift of the two LAGEOS satellites. In subsect. 2 we analyze some of the most important sources of systematic errors: the even zonal harmonics of the static part of the geopotential, the Earth solid and ocean tidal perturbations, the direct solar radiation pressure and the mismodelling of the inclination. Subsect. 3 is devoted to the discussion of the obtained results and to the conclusions.

5˙1. *The relativistic perigee precession of LAGEOS type satellites.* – As known, in the slow-motion and weak-field approximation, the Schwarzschild metric generated by a static, spherically symmetric distribution of mass-energy induces an additional post-Newtonian "gravitoelectric" force which acts on the orbit of a test body by shifting its pericenter; in the PPN formalism the pericenter rate can be written as

$$(150) \qquad \dot{\omega}_{\mathrm{GR}} = \frac{3nGM}{c^2 a(1-e^2)} \times \frac{2+2\gamma-\beta}{3}.$$

In the following we define $\nu \equiv \frac{2+2\gamma-\beta}{3}$. General Relativity predicts that the perigee shifts for LAGEOS and LAGEOS II amount to 3,312.35 mas/y and 3,387.46 mas/y, respectively.

Following ref.[14] the actual experimental precision allows for detecting such rates for both LAGEOS. Indeed, for the perigee the observable quantity is $r \equiv ea\dot{\omega}$ and at present its measurement error amounts to about $\delta r_{\mathrm{exp}} \leq 1$ cm for the two LAGEOS, over several orbits and for a given set of force models (i.e. not including modelling errors). Since the LAGEOS eccentricity is $e_{\mathrm{I}} = 4.5 \times 10^{-3}$ the accuracy in detecting the perigee is $\delta\omega^{\mathrm{I}}_{\mathrm{exp}} = \delta r_{\mathrm{exp}}/(e_{\mathrm{I}}a_{\mathrm{I}}) \simeq 37$ mas. So, over 1 year the relative accuracy of the measurement of the relativistic perigee shift would be $\sim 1 \times 10^{-2}$. For LAGEOS II this measurement accuracy is better than that of LAGEOS indeed the LAGEOS II eccentricity is $e_{\mathrm{II}} = 1.4 \times 10^{-2}$, so that $\delta\omega^{\mathrm{II}}_{\mathrm{exp}} \simeq 12$ mas; this may yield an accuracy of about 3×10^{-3} over 1 year. These considerations rule out the possibility of directly using the perigee of the other existing spherical geodetic laser-ranged satellites Etalon-1, Etalon-2, Ajisai, Stella, Westpac-1 because their eccentricities are even smaller than that of LAGEOS. On the contrary, Starlette has an eccentricity of the order of 2×10^{-2}; however, since it orbits at a lower altitude it is more sensitive than the LAGEOS satellites to atmospheric drag and to Earth's zonal harmonics, so that it would be difficult to process its data at an acceptable level of accuracy. Accordingly, we will focus on the

perigee of LAGEOS and especially of LAGEOS II in order to accurately detect the gravitoelectric relativistic shift in the gravitational field of Earth.

5˙2. *The systematic errors.* – The most important source of systematic error in such measurements is represented by the mismodelling induced by the even zonal harmonics of the Earth gravitational field [1] on the classical perigee precession. By using the covariance matrix of the EGM96 Earth gravity model [19] and adding the correlated terms in a root-sum-square fashion up to degree $l = 20$ we obtain for LAGEOS a systematic error $\delta\nu/\nu_{\mathrm{zonals}} = 8.1 \times 10^{-3}$, whereas for LAGEOS II we have $\delta\nu/\nu_{\mathrm{zonals}} = 1.5 \times 10^{-2}$.

Since the major source of uncertainty lies in the first two even zonal harmonics δJ_2 and δJ_4, following [14] for the Lense-Thirring LAGEOS experiment, we search for suitable combinations of orbital residuals of the existing SLR satellites in order to eliminate most static and dynamical even zonal terms of the geopotential. In Table XVI we report the most promising combinations: their general form is

$$(151) \qquad \delta\dot{\omega}^{\mathrm{II}} + \sum_{j=1}^{N} c_j \delta\dot{\Omega}^j + c_{\mathrm{N}+1}\delta\dot{\omega}^{\mathrm{I}} = x_{\mathrm{GR}}\ \nu,$$

in which N is the number of the nodes of different SLR satellites employed, x_{GR} is the slope, in mas/y, of the relativistic trend to be measured and $\delta\nu/\nu_{\mathrm{zonals}}$ is the systematic error induced by the even zonal harmonics up to degree $l = 20$ calculated with EGM96 covariance matrix. It is important to stress that the use of LAGEOS, due to their altitude, makes our measurement substantially insensitive to the errors in the zonal harmonics of degree $l > 20$, so that our estimates of $\delta\nu/\nu_{\mathrm{zonals}}$ presented here are valid even in the case that the EGM96 covariance matrix for higher degrees $l > 20$ would not be accurate enough. In addition to LAGEOS and LAGEOS II, we have only considered Ajisai since

TABLE XVI. – *PPN combined residuals.*

κ	Ω^{II} c_1	Ω^{I} c_2	Ω^{Aj} c_3	ω^{I} c_4	x_{GR} (mas/y)	$\delta\nu/\nu_{\mathrm{zonals}}$
1	-0.868	-2.855	0	0	3,387.46	6.59×10^{-3}
2	-2.514	-4.372	0	2.511	11,704.92	1.1×10^{-3}
3	-1.962	-3.693	0.0366	1.370	7,928.51	8.1×10^{-4}

it is well tracked, contrary to, e.g., the Etalons, and it would be less demanding than the other satellites to reduce its laser ranged data to a level of accuracy comparable to that of LAGEOS and LAGEOS II. Moreover, the other SLR satellites orbit at lower altitudes, therefore they are more sensitive to the higher degree terms of the geopotential. Consequently, as confirmed by numerical calculations, the inclusion in their data in the combined residuals would increase $\delta\nu/\nu_{\mathrm{zonals}}$,.

Note that the systematic error induced by the mismodelled secular rates of the even zonal harmonics of the geopotential is really critical because it can be considered as an unavoidable part of the total error in the experiment. Indeed, the resulting aliasing trend cannot be removed from the data and nothing can be done about it apart from assessing

as more reliably as possible the related error.(^{9})

It is important to point out that the values quoted in Table XVI for $\delta\nu/\nu_{\mathrm{zonals}}$ will be reduced in the near future when the data from the CHAMP mission will be released.

In regard to the evaluation of the impact of other sources of systematic errors in this section we consider in detail only the combination *1* of Table XVI so to exploit the background acquired with the Lense-Thirring LAGEOS experiment [112, 66, 15]. Moreover, reducing the Ajisai' s data to an acceptable level of accuracy for our measurement would neither be a trivial nor an immediate task to be performed and the inclusion of the perigee of LAGEOS would raise the experimental error. E.g., for combination *2* of Table XVI, over 1 year, the impact of the error in measuring the perigee rate of LAGEOS amounts to $2.5 \times (3.1 \times 10^{-3}) = 7.7 \times 10^{-3}$ while for combination *3* it is $1.370 \times (4.7 \times 10^{-3}) = 6.4 \times 10^{-3}$.

5˙**3.** *Discussion and conclusions*. – In Table XVII we summarize the results obtained for a 8 years long time span with 7 days arc lengths. The results and the methods of sections 3 and 4 and of ref.[87, 113] have been used.

TABLE XVII. – *Preliminary error budget: $T_{obs} = 8$ years, $\Delta t = 7$ days.*

Even zonal harmonics	6.59×10^{-3}
J_3 geopotential	3.2×10^{-4}
Tides	4.4×10^{-4}
Non-gravitational effects	1×10^{-4}
Measurement error in LAGEOS II perigee	4×10^{-4}
Total systematic error	7.3×10^{-3}

In regard to the non–gravitational errors, according to the results of ref.[87] for the direct solar radiation pressure and the Earth's albedo and to the results of ref.[113] for the thermal thrust perturbations and the asymmetric reflectivity, the corresponding uncertainty would amount to almost 1×10^{-2} over 7 years. In obtaining this result a very pessimistic approach has been adopted by assuming a mismodeling of 20% for all the perturbing effects except for the direct solar radiation pressure which has been assumed to have an uncertainty at the 0.5% level. However, we stress that only the Earth's thermal thrust, or Yarkovski-Rubincam effect, induces a mismodeled linear trend whose impact would amount to about 1×10^{-4}: the other non–gravitational forces are time–varying with known periodicities and can be fitted and removed from the signal as done for the tidal perturbations.

In assessing the total systematic error we have accounted for the fact that the gravitational errors are not independent simply by summing them up. Then, we have added them and the other independent sources of errors in a root-sum-square fashion. Note that the error in the LAGEOS II perigee refers to 1 year only by assuming an error of 1 cm in its radial position. Moreover, the estimate of the statistical formal error has been

---

(^{9}) About combination *3*, it should be noted that in order to obtain more reliable and accurate estimates of the systematic error due to the even zonal harmonics of the geopotential it should be better to extend the calculations to higher degrees than $l = 20$ due to the sensitivity of Ajisai to such higher degree terms.

obtained by considering the noise level in the LAGEOS data of 1998 Lense-Thirring experiment; in the near future and for longer time spans these uncertainties will be reduced. Moreover, it is important to emphasize that the data from the CHAMP and GRACE missions will soon yield a notable reduction of the systematic error due to the higher degree static even zonal harmonics of the geopotential and of the solid and ocean tides systematic errors as well. In particular, a very significant reduction of the systematic errors will take place due to the static part of the geopotential, which has turned out to be the most important source of uncertainty.

The results obtained for the combination *1* examined here together with those released in ref.[98] for the combination η would allow to measure $\beta = \frac{2}{7}\eta + \frac{3}{7}\nu + \frac{4}{7}$ independently of other measurements of γ with $\sim 3.3 \times 10^{-3}$ accuracy over 8 years; this result, which is of the same order of magnitude of that obtained with the radar ranging technique [102], should be compared with the most recent $\delta\beta = 4.7 \times 10^{-4}$ obtained from the LLR data [98]. The parameter γ, given by $\gamma = \frac{1}{7}\eta + \frac{12}{7}\nu - \frac{5}{7}$, could be measured less precisely over the same time span: $\delta\gamma \sim 1.2 \times 10^{-2}$.

6. – The LARES mission revisited: some alternative scenarios

6˙1. *Introduction*. – In order to measure the Lense-Thirring drag with an accuracy of few percent, in [12] it was proposed to launch a passive geodetic laser-ranged satellite-the former LAGEOS III - with the same orbital parameters of LAGEOS apart from its inclination which should be supplementary to that of LAGEOS.

This orbital configuration would be able to cancel out exactly the classical nodal precessions provided that the observable to be adopted is the sum of the residuals of the nodal precessions of LAGEOS III and LAGEOS

$$(152) \qquad\qquad \delta\dot{\Omega}^{\mathrm{III}} + \delta\dot{\Omega}^{\mathrm{I}} = 62\mu_{\mathrm{LT}}.$$

Later on the concept of the mission slightly changed. The area-to-mass ratio of LAGEOS III was reduced in order to make less relevant the impact of the non-gravitational perturbations and the eccentricity was enhanced in order to be able to perform other general relativistic tests: the LARES was born. The most recent error budget of the LARES Lense-Thirring experiment claim an accuracy of the order of 3%. Unfortunately, at present we do not know if the LARES mission will be approved by any space agency.

In this section we investigate the possibility of further reducing the error in this important proposed mission. This section is organized as follows. In subsect. 2 we analyze in detail the impact of the unavoidable injection errors in the orbital parameters of LARES on the systematic error induced by the mismodelling in the even zonal harmonics of the geopotential according to the most recently released Earth gravity model. Moreover, in subsect. 3 we propose an alternative configuration which should be able to reduce this error by one order of magnitude. It adopts as observable a suitable combination of the orbital residuals of the nodes of LAGEOS, LAGEOS II and LARES, and the perigees of LAGEOS II and LARES. It presents also the important advantage that it is almost insensitive to the errors in the inclination of LARES, contrary to the original LAGEOS/LARES only configuration. The negative implications of placing the LARES in a low-altitude polar orbits are examined in subsect. 4. Subsect. 5 is devoted to the conclusions.

6˙2. *The impact of the even zonal harmonics of the geopotential on the original LARES mission*. – Let us calculate the systematic error induced by the mismodelling in the even degree zonal coefficients J_2, J_4,... of the geopotential on the sum of the classical precessions of the nodes of LAGEOS and LARES. It is important to stress that it is the major source of systematic error and it cannot be eliminated in any way. We will use the covariance matrix of the Earth gravity field model EGM96 [19] by summing up in a root sum square fashion the correlated contributes up to degree $l = 20$[10]. The relative error obtained by using the nominal values amounts to

$$(153) \qquad\qquad \frac{\delta\mu_{\mathrm{LT}}}{\mu_{\mathrm{LT}}}_{\mathrm{zonals}} = 3 \times 10^{-3}.$$

It is not equal to zero because we have assumed $e_{\mathrm{LR}} = 0.04$ while $e_{\mathrm{LAGEOS}} = 0.0045$. If it was $e_{\mathrm{LR}} = e_{\mathrm{LAGEOS}}$, then the classical nodal precessions would be exactly equal in value and opposite in sign and would cancel out. Notice that the coefficients with which $\delta\dot{\Omega}^{\mathrm{III}}$ and $\delta\dot{\Omega}^{\mathrm{I}}$ enter the combination of eq. (152) do not depend on any orbital parameters: they are constants equal to 1. Moreover, eq. (152) is affected by all the classical nodal precessions, including those induced by J_2 and J_4 which, instead, are cancelled out *a priori* in the combination used in the LAGEOS experiment [14]. They are the most effective in aliasing the Lense-Thirring precessional rates.

Now we will focus on the sensitivity of $\frac{\delta\mu_{\mathrm{LT}}}{\mu_{\mathrm{LT}}}_{\mathrm{zonals}}$ to the unavoidable orbital injection errors in the possible orbital parameters of LARES. For a former analysis see ref.[114]. It is particularly interesting to consider the impact of the errors in the inclination and the semimajor axis. The ranges of variation for them have been chosen in a very conservative way in order to take into account low-precision and low-costs injection scenarios.

From fig. 3 it is interesting to notice that the minimum value of the systematic zonal error, which amounts to 2.1×10^{-3}, does not correspond to $i_{\mathrm{LR}} = 70$ deg but it is obtained for a slightly smaller value. It is possible to show that for $e_{\mathrm{LR}} = e_{\mathrm{LAGEOS}}$ the minimum is 0 and that it is attained at $i_{\mathrm{LR}} = 70$ deg. The maximum error amounts to 1.6×10^{-2}. This suggests that the original LARES project is rather sensitive to small departures of i_{LR} from its nominal value. Fig. 4 shows that even more relevant is the sensitivity to the LARES semimajor axis. Also in this case the minimum is attained at a value of a_{LR} smaller than the nominal $a_{\mathrm{LR}} = 12,270$ km. For $e_{\mathrm{LR}} = e_{\mathrm{LAGEOS}}$ the minimum error amounts to 0 and it is obtained for $a_{\mathrm{LR}} = 12,270$ km, as expected. In obtaining fig. 4 we have accounted for the dependence of the nodal Lense-Thirring precession on a by varying, accordingly, the slope of the general relativistic trend. The sensitivity to eccentricity variations is less relevant: indeed, by varying it from 0.03 to 0.05 the relative systematic zonal error passes from 1.6×10^{-3} to 4.6×10^{-3}

6˙3. *An alternative LARES scenario*. – Here we will look for an alternative observable involving the orbital elements of LARES which
• yields a smaller value for the systematic error due to the mismodelled even zonal harmonics of the geopotential than that of the simple sum of the nodes of LAGEOS and LARES

---

[10] It is important to notice that using satellites of the LAGEOS family allows one to obtain reliable estimates with EGM96. Indeed, the LAGEOS' orbits are not affected by the terms of degree $l > 20$, for which the EGM96 covariance matrix elements are determined less accurately.
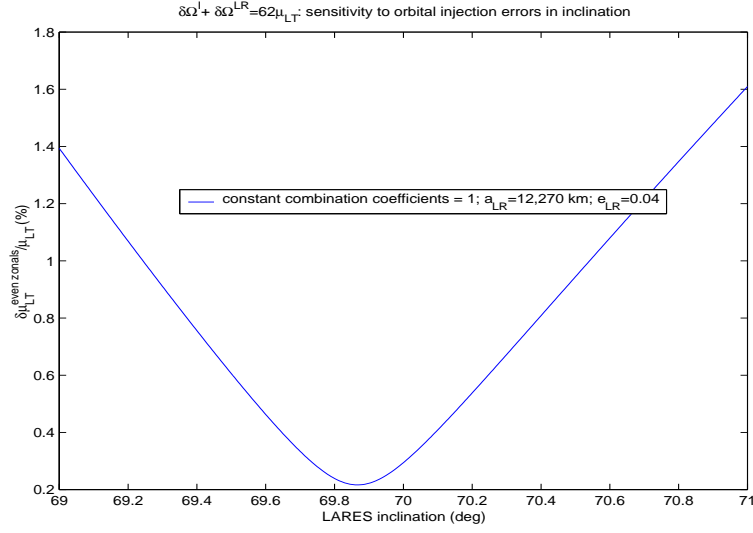
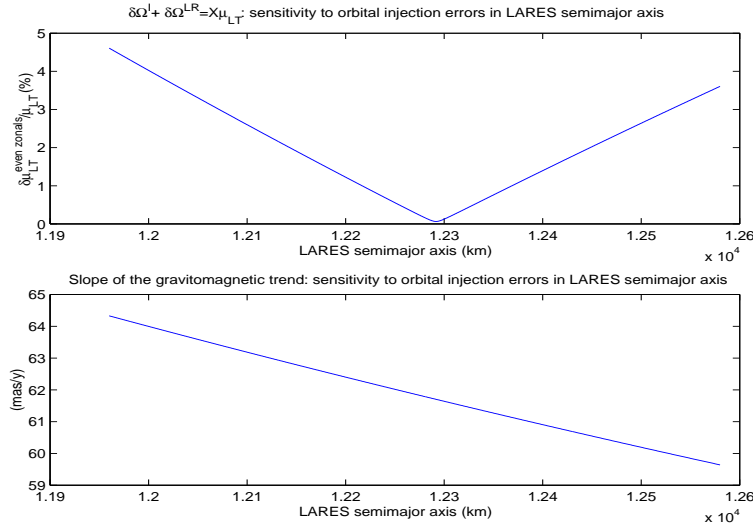Fig. 3. – Influence of the injection errors in the LARES inclination on the zonals' error.

Fig. 4. – Influence of the injection errors in the LARES semimajor axis on the zonals' error.

• is less sensitive to the departures of the possible orbital elements of LARES from the nominal values. The first requirement could be implemented by setting up a suitable orbital combination which cancels out the contributions of as many mismodelled even zonal harmonics as possible, following the strategy of the LAGEOS experiment outlined in [14]. To this aim we will consider only the satellites of the LAGEOS family both because they are the best laser-ranged tracked targets and because the gravitational and

non-gravitational perturbations affecting their orbits have been extensively and thoroughly analyzed.

Our result is

$$(154) \quad \delta\dot{\Omega}^{\text{LAGEOS}} + c_1\delta\dot{\Omega}^{\text{LAGEOS II}} + c_2\delta\dot{\Omega}^{\text{LARES}} + c_3\delta\dot{\omega}^{\text{LAGEOS II}} + c_4\delta\dot{\omega}^{\text{LARES}} = 61.8\mu_{\text{LT}},$$

with

$$(155) \qquad\qquad\qquad\qquad c_1 = 6 \times 10^{-3},$$
$$(156) \qquad\qquad\qquad\qquad c_2 = 9.83 \times 10^{-1},$$
$$(157) \qquad\qquad\qquad\qquad c_3 = -1 \times 10^{-3},$$
$$(158) \qquad\qquad\qquad\qquad c_4 = -2 \times 10^{-3}.$$

It is important to notice that the coefficients given by eqs. (155)-(158) depend on the orbital parameters of the satellites entering the combination and, among them, of LARES. The values released here are calculated for the nominal LARES parameters, as is the case for the slope in mas/y of the general relativistic trend. The observable of eq. (154) allows one to cancel out the static and dynamical contributions of the first four even zonal harmonics. The relative systematic error due to the J_{2n}, $n \geq 5$, according to EGM96 up to degree $l = 20$, amounts to:

$$(159) \qquad\qquad\qquad \frac{\delta\mu_{\text{LT}}}{\mu_{\text{LT}}}\bigg|_{\text{zonals}} = 2 \times 10^{-4},$$

which is one order of magnitude better than the result of eq. (153).

Fig. 5 and fig. 6 show the important achievements realized in reducing the sensitivity of the proposed combined residuals to the orbital injection errors in the LARES orbital elements. In obtaining fig. 5 and fig. 6 we have accounted for the dependence on a_{LR} and i_{LR} of both the coefficients and the Lense-Thirring precessions: it turns out that the variations in the slope of the general relativistic trend are very smooth with respect to the nominal value of 61.8 mas/y amounting to few mas/y. Now the values of the zonals' error are much more close to the nominal one given by eq. (159). Also in this case, the minima are attained at slightly different values of the LARES orbital elements with respect to the nominal ones. It is interesting to notice in fig. 5 that over a 3% variation of i_{LARES} the error due to the mismodeled zonal harmonics remain almost constant, while over a 5% variation of a_{LARES} it changes of 1 order of magnitude, as it turns out from fig. 6. It is worthwhile noting that the time-varying gravitational and non-gravitational orbital perturbations which affect the proposed combined residuals are depressed by the small values of the coefficients with which some orbital elements enter the combination. Moreover, the observational error in the LAGEOS II and LARES perigees, which are difficult to measure for low eccentric satellites as LAGEOSdue to the small value of their eccentricity, would have an impact of the order of 1×10^{-4} by assuming an uncertainty of 1 cm over 1 year in the satellite's position.

6'4. *Conclusions*. – If analyzed from the point of view of the impact of the systematic error induced by the mismodelling in the even zonal harmonics of the geopotential, which is the most important source of systematic error, the original LARES mission seems to be affected by a certain sensitivity to the unavoidable departures of the LARES orbital
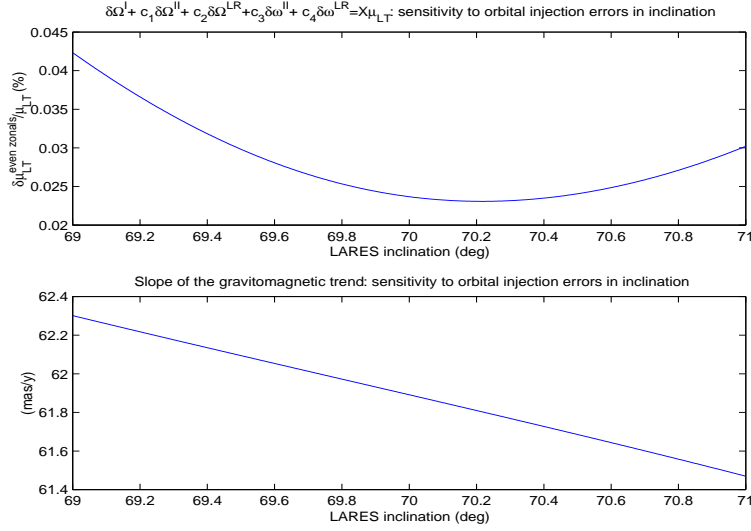
Fig. 5. – Alternative combined residuals: influence of the injection errors in the LARES inclination on the zonals' error.
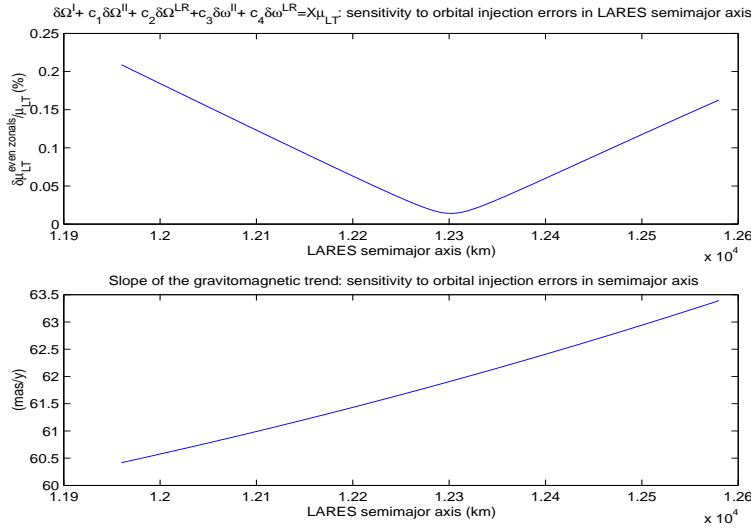

Fig. 6. – Alternative combined residuals: influence of the injection errors in the LARES semimajor axis on the zonals' error.

parameters from their nominal values due to orbital injection errors. In such a refined experiment, which would compete with the ambitious Stanford GP-B mission and its claimed global 1% accuracy level, it could be a serious drawback. It could be enhanced if LARES will be finally put in orbit with a low-cost launcher which, inevitably, would induce relatively large injection errors.

The adoption of the alternative combined residuals proposed here, including also the node of LAGEOS II and the perigees of LAGEOS II and LARES, would reduce by one order of magnitude the systematic error due to the even zonal harmonics of the geopotential passing from 0.3% to 0.02%, and would reduce greatly the sensitivity of such result to errors in the LARES orbital parameters. This would yield to less stringent requirements on the quality and the costs of the launcher to be adopted. It is very important to notice that the estimates presented here are based on the most recent Earth gravity model EGM96. When the new data on the terrestrial gravitational field from the CHAMP and GRACE missions will be available, the systematic zonal error will greatly reduce. The impact of the errors related to the quality of laser data will further reduce in the near future as well. Preliminary estimates of the standard statistical error in the solve-for least square parameter μ_{LT}, based on the present models of the time-dependent LAGEOS perturbations worked out in section 3 and the noise level reported in the Lense-Thirring LAGEOS experiment, yield a value of the order of 10^{-3}. If confirmed by further analysis of the impact of the time-dependent gravitational and non-gravitational perturbations, this result is very important because the total error of this improved version of the LARES mission would be $\leq 1\%$.

7. – Conclusions and recommendations for future work

The general relativistic features considered here are
• The gravitomagnetic LAGEOS experiment devoted to the measurement of the Lense-Thirring drag of inertial frames, currently carried on by analyzing the combined residuals of the nodes of LAGEOS and LAGEOS II and the perigee of LAGEOS II. The assessment of the systematic error induced by the time–dependent part of the terrestrial gravitational field has been extensively discussed so to extend its evaluation also to future measurements over longer time spans. The role of the proposed LARES in a new context is also taken into account. The proposed new observable would allow to reduce by one order of magnitude the total systematic error
• The pericenter shift of a test particle due to the Schwarzschild's gravitoelectric part of the gravitational field of a central, static body and the possibility of measuring it at a 10^{-3} level in the field of the Earth with LAGEOS, LAGEOS II, and, perhaps, other SLR satellites

It is very important to stress that in the near future, when the new and more precise data relative to the static and dynamical parts of the Earth's gravitational field from the CHAMP and GRACE missions will be available, it will be possible to reduce sensibly the uncertainties of many source of systematic errors of gravitational origin. This is particularly true for the even zonal harmonics of the static part of the geopotential. In regard to the gravitomagnetic LAGEOS experiment, this would probably allow to reduce the total geopotential error from the present 12.9% to some percent. Moreover, the zonals error in the PPN measurement could reach the level of $10^{-4}-10^{-5}$ according to the observable adopted. These improvements would extend also to the LARES project. So, it could be possible to proceed in the future by updating the orbit determination softwares like GEODYN II with the new data of the geopotential and, subsequently, by reanalyzing the data of the gravitomagnetic LAGEOS experiment. In the framework of the gravitomagnetic LAGEOS experiment, it could be useful to look for alternative combinations of orbital residuals involving also other SLR satellites in order to reduce, on one hand, the systematic error due to the geopotential, on the other, the systematic error due to the non–gravitational perturbations. It would be the follow-on of the work

presented in ref.[114]. A first attempt can be found in ref.[115].

APPENDIX A.

The classical orbital precessions

Here we show the explicitly calculated coefficients

$$\text{(A.1)} \qquad \dot\Omega_{.2n} \equiv \frac{\partial \dot\Omega_{\text{class}}}{\partial(J_{2n})}$$

and

$$\text{(A.2)} \qquad \dot\omega_{.2n} \equiv \frac{\partial \dot\omega_{\text{class}}}{\partial(J_{2n})}$$

of the satellites' classical nodal and apsidal precessions due to the even ($l = 2n$, $n = 1, 2, 3...$) zonal ($m = 0$) harmonics of the geopotential up to $l = 20$. Recall that $J_l \equiv -C_{l0}$, $l = 2n$, $n = 1, 2, 3...$ where the unnormalized adimensional Stokes coefficients C_{lm} of degree l and order m can be obtained from the normalized $\overline{C}_{lm}$ with

$$\text{(A.3)} \qquad C_{lm} = N_{lm}\overline{C}_{lm}.$$

In it

$$\text{(A.4)} \qquad N_{lm} = \left[\frac{(2l+1)(2-\delta_{0m})(l-m)!}{(l+m)!}\right]^{\frac{1}{2}}.$$

For the general expression of the classical rates of the near Earth satellites' Keplerian orbital elements due to the geopotential $\dot a_{\text{class}}$, $\dot e_{\text{class}}$, $\dot i_{\text{class}}$, $\dot\Omega_{\text{class}}$, $\dot\omega_{\text{class}}$, $\dot{\mathcal{M}}_{\text{class}}$, see ref.[1]. The coefficients $\dot\Omega_{.2n}$ and $\dot\omega_{.2n}$ are of crucial importance in the evaluation of the systematic error due to the mismodelled even zonal harmonics of the geopotential; moreover, they enter the combined residuals' coefficients c_i, $i = 1, 2...N$ of sect. 5 and sect. 6. See also ref.[14]. Since the general relativistic effects investigated are secular perturbations, we have considered only the perturbations averaged over one satellite' s orbital period. This has been accomplished with the condition $l - 2p + q = 0$. Since the eccentricity functions G_{lpq} are proportional to $e^{|q|}$, for a given value of l we have considered only those values of p which fulfil the condition $l - 2p + q = 0$ with $q = 0$, i.e. $p = \frac{l}{2}$. This implies that in the summations

$$\text{(A.5)} \qquad \sum_{p=0}^{l} \frac{dF_{l0p}}{di} \sum_{q=-\infty}^{+\infty} G_{lpq}$$

and

$$\text{(A.6)} \qquad \sum_{p=0}^{l} F_{l0p} \sum_{q=-\infty}^{+\infty} \frac{dG_{lpq}}{de}$$

involved in the expressions of the classical rates we have considered only $F_{l0\frac{l}{2}}$ and $G_{l\frac{l}{2}0}$. Moreover, in working out the $G_{l\frac{l}{2}0}$ we have neglected the terms of order $\mathcal{O}(e^k)$ with $k > 2$.

The nodal coefficients, proportional to

$$
(A.7) \qquad \frac{1}{\sin i} \sum_{q=-\infty}^{+\infty} G_{lpq} \sum_{p=0}^{l} \frac{dF_{lmp}}{di},
$$

are

$$
(A.8)\ \dot{\Omega}_{.2} = -\frac{3}{2}n\left(\frac{R}{a}\right)^2 \frac{\cos i}{(1-e^2)^2},
$$

$$
(A.9)\ \dot{\Omega}_{.4} = \dot{\Omega}_{.2}\left[\frac{5}{8}\left(\frac{R}{a}\right)^2 \frac{(1+\frac{3}{2}e^2)}{(1-e^2)^2}\left(7\sin^2 i - 4\right)\right],
$$

$$
(A.10)\ \dot{\Omega}_{.6} = \dot{\Omega}_{.2}\left[\frac{35}{8}\left(\frac{R}{a}\right)^4 \frac{(1+5e^2)}{(1-e^2)^4}\left(\frac{33}{8}\sin^4 i - \frac{9}{2}\sin^2 i + 1\right)\right],
$$

$$
\dot{\Omega}_{.8} = \dot{\Omega}_{.2}\left[\frac{105}{16}\left(\frac{R}{a}\right)^6 \frac{(1+\frac{21}{2}e^2)}{(1-e^2)^6}\left(\frac{715}{64}\sin^6 i - \frac{143}{8}\sin^4 i + \right.\right.
$$

$$
(A.11)\qquad \left.\left. + \frac{33}{4}\sin^2 i - 1\right)\right],
$$

$$
\dot{\Omega}_{.10} = \dot{\Omega}_{.2}\left[\frac{1,155}{128}\left(\frac{R}{a}\right)^8 \frac{(1+18e^2)}{(1-e^2)^8}\left(\frac{4,199}{128}\sin^8 i - \frac{1,105}{16}\sin^6 i\right.\right.
$$

$$
(A.12)\qquad \left.\left. + \frac{195}{4}\sin^4 i - 13\sin^2 i + 1\right)\right],
$$

$$
\dot{\Omega}_{.12} = \dot{\Omega}_{.2}\left[\frac{3,003}{256}\left(\frac{R}{a}\right)^{10} \frac{(1+\frac{55}{2}e^2)}{(1-e^2)^{10}}\left(\frac{52,003}{512}\sin^{10} i - \frac{33,915}{128}\sin^8 i\right.\right.
$$

$$
(A.13)\qquad \left.\left. + \frac{8,075}{32}\sin^6 i - \frac{425}{4}\sin^4 i + \frac{75}{4}\sin^2 i - 1\right)\right],
$$

$$
\dot{\Omega}_{.14} = \dot{\Omega}_{.2}\left[\frac{15,015}{1,024}\left(\frac{R}{a}\right)^{12} \frac{(1+\frac{91}{2}e^2)}{(1-e^2)^{12}}\left(\frac{334,305}{1,024}\sin^{12} i - \frac{260,015}{256}\sin^{10} i\right.\right.
$$

$$
(A.14)\qquad \left.\left. + \frac{156,009}{128}\sin^8 i - \frac{11,305}{16}\sin^6 i + \frac{1,615}{8}\sin^4 i - \frac{51}{2}\sin^2 i + 1\right)\right],
$$

$$
\dot{\Omega}_{.16} = \dot{\Omega}_{.2}\left[\frac{36,465}{2,048}\left(\frac{R}{a}\right)^{14} \frac{(1+\frac{105}{2}e^2)}{(1-e^2)^{14}}\left(\frac{17,678,835}{16,384}\sin^{14} i - \right.\right.
$$

$$
-\frac{3,991,995}{1,024}\sin^{12} i + \frac{2,890,755}{512}\sin^{10} i - \frac{535,325}{128}\sin^8 i + \frac{107,065}{64}\sin^6 i
$$

$$
(A.15)\qquad \left.\left. - \frac{2,793}{8}\sin^4 i + \frac{133}{4}\sin^2 i - 1\right)\right],
$$

$$\dot{\Omega}_{.18} = \dot{\Omega}_{.2} \left[\frac{692,835}{32,768} \left(\frac{R}{a} \right)^{16} \frac{(1+68e^2)}{(1-e^2)^{16}} \left(\frac{119,409,675}{32,768} \sin^{16} i - \right. \right.$$

$$- \frac{30,705,345}{2,048} \sin^{14} i + \frac{6,513,255}{256} \sin^{12} i - \frac{1,470,735}{64} \sin^{10} i +$$

$$+ \frac{760,725}{64} \sin^8 i - \frac{28,175}{8} \sin^6 i +$$

$$(A.16) \quad + \frac{1,127}{2} \sin^4 i - 42 \sin^2 i + 1 \bigg) \bigg] ,$$

$$\dot{\Omega}_{.20} = \dot{\Omega}_{.2} \left[\frac{1,616,615}{65,536} \left(\frac{R}{a} \right)^{18} \frac{(1+\frac{171}{2}e^2)}{(1-e^2)^{18}} \left(\frac{1,641,030,105}{131,072} \sin^{18} i \right. \right.$$

$$- \frac{1,893,496,275}{32,768} \sin^{16} i + \frac{460,580,175}{4,096} \sin^{14} i - \frac{30,705,345}{256} \sin^{12} i$$

$$+ \frac{19,539,765}{256} \sin^{10} i - \frac{1,890,945}{64} \sin^8 i + \frac{108,675}{16} \sin^6 i -$$

$$(A.17) \quad - \frac{1,725}{2} \sin^4 i + \frac{207}{4} \sin^2 i - 1 \bigg) \bigg] .$$

The coefficients of the classical perigee precession are much more involved because they are proportional to

$$(A.18) \quad - \left(\frac{\cos i}{\sin i} \right) \sum_{q=-\infty}^{+\infty} G_{lpq} \sum_{p=0}^{l} \frac{dF_{lmp}}{di} + \frac{(1-e^2)}{e} \sum_{q=-\infty}^{+\infty} \frac{dG_{lpq}}{de} \sum_{p=0}^{l} F_{lmp}.$$

We can pose $\dot{\omega}_{.2n} = \dot{\omega}^a_{.2n} + \dot{\omega}^b_{.2n}$.
The first set is given by

$$(A.19) \quad \dot{\omega}^a_{.2} = \frac{3}{2} n \left(\frac{R}{a} \right)^2 \frac{\cos^2 i}{(1-e^2)^2},$$

$$(A.20) \quad \dot{\omega}^a_{.4} = \dot{\omega}^a_{.2} \left[\frac{5}{8} \left(\frac{R}{a} \right)^2 \frac{(1+\frac{3}{2}e^2)}{(1-e^2)^2} \left(7 \sin^2 i - 4 \right) \right],$$

$$(A.21) \quad \dot{\omega}^a_{.6} = \dot{\omega}^a_{.2} \left[\frac{35}{8} \left(\frac{R}{a} \right)^4 \frac{(1+5e^2)}{(1-e^2)^4} \left(\frac{33}{8} \sin^4 i - \frac{9}{2} \sin^2 i + 1 \right) \right],$$

$$\dot{\omega}^a_{.8} = \dot{\omega}^a_{.2} \left[\frac{105}{16} \left(\frac{R}{a} \right)^6 \frac{(1+\frac{21}{2}e^2)}{(1-e^2)^6} \left(\frac{715}{64} \sin^6 i - \right. \right.$$

$$(A.22) \quad - \frac{143}{8} \sin^4 i + \frac{33}{4} \sin^2 i - 1 \bigg) \bigg],$$

$$\dot{\omega}^a_{.10} = \dot{\omega}^a_{.2} \left[\frac{1,155}{128} \left(\frac{R}{a} \right)^8 \frac{(1+18e^2)}{(1-e^2)^8} \left(\frac{4,199}{128} \sin^8 i - \frac{1,105}{16} \sin^6 i \right. \right.$$

$$\text{(A.23)} \quad + \frac{195}{4}\sin^4 i - 13\sin^2 i + 1\Big)\Big],$$

$$\dot\omega^a_{.12} = \dot\omega^a_{.2}\left[\frac{3{,}003}{256}\left(\frac{R}{a}\right)^{10}\frac{(1+\frac{55}{2}e^2)}{(1-e^2)^{10}}\left(\frac{52{,}003}{512}\sin^{10} i - \frac{33{,}915}{128}\sin^8 i\right.\right.$$

$$\text{(A.24)} \quad + \frac{8{,}075}{32}\sin^6 i - \frac{425}{4}\sin^4 i + \frac{75}{4}\sin^2 i - 1\Big)\Big],$$

$$\dot\omega^a_{.14} = \dot\omega^a_{.2}\left[\frac{15{,}015}{1{,}024}\left(\frac{R}{a}\right)^{12}\frac{(1+\frac{91}{2}e^2)}{(1-e^2)^{12}}\left(\frac{334{,}305}{1{,}024}\sin^{12} i - \frac{260{,}015}{256}\sin^{10} i+\right.\right.$$

$$+ \frac{156{,}009}{128}\sin^8 i - \frac{11{,}305}{16}\sin^6 i + \frac{1{,}615}{8}\sin^4 i-$$

$$\text{(A.25)} \quad - \frac{51}{2}\sin^2 i + 1\Big)\Big],$$

$$\dot\omega^a_{.16} = \dot\omega^a_{.2}\left[\frac{36{,}465}{2{,}048}\left(\frac{R}{a}\right)^{14}\frac{(1+\frac{105}{2}e^2)}{(1-e^2)^{14}}\left(\frac{17{,}678{,}835}{16{,}384}\sin^{14} i - \frac{3{,}991{,}995}{1{,}024}\sin^{12} i\right.\right.$$

$$+ \frac{2{,}890{,}755}{512}\sin^{10} i - \frac{535{,}325}{128}\sin^8 i + \frac{107{,}065}{64}\sin^6 i$$

$$\text{(A.26)} \quad - \frac{2{,}793}{8}\sin^4 i + \frac{133}{4}\sin^2 i - 1\Big)\Big],$$

$$\dot\omega^a_{.18} = \dot\omega^a_{.2}\left[\frac{692{,}835}{32{,}768}\left(\frac{R}{a}\right)^{16}\frac{(1+68e^2)}{(1-e^2)^{16}}\left(\frac{119{,}409{,}675}{32{,}768}\sin^{16} i-\right.\right.$$

$$- \frac{30{,}705{,}345}{2{,}048}\sin^{14} i + \frac{6{,}513{,}255}{256}\sin^{12} i - \frac{1{,}470{,}735}{64}\sin^{10} i +$$

$$+ \frac{760{,}725}{64}\sin^8 i - \frac{28{,}175}{8}\sin^6 i + \frac{1{,}127}{2}\sin^4 i-$$

$$\text{(A.27)} \quad - 42\sin^2 i + 1\Big)\Big],$$

$$\dot\omega^a_{.20} = \dot\omega^a_{.2}\left[\frac{1{,}616{,}615}{65{,}536}\left(\frac{R}{a}\right)^{18}\frac{(1+\frac{171}{2}e^2)}{(1-e^2)^{18}}\left(\frac{1{,}641{,}030{,}105}{131{,}072}\sin^{18} i\right.\right.$$

$$- \frac{1{,}893{,}496{,}275}{32{,}768}\sin^{16} i + \frac{460{,}580{,}175}{4{,}096}\sin^{14} i - \frac{30{,}705{,}345}{256}\sin^{12} i$$

$$+ \frac{19{,}539{,}765}{256}\sin^{10} i - \frac{1{,}890{,}945}{64}\sin^8 i + \frac{108{,}675}{16}\sin^6 i-$$

$$\text{(A.28)} \quad - \frac{1{,}725}{2}\sin^4 i + \frac{207}{4}\sin^2 i - 1\Big)\Big].$$

The second set is given by

(A.29) $\quad w_{.2} = -\dfrac{3}{2}n\left(\dfrac{R}{a}\right)^2$,

(A.30) $\quad \dot{\omega}_{.2}^b = w_{.2}\left\{\left[\dfrac{1}{(1-e^2)^2}\right]\left(\dfrac{3}{2}\sin^2 i - 1\right)\right\}$,

$\qquad \dot{\omega}_{.4}^b = w_{.2}\left\{\dfrac{5}{8}\left(\dfrac{R}{a}\right)^2\left[\dfrac{3}{(1-e^2)^3} + 7\dfrac{(1+\frac{3}{2}e^2)}{(1-e^2)^4}\right]\left(\dfrac{7}{4}\sin^4 i - \right.\right.$

(A.31) $\qquad \left.\left. - \ 2\sin^2 i + \dfrac{2}{5}\right)\right\}$,

$\qquad \dot{\omega}_{.6}^b = w_{.2}\left\{\dfrac{35}{8}\left(\dfrac{R}{a}\right)^4\left[\dfrac{10}{(1-e^2)^5} + 11\dfrac{(1+5e^2)}{(1-e^2)^6}\right]\left(\dfrac{33}{48}\sin^6 i\right.\right.$

(A.32) $\qquad \left.\left. - \ \dfrac{9}{8}\sin^4 i + \dfrac{1}{2}\sin^2 i - \dfrac{1}{21}\right)\right\}$,

$\qquad \dot{\omega}_{.8}^b = w_{.2}\left\{\dfrac{105}{16}\left(\dfrac{R}{a}\right)^6\left[\dfrac{21}{(1-e^2)^7} + 15\dfrac{(1+\frac{21}{2}e^2)}{(1-e^2)^8}\right]\left(\dfrac{715}{512}\sin^8 i\right.\right.$

(A.33) $\qquad \left.\left. - \ \dfrac{143}{48}\sin^6 i + \dfrac{33}{16}\sin^4 i - \dfrac{1}{2}\sin^2 i + \dfrac{1}{36}\right)\right\}$,

$\qquad \dot{\omega}_{.10}^b = w_{.2}\left\{\dfrac{1,155}{128}\left(\dfrac{R}{a}\right)^8\left[\dfrac{36}{(1-e^2)^9} + 19\dfrac{(1+18e^2)}{(1-e^2)^{10}}\right]\left(\dfrac{4,199}{1,280}\sin^{10} i\right.\right.$

(A.34) $\qquad \left.\left. - \ \dfrac{1,105}{128}\sin^8 i + \dfrac{195}{24}\sin^6 i - \dfrac{13}{4}\sin^4 i + \dfrac{1}{2}\sin^2 i - \dfrac{1}{55}\right)\right\}$,

$\qquad \dot{\omega}_{.12}^b = w_{.2}\left\{\dfrac{3,003}{256}\left(\dfrac{R}{a}\right)^{10}\left[\dfrac{55}{(1-e^2)^{11}} + 23\dfrac{(1+\frac{55}{2}e^2)}{(1-e^2)^{12}}\right]\left(\dfrac{52,003}{6,144}\sin^{12} i\right.\right.$

$\qquad - \ \dfrac{6,783}{256}\sin^{10} i + \dfrac{8,075}{256}\sin^8 i - \dfrac{425}{24}\sin^6 i + \dfrac{75}{16}\sin^4 i$

(A.35) $\qquad \left.\left. - \ \dfrac{1}{2}\sin^2 i + \dfrac{1}{78}\right)\right\}$,

$\qquad \dot{\omega}_{.14}^b = w_{.2}\left\{\dfrac{15,015}{1,024}\left(\dfrac{R}{a}\right)^{12}\left[\dfrac{91}{(1-e^2)^{13}} + 27\dfrac{(1+\frac{91}{2}e^2)}{(1-e^2)^{14}}\right] \times\right.$

$\qquad \times \left(\dfrac{334,305}{14,336}\sin^{14} i - \dfrac{260,015}{3,072}\sin^{12} i + \dfrac{156,009}{1,280}\sin^{10} i - \right.$

$\qquad - \ \dfrac{11,305}{128}\sin^8 i + \dfrac{1,615}{48}\sin^6 i - \dfrac{51}{8}\sin^4 i +$

(A.36) $\qquad \left.\left. + \ \dfrac{1}{2}\sin^2 i - \dfrac{1}{105}\right)\right\}$,

$$\dot{\omega}_{.16}^{b} = w_{.2} \left\{ \frac{36,465}{2,048} \left(\frac{R}{a}\right)^{14} \left[\frac{105}{(1-e^2)^{15}} + 31\frac{(1+\frac{105}{2}e^2)}{(1-e^2)^{16}} \right] \times \right.$$

$$\times \left(\frac{17,678,835}{262,144} \sin^{16} i - \frac{570,285}{2,048} \sin^{14} i + \frac{963,585}{2,048} \sin^{12} i - \right.$$

$$- \frac{107,065}{256} \sin^{10} i + \frac{107,065}{512} \sin^8 i - \frac{931}{16} \sin^6 i +$$

(A.37) $$\left. \left. + \frac{133}{16} \sin^4 i - \frac{1}{2} \sin^2 i + \frac{1}{136} \right) \right\},$$

$$\dot{\omega}_{.18}^{b} = w_{.2} \left\{ \frac{692,835}{32,768} \left(\frac{R}{a}\right)^{16} \left[\frac{136}{(1-e^2)^{17}} + 35\frac{(1+68e^2)}{(1-e^2)^{18}} \right] \times \right.$$

$$\times \left(\frac{39,803,225}{196,608} \sin^{18} i - \frac{30,705,345}{32,768} \sin^{16} i + \frac{930,465}{512} \sin^{14} i - \right.$$

$$- \frac{490,245}{256} \sin^{12} i + \frac{152,145}{128} \sin^{10} i - \frac{28,175}{64} \sin^8 i +$$

(A.38) $$\left. \left. + \frac{1,127}{12} \sin^6 i - \frac{21}{2} \sin^4 i + \frac{1}{2} \sin^2 i - \frac{1}{171} \right) \right\},$$

$$\dot{\omega}_{.20}^{b} = w_{.2} \left\{ \frac{1,616,615}{65,536} \left(\frac{R}{a}\right)^{18} \left[\frac{171}{(1-e^2)^{19}} + 39\frac{(1+\frac{171}{2}e^2)}{(1-e^2)^{20}} \right] \times \right.$$

$$\times \left(\frac{328,206,021}{524,288} \sin^{20} i - \frac{210,388,475}{65,536} \sin^{18} i + \frac{460,580,175}{65,536} \sin^{16} i - \right.$$

$$- \frac{30,705,345}{3,584} \sin^{14} i + \frac{6,513,255}{1,024} \sin^{12} i - \frac{378,189}{128} \sin^{10} i +$$

$$+ \frac{108,675}{128} \sin^8 i - \frac{575}{4} \sin^6 i + \frac{207}{16} \sin^4 i -$$

(A.39) $$\left. \left. - \frac{1}{2} \sin^2 i + \frac{1}{210} \right) \right\}.$$

The results previously obtained can be used in working out explicitly the contributions of the mismodelled classical nodal and apsidal precessions up to degree $l = 20$ of the existing spherical passive laser-ranged geodetic satellites and of LARES. They are of the form $\delta\dot{\Omega}_{(2n)} = \dot{\Omega}_{.2n} \times \delta J_{2n}$, $n = 1, 2, ...10$ and $\delta\dot{\omega}_{(2n)} = \dot{\omega}_{.2n} \times \delta J_{2n}$, $n = 1, 2, ...10$. The values employed for $\delta J_{2n} = \sqrt{4n+1} \times \delta\overline{C}_{2n\ 0}$, $n = 1, 2, ...10$ would be those quoted in, e.g., EGM96 model.

APPENDIX B.

Some useful parameters used in the text

The data employed for the terrestrial space environment and the LAGEOS satellites are in the following table. In it ε is the angle between the ecliptic and the equatorial

plane, $R_\oplus$ is the Earth mean equatorial radius, G is the Newtonian gravitational constant, $GM_\oplus$ and $\delta(GM_\oplus)$ are the Newtonian gravitational constant times the Earth's mass and its error according to IERS standard [56], J_2, J_4, δJ_2 and δJ_4 are the first two even zonal geopotential's coefficients and their errors according to EGM96 [19], $J_\oplus$ is the Earth's angular momentum, $\omega_\oplus$ is the mean Earth angular velocity.

The conversion factor from rad/s to mas/y is 1 rad/s=6.509×10^{15} mas/y.

TABLE XVIII. – *Earth's and LAGEOS parameters used in the text.*

Parameter	Numerical value	Units
ε	23.44	deg
$R_\oplus$	$6,378 \times 10^5$	cm
G	6.67259×10^{-8}	cm^3 g^{-1} s^{-2}
$GM_\oplus$	3.986×10^{20}	cm^3 s^{-2}
$\delta(GM_\oplus)$	8×10^{11}	cm^3 s^{-2}
J_2	1.0826×10^{-3}	-
J_4	-1.6194×10^{-6}	-
δJ_2	7.9626×10^{-11}	-
δJ_4	3.126×10^{-10}	-
$J_\oplus$	5.9×10^{40}	g cm^2 s^{-1}
$J_\oplus/(cM_\oplus)$	3.3×10^2	cm
$\omega_\oplus$	7.29×10^{-5}	rad s^{-1}
G/c^2	7.42×10^{-29}	cm g^{-1}
$(GJ_\oplus)/c^2$	4.37×10^{12}	cm^3 s^{-1}
$(GM_\oplus)/c^2$	4.43×10^{-1}	cm
a_{LAGEOS}	1.2270×10^9	cm
$a_{\text{LAGEOS II}}$	1.2163×10^9	cm
a_{LARES}	1.2270×10^9	cm
e_{LAGEOS}	0.0045	-
$e_{\text{LAGEOS II}}$	0.014	-
e_{LARES}	0.04	-
i_{LAGEOS}	110	deg
$i_{\text{LAGEOS II}}$	52.65	deg
i_{LARES}	70	deg
n_{LAGEOS}	4.643×10^{-4}	s^{-1}
$n_{\text{LAGEOS II}}$	4.710×10^{-4}	s^{-1}
n_{LARES}	4.643×10^{-4}	s^{-1}

APPENDIX C.

WEB resources

- **http://wugrav.wustl.edu/People/CLIFF/tegp.html**, the experimental gravity web page.

- **http://www.livingreviews.org/Articles/Volume4/2001-4will/index.html**, recent review of the current status of the empirical basis of General Relativity.

- **http://www.laeff.esa.es/eng/laeff/activity/lageos3.html**, on LAGEOS III project.

- **http://w3.ing.uniroma1.it/tildespacedpt/lares.html**, on LARES project.

- **http://earth.agu.org/revgeophys/marsha01/node1.html**, on the force models acting on LAGEOS satellites.

- **http://einstein.stanford.edu/index.html**, on the GP-B mission.

- **http://www.nas.edu/ssb/gpbexe.html**, on the GP-B mission.

- **http://op.gfz-potsdam.de/champ/**, on the CHAMP mission.

- **http://op.gfz-potsdam.de/grace/**, on the GRACE missions

- **http://ilrs.gsfc.nasa.gov/**, the International Laser Ranging Service web site.

- **http://www.ee.surrey.ac.uk/SSC/SSHP/**, small satellites web site.

- **http://cddisa.gsfc.nasa.gov/926/egm96/egm96.html**, the EGM96 Earth gravity model.

- **http://co-ops.nos.noaa.gov/restles1.html**, on the phenomenon of Earth tides.

- **http://www.astro.oma.be/D1/EARTH_TIDES/wgtide.html**, home page of the Working Group of Theoretical Tidal Model of the Earth Tide Commission.

- **http://www.ill.fr/tas/matlab/doc/mfit.html**, useful collection of MATLAB least squares programs and other routines.

REFERENCES

[1] W.M. KAULA, *Theory of Satellite Geodesy*, (Blaisdell Publishing Company, Waltham, 1966).

[2] A. MILANI, P. FARINELLA and A.M. NOBILI, *Non-Gravitational Perturbations and Satellite Geodesy*, (Adam Hilger, Bristol, 1987).

[3] C. LÄMMERZAHL, C.W.F. EVERITT and F.W. HEHL, *Gyros, Clocks, Interferometers...:Testing Relativistic Gravity in Space,* Lecture Note in Physics 562, (Springer Verlag, Berlin, 2001).

[4] O. MONTENBRUCK and E. GILL, *Satellite Orbits: Models, Methods, Applications,* (Springer, Berlin, 2000).

[5] M.H. SOFFEL, *Relativity in Astrometry, Celestial Mechanics and Geodesy*, (Springer, Berlin, Heidelberg, 1989).

[6] E.W. GRAFAREND and G. JOOS, in *Proceedings of the 21nd International Workshop on High Precision Navigation,* edited by K. LINKWITZ and U. HANGLEITER (Dümmler Verlag, Bonn, 1992), p.19.

[7] J. LENSE and H. THIRRING, *Phys. Z.,* **19**, 156, (1918), translated by B. MASHHOON, F.W. HEHL and D.S. THEISS, *Gen. Rel. Grav.,* **16**, 711, (1984).

[8] I. CIUFOLINI and J.A. WHEELER, *Gravitation and Inertia*, (Princeton University Press, New York, 1995).

[9] B. MASHHOON, F. GRONWALD and H.I.M. LICHTENEGGER, in *Gyros, Clocks, Interferometers...:Testing Relativistic Gravity in Space,* Lecture Note in Physics 562, edited by C. LÄMMERZAHL, C.W.F. EVERITT and F.W. HEHL, (Springer Verlag, Berlin, 2001), p.83.

[10] B. Mashhoon, in *Proceedings of the XXIII Spanish Relativity Meeting on Reference Frames and Gravitomagnetism*, edited by J.F. Pascual-Sánchez, L. Floría, A. San Miguel and F. Vicente, (World Scientific, Singapore, 2001), p.121.

[11] C.W.F. Everitt and other members of the Gravity Probe B team, in *Gyros, Clocks, Interferometers…:Testing Relativistic Gravity in Space,* Lecture Note in Physics 562, edited by C. Lämmerzahl, C.W.F. Everitt and F.W. Hehl, (Springer Verlag, Berlin, 2001), p.52.

[12] I. Ciufolini, *Phys. Rev. Lett.,* **56**, 278, (1986).

[13] I. Ciufolini and R. Matzner, in *LARES Phase-A Study*, (Rome, 1998), p.2.

[14] I. Ciufolini, *Il Nuovo Cimento,* **109A**, 1709, (1996).

[15] I. Ciufolini, E. Pavlis, F. Chieppa, E. Fernandes-Vieira and J. Pérez-Mercader, *Science,* **279**, 2100, (1998).

[16] I. Ciufolini, *Class. Quantum Grav.,* **17**, 2369, (2000).

[17] T.E. Sterne, *An Introduction to Celestial Mechanics*, (Interscience, New York, 1960).

[18] T. Allison and N. Ashby, *Celest. Mech.,* **57**, 537, (1993).

[19] F.G. Lemoine et al., *NASA/TP-1998-206861*, (1998).

[20] P. Melchior, *The Tides Of The Planet Earth*, (Pergamon Press, New York, 1983).

[21] D.E. Cartwright, *Tides A Scientific History,* (Cambridge, 2000).

[22] L. Iorio, *Celest. Mech.,* **79**, 201, (2001).

[23] L. Iorio and E.C. Pavlis, *J. of the Geod. Soc. of Japan,* **47**, 169, (2001).

[24] E.C. Pavlis and L. Iorio, to be published in *Int. J. of Mod. Phys. D,* (2002).

[25] L. Iorio, *Il Nuovo Cimento*, **116B**, 777, (2001).

[26] B. Bertotti and P. Farinella, *Physics of the Earth and the Solar System*, (Kluwer Academic Publishers, Dordrecht, 1990).

[27] J.P. Vinti, *Orbital and Celestial Mechanics*, edited by G.J. Der and N.L. Bonavito, Progress in Astronautics and Aeronautics, Volume 177, (1998).

[28] A. Einstein:, *The meaning of Relativity,* 5th ed. (Princeton University Press, New York, 1975).

[29] Y. Vladimirov, N. Miskievich and J. Horsky, *Space Time Gravitation*, (Mir Publishers, Moscow, 1987).

[30] B. Mashhoon, *Phys. Lett. A*, **173**, 347, (1993).

[31] L.D. Landau and E.M. Lifshitz, *The Classical Theory of Fields*, (Oxford University Press, 1979).

[32] C.W. Misner, K.S. Thorne and J.A. Wheeler, *Gravitation*, (Freeman, San Francisco, 1973).

[33] V.I. Arnold, *Geometrical Methods in the Theory of Ordinary Differential Equations*, (Springer Verlag, 1983).

[34] V.I. Arnold, *Mathematical Methods of Classical Mechanics*, (Springer Verlag, 1989).

[35] J.M. Dow, Ph.D. thesis: Technische Universität München, (München, 1988).

[36] D. Christodoulidis, D.E. Smith, R.G. Williamson and S.M. Klosko, *J. Geophys. Res.,* **93**(B6), 6216, (1988).

[37] S. Casotto, Ph.D. thesis: The University of Texas, (Austin, 1989).

[38] J.J. Dronkers, *Tidal Computations*, (North-Holland Publishing Company, Amsterdam, 1964).

[39] K. Lambeck, *Phil. Trans. R. Soc. Lond. A.,* **287**, 545, (1977).

[40] A.T. Doodson, *Proc. R. Soc. A.,* **100**, 305, (1921).

[41] D.E. Cartwright and R.J. Tayler, *Geophys. J. R. Astron. Soc.,* **23**, 45, (1971).

[42] D.E. Cartwright and A.C. Edden, *Geophys. J. R. Astron. Soc.,* **33**, 253, (1973).

[43] F.J. Buellesfeld, *Deutsche Geodätische Kommission, Reihe C, Heft* **314**, (München, Germany, 1985).

[44] Y. Tamura, *Bull. Info. Marées Terrestres,* **99**, 6813, (1987).

[45] Q. Xi, *Bull. Info. Marées Terrestres,* **99**, 6766, (1987).

[46] T. Hartmann and H.G. Wenzel, *Bull. Info. Marées Terrestres,* **123**, 9278, (1995).

[47] F. Roosbeek, *Geophys. J. Int.,* **126**, 197, (1996).

[48] A.E.H. Love, A Treatise on the Mathematical Theory of Elasticity, 4th ed., (Dover, Mineola, New York, 1926).

[49] K. Lambeck, A. Cazenave and G. Balmino, *Rev. Geophys. Space Phys.,* **12**, 421, (1974).

[50] R. Wang, in *Tidal Phenomena*, edited by H. Wilhelm, W. Zürn and H.G. Wenzel (Springer, Heidelberg, 1997), p.27.

[51] B. Bertotti and M. Carpino, in *Measurement of the Gravitomagnetic Field Using a Pair of Laser Ranged Satellites*, ASI final report, (Frascati, 1989), p.105.

[52] J.M. Wahr, *Geophys. J. R. Astron. Soc.,* **64**, 677, (1981).

[53] J.M. Wahr, *Geophys. J. R. Astron. Soc.,* **64**, 651, (1981).

[54] M. Chapront-Touzé and J. Chapront, *Astron. Astrophys.,* **190**, 342, (1988).

[55] P. Bretagnon and G. Francou, *Astron. Astrophys.,* **202**, 309, (1988).

[56] D.D. McCarthy, IERS conventions (1996), IERS Technical Note 21, (U. S. Naval Observatory, 1996).

[57] P.M. Mathews, B.A. Buffet and I.I. Shapiro, *Geophys. Res. Lett.,* **22**, 579, (1995).

[58] F.A. Dahlen, *Geophys. J. R. Astr. Soc.,* **28**, 357, (1972).

[59] M.L. Smith, *Geophys. J. R. Astr. Soc.,* **37**, 491, (1974).

[60] R. Wang, *Geophys., J. Int.,* **117**, 562, (1994).

[61] V. Dehant, P. Defraigne and J.M. Wahr, *J. Geophys. Res.*, **104**(B1), 1035, (1999).

[62] F. Gilbert and A.M. Dziewonski, *Philos. Trans. R., Soc. London, Ser. A,* **278**, 187, (1975).

[63] A.D. Dziewonski and D.L. Anderson, *Phys. Earth Planet Inter.*, **25**, 297, (1981).

[64] P. Varga, in *Proceedings of the Thirteenth International Symposium on Earth Tides*, edited by B. Ducarme and P. Paquet Observatoire Royal de Belgique, (Brussels, 1998), p. 297.

[65] G. Balmino, *The Use of Artificial Satellites for Geodesy and Geodynamics*, edited by G. Veis, (National Technical University, Athens, 1974).

[66] I. Ciufolini, F. Chieppa, D. Lucchesi and F. Vespe, *Class. Quantum Grav.*, **14**, 2701, (1997).

[67] D. Christodoulidis, Lehrstuhl für Astronomische und Physikalische Geodäsie, (Technische Universität München, 1978).

[68] I. Ciufolini, *Int. J. of Mod. Phys. A,* **4**, 3083, (1989).

[69] W. Zahel, in *Tidal Phenomena*, edited by H. Wilhelm, W. Zürn and H.G. Wenzel (Springer, Heidelberg, 1997), p.113.

[70] A. Defant, *Physical Oceanography, vol. 2*, (Pergamon Press, New York, 1961).

[71] M.C. Hendershott and W. Munk, *A. Rev. Fluid Mech.*, **21**, 205, (1970).

[72] E.W. Schwiderski, *Rev. Geophys. Space Phys.,* **18**, 243, (1980).

[73] G. Neumann, and W.J. Pierson jr., *Principles Of Physical Oceanography*, (Prentice-Hall, Englewood Cliffs, N. Y., 1966).

[74] C.L. Pekeris and Y. Akkad, *Phil. Trans. R. Soc.*, **265**, 413, (1969).

[75] M.C. Hendershott, *Geophys. J. R. Astr. Soc.*, **29**, 399, (1972).

[76] M.C. Hendershott, *EOS Trans., American Geophys. Union*, **54**, 76, (1973).

[77] A. Gill, *Atmosphere-Ocean Dynamics*, International Geophysics Series, vol. 30, (Academic Press, New York, 1982).

[78] C.K. Shum, J.C. Ries and B.D. Tapley, *Geophys. J. Int.,* **121**, 321, (1995).

[79] W.E. Farrell, *Rev. Geophys. Space Phys.,* **10**, 761, (1972).

[80] S.D. Pagiatakis, *Geophys. J. Int,* **103**, 541, (1990).

[81] T.L. Felsentreger and J.G. Marsh, *J. Geophys. Res.,* **83**(B4), 1837, (1978).

[82] C.C. Goad and B.C. Douglas, *J. Geophys. Res.,* **83**(B5), 2306, (1978).

[83] M.K. Cheng, C.K. Shum and B.D. Tapley, in *Proc. IUGG, XII General Assembly*, (Boulder, Colorado, July 1995).

[84] R.J. Eanes and S.V. Bettadpur, in *Proc. IUGG, XII General Assembly*, (Boulder, Colorado, July 1995).

[85] Y. Bard, *Nonlinear Parameter Estimation,* (Academic Press, New York, 1974).

[86] N.R. Draper and H. Smith, *Applied Regression Analysis,* 2nd edition, Wiley Series in Probability and Mathematical Statistics, (Wiley, 1981).

[87] D.M. Lucchesi, *Planetary Space Sci.* **40**, 447, (2001).

[88] G. Godin, *The analysis of tides*, (Liverpool University Press, Liverpool, 1972).

[89] M.B. Priestley, *Spectral analysis and time series,* Vol. 1-2, (Academic Press, 1981).

[90] Vespe, F., *Adv. Space Res.,* **23**, 699, (1999).

[91] C.M. Will, *Theory and Experiment in Gravitational Physics*, 2nd edition, (Cambridge University Press, Cambridge, 1993).

[92] C.M. Will, *Living Rev. Relativity 2001-4* (January, 2001), [Article in Online Journal] cited on: 09 Aug 2001, http://www.livingreviews.org/Articles/Volume4/2001-4will.

[93] R.D. Reasenberg, *Astrophys. Jou.,* **234**, L219, (1979).

[94] M. Frœschlé, F. Mignard and F. Arenou, *ESA SP-***402**, (1997).

[95] D.E. Lebach et al., *Phys. Rev. Lett.,* **75**, 1439, (1995).

[96] GAIA Science Advisory Group, GAIA: Composition, formation and evolution of the galaxy. Results of the Concept and Technology Study. Draft version available on as `http://astro.estec.esa.nl/GAIA` march-report.pdf, version 1.6, (2000).

[97] J.G. Williams, X.X. Newhall and J.O. Dickey, *Phys. Rev. D*, **53**, 6730, (1996).

[98] J.D. Anderson and J.G. Williams, *Class. and Quant. Grav.,* **18**, 2447, (2001).

[99] K. Nordvedt, *Phys. Rev. D,* **43**, 3131, (1991).

[100] I. Shapiro, C. Counselman and R. King, *Phys Rev. Lett.,* **36**, 555, (1976).

[101] I. Shapiro et al., *Phys Rev. Lett.,* **28**, 1594, (1972).

[102] I. Shapiro, in *Proceedings of the 12th International Conference on General Relativity and Gravitation,* edited by N. Ashby, D. Bartlett and W. Wyss (Cambridge University Press, Cambridge, 1990), p. 313.

[103] E.V. Pitjeva, *Celest. Mech.,* **55**, 313, (1993).

[104] S. Pireaux, J.-P. Rozelot and S. Godier, preprint astro-ph/0109032, submitted to *Astrophysics and Space Sciences*, (2001).

[105] A. Cacciani et al., in *Proceedings Oji International Seminar on Progress of Seismology of the Sun and the Stars,* edited by Y. Osaki and H. Shibahashi (Lecture Notes in Physics, 1989).

[106] I. Shapiro, *Rev. Mod. Phys.,* **71**, S41, (1999).

[107] S. Godier and J.-P. Rozelot, *Astron. and Astrophys.,* **355**, 365, (2000).

[108] W-T. Ni, in *Gyros, Clocks, Interferometers...:Testing Relativistic Gravity in Space,* Lecture Note in Physics, edited by C. Lämmerzahl, C.W.F. Everitt and F.W. Hehl 562, (Springer Verlag, Berlin, 2001), p.330.

[109] I. Ciufolini and R. Matzner, *Int. J. of Mod. Phys., A* **7**, 843, (1992).

[110] Balogh, et al., *ESA-SCI,* **1** p. 21 and p. 35, (2000).

[111] A. Milani, A. Rossi, D. Vokrouhlický, D. Villani and C. Bonanno, *Planetary Space Sci.*, **49**, 1579, (2001).

[112] I. Ciufolini, F. Vespe, and A. Mandiello, *Il Nuovo Cimento,* **109A**, 575, (1996).

[113] D.M. Lucchesi, *Planet. Space Sci.*, in press, (2002).

[114] S. Casotto, I. Ciufolini, F. Vespe and G. Bianco, *Il Nuovo Cimento,* **105B**, 589, (1990).

[115] L. Iorio, *J. of the Geod. Soc. of Japan,* **48**, 13, (2002).